Development and demonstration of an automated, modular and environmentally friendly multi-functional platform for open sea farm installations of the Blue Growth Industry

D2.2 – Representative site selection and associated climatology characteristics

Project main data		
Grant Agreement No.	774426	
Specific Work Programme	Food security, sustainable agriculture and forestry, marine and maritime and inland water research and the bioeconomy	
Type of Action	Innovation Action	
Call identifier	HRZ2020 BG-04-2017	
Call topic:	Multi-use of the oceans marine space, offshore and near-shore: enabling technologies	
Document data		
Document title:	D 2.2 – Representative site selection and associated climatology characteristics	
Document ID:	The Blue Growth Farm-WP2-CHL-D2.2 – PU_R1.0	
Date	31st, July 2018	
Issue	1.0	
Dissemination level		
PU	Public	**X**
RE	Restricted to a group identified by the Consortium	
CO	Confidential (only Consortium members including EC services)	

Document modifications record table					
Revision	**Edition date (day/month/year)**	**Author**	**Partner short name**	**Changed sections / pages of the current revision**	**Comment(s)**
1.0	31/07/2018	Giulio Brizzi Maroua Sabbagh Tim Atack Lorenzo Facco	CHL SAGRO RINA-C	All	First issue

LIST OF CONTENTS

LIST OF FIGURES

LIST OF TABLES

LIST OF ANNEXES

LIST OF ACRONYMS AND ABBREVIATIONS

EC	European Commission
GA	Grant Agreement
H&S	Health & Safety
HVAC	Heating, Ventilation, Air Conditioning
IFIs	International Financial Institutions
LCA	Life Cycle Analysis
MSPFD	Maritime Spatial Planning Framework Directive
MOI	Multipurpose Offshore Installation
MOM	Minutes of the Meeting
MS	Milestone
MSFD	Marine Strategy Framework Directive
O&M	Operation & Maintenance
PO	Project Officer
R&D	Research and Development
SHM	Structural Health Monitoring
WP	Work Packages

APPLICABLE DOCUMENTS

[AD1] European Commission, Directorate-General for Research & Innovation, Grant Agreement Number 774426 The Blue Growth Farm (GA-2018-774426), 2018.

[AD2] Technical Annex I to the Grant Agreement Number 774426: "Description of Work", April 2018, Part A and Part B.

1. INTRODUCTION

The present report has been produced as the result of the Task 2.2 (WP2) of the Blue Growth Farm contract [AD1].

Within the goals of WP2, which is to configure the development of the Blue Growth Farm design for at both full scale size and at prototype level, the aim of Task 2.2 is to collect and organize the climatic data relating to a number of marine sites, representative of the likely environmental conditions affordable by the Blue Growth Farm Platform.

Based on the preliminary Blue Growth Farm features assessed in task 2.1, three sites will be selected as representative of the climatic condition encountered during platform life, from deployment to operation. Specific attention is given to sea state and wind conditions, which must be in accordance with a suitable temperature range for the species selected for farming within the platform facilities, in order to provide an optimal farming environment and at the same time maximize the wind/wave energy exploitation. The site selection will be carried out with a view to optimizing integration within all platform systems and components, leading to the best exploitation of all platform functionalities.

The results of the present task will be used as the basis for subsequent Tasks 2.3 and 2.4.

1.1 Identification of the document and its structure

The present document is identified as Deliverable D2.2 “Representative site selection and associated climatology characteristics” of the Blue Growth Farm contract [AD1]. This document identifies and describes the environmental features of a number of sites considered suitable for the Blue Growth Farm Platform operational life.

The contents of the document are as follows:

- Section 1 provides an introduction to the present document;
- Section 2 gives a description of methods used and data sources;
- Section 3 describes site selection in the Mediterranean;
- Section 4 describes site selection in the North Atlantic;
- Section 5 describes site selection in the Subtropical Atlantic Ocean;
- Section 6 presents the conclusions of the document.

2 MATERIALS AND METHODS

2.1 Data sources

Data relating to **Mediterranean** sites are derived from the computations available through the **MEDSEA ANAYSIS FORECAST SYSTEM**, contained into the Copernicus product *MEDSEA ANALYSYS FORECAST WAV 006 017*, including hourly wave parameters at 1/24° horizontal resolution covering the whole Mediterranean Sea and partially the Atlantic Ocean. The System is a wave model, the WAM Cycle 4.5.4, considered to be the state-of-the-art model used over the last 20 years for wave hindcasting and forecasting. The Model performs an optimal interpolation of significant wave heights observed by satellite altimeters and then a readjustment of the wave spectrum at each grid point. WAM solves the wave transport equation explicitly without any presumption on wave spectrum shape. Input sorces are the wind, the white capping dissipation, the non-linear transfer and the bottom friction. In the wave model the continuous wave spectrum is approximated by step functions, which are constant in a frequency-direction bin. The spectrum is discretized in 32 frequencies and 24 directions of 15 degrees. The model solution is corrected by an optimal interpolation data assimilation scheme of along track satellite significant wave height observation, which rescales the wave spectrum, after separating it into wind and swell components. The model running in shallow waters considers wave refraction due to depth and current in addition to wave breaking due to depth. The system is forced by 10m-above-sea-surface wind fields obtained by the ECMWF Integrated Forecasting System at 1/8° resolution. The model is also forced by daily averaged surface currents from the Med MFC V3 model at 1/24° resolution. The Mediterranean set-up includes a nested fine grid domain at a resolution of 0,0416°, approximately 4 km. Data are graphically available as hourly observation from 01.01.2016 to current date (15.07.2018) through the Copernicus server. Data have been retrieved in graphic form.

Data concerning the **North Sea** sites are recovered through the **ATLANTIC-EUROPEAN NORTH-WEST SHELF-OCEAN WAVE ANALYSIS AND FORECAST**, and are generated using a WAVEWATCH III model, a 7 km Atlantic Margin Model, which became operational within CMEMS in April 2017. The wave model provides a description of ocean surface gravity wave (periods 3-30 seconds) characteristics as an extension to the existing physical and ecosystem model products provided by the North-West Shelf MFC. The WWIII-AMM7 model is a nested regional wave model configuration, defined on an identical grid to other North-West Shelf MFC modelling systems for hydrodynamics and ecosystems. The model is located on the North-West European continental shelf (NWS), from 40°N, 20°W to 65°N, 13°E, and uses a regular latitude-longitude grid with 1/15° latitudinal resolution and 1/9° longitudinal resolution (approximately 7 km square). The domain extends beyond the continental shelf in order to place the model's boundary region in the deep waters of the adjacent North-East Atlantic, but the focus region for the model comprises open waters of the shelf seas, i.e. the North Sea, Irish Sea, English Channel, Celtic Sea and Bay of Biscay. The present 7 km resolution of the model restricts its utility in the coastal zone, where topographic sheltering (e.g. reductions in wave height in the lea of headlands) and strong sub-grid scale variability in shallow water bathymetry will affect the wave field. In order to match the grid set-up in the hydrodynamic model, but improve the estimate of wave energy transmission in the vicinity of sub grid scale topographic features such as small islands and coastal headlands, a number of sub grid blocking cells are defined. The model predicts the evolution of the two dimensional (frequency-direction) wave energy spectrum in time and space. Shallow water effects cannot be fully resolved at the model's 7 km resolution, but are partially parameterised using bottom friction dissipation following the JONSWAP formula and depth induced wave breaking. Forcing for the model is provided by two models run operationally at the Met Office. Hourly surface (10m) wind forcing is taken from the global configuration of the Unified Model, interpolated onto the wave model grid. Surface current effects on the wave field are included by using surface zonal and meridional current fields from the NWS FOAM-AMM7 model. Since wave and hydrodynamic models use the same grid, no interpolation is applied. The role of the hind cast is to apply analysed wind and surface current data to the wave model, so that the model is forced by the best available descriptions of atmosphere and ocean. Data have been retrieved in graphic form.

The data series regarding waves on the **Canary Islands** have been obtained through the **ATLANTIC IBERIAN BISCAY IRISH-OCEAN WAVE ANALYSIS AND FORECAST** system, which provide a short-term high resolution wave forecast product for the Iberian-Biscay -Ireland area. The model is run twice daily on a grid of 10 km horizontal resolution and forced by ECMWMF wind data. This model is currently used as operational wave model in Meteo France. The model is driven by three-hourly analysed wind from ECMWF and uses boundary conditions from the global CMEMS wave system. The model performs a partitioning on wave spectra over all ocean grid points, allowing for the separation between wind sea and swell sea system. The model has a spectral resolution of 24 direction and 30 frequencies. The wave forecast CMEMS product *IBI ANALYSIS FORECAST WAV 005 005* has a temporal coverage from 2014 to present, with the historical data stored composed by best estimates. Data have been retrieved in graphic form.

The data series concerning seawater potential temperature and current have been retrieved from the **IBI OCEAN REANALYSIS SYSTEM** (CMEMS product *IBI REANALYSIS PHYS 005 002*) which provide monthly and hourly averages of temperature, salinity, mixed layer depth, sea surface height and current. The IBI model is based on the NEMO V3.6 ocean general circulation model, running at 1/12° horizontal resolution. Other data from AVHRR satellite sensors and in situ temperature and salinity are assimilated into the model. Data have been retrieved in graphic form.

Wind speed and wind stress series have been retrieved from the **GLOBAL OCEAN WIND OBSERVATION CLIMATOLOGY (MONTHLY MEANS)- REPROCESSED** system (CMEMS product: *WIND GLO L4 REP OBSERVATION*). The time series are monthly averaged wind variables calculated over global oceans, estimated from daily wind fields calculated from retrieval from ASCAT scatterometer on satellites from 2007 to 2017. The resulting fields are estimated as equivalent neutral-stability 10 m daily winds, with a spatial resolution of 0,25° in latitude and longitude. The monthly winds are estimated at grid points from at least 25 values/day on the same grid point. Data have been retrieved in graphic form.

Other data have been obtained from scientific paper, as given in the Reference.

2.2 Methods

2.2.1 Site selection criteria

Some authors (Zanuttigh at al., 2016), within the frame of the MERMAID EU FP7 project, have described a method to identify the best design solution, including the technological features of either single- or multi-use platform, to be selected for a given site. This method proposes a pre-screening phase, where the basic question on the site potential is addressed, and a ranking phase where a value is associated to each envisaged technological solution.

In the present case, since the Blue Growth Farm Platform is a multi-use platform aiming at a high degree of environmental flexibility, this method is not applicable, although the method we intend to use is similar. It is separated into a preliminary phase (excluding pre-screening) and a ranking phase where the best and worst factor combination is identified on the basis of ranks assigned to significant site characteristics.

Table 1: Excluding criteria for site selection, where in the presence of EVEN ONE CRITERION, the site is excluded from further selection.

Site name:	Position:

CRITERION	EXCLUDING
Protected areas	*
Other uses of the sea	*
Naval routes	*
Depth outside range 70- 200m	*
Distance from coast > 15nm	*
Distance from port > 15nm	*
Temp. salmon outside range 4°-20°	*
Temp. bream/bass outside range 12°-28°	*

In a second step, after identifying the boundaries of a possible area where the use of marine space is not under any constraints ideally preventing it from the deployment of a Blue Growth Platform, the TOPSYS method, a multi-criteria decision analysis tool, has been adopted. The described method, in Hwang and Yoon, (1981) and Hwang et al. (1993), is based on the comparison of a set of alternatives, after giving a weight for each criterion, and normalising scores for any given criterion. Then the geometric distance between each alternative and the best alternative is computed, and considered as the best score for each criterion. The highest sum of weighted and normalized scores gives the minimal distance from the ideal solution, either the best or worst ones.

2.2.2 Criteria for Fish farming: Fish Swimming Behaviour And Endurance To Current Velocity - Application to the Offshore Environment.

Exposed sites are associated with greater wave action and stronger water currents compared to coastal locations; several papers have looked at how fish farmed in offshore cages would cope in exposed environments with marine currents in terms of growth, stress levels, behaviour and welfare.

Endurance and swimming behaviour of Atlantic salmon (*Salmo salar*) in relation to current velocity was studied in offshore cages (Hvas et al., 2017; Johansson et al., 2014).

At sheltered farming sites current velocities are below 20 cm.s^{-1} outside the cages (Johansson et al., 2007), the swimming speed of *S.salar* is independent of the current velocity and caged fish form circular schooling structures cruising at varing speeds of **0.3-1.1 body lengths per second (BL.s^{-1})**, (Demster et al., 2009 ; Stien et al., 2016).

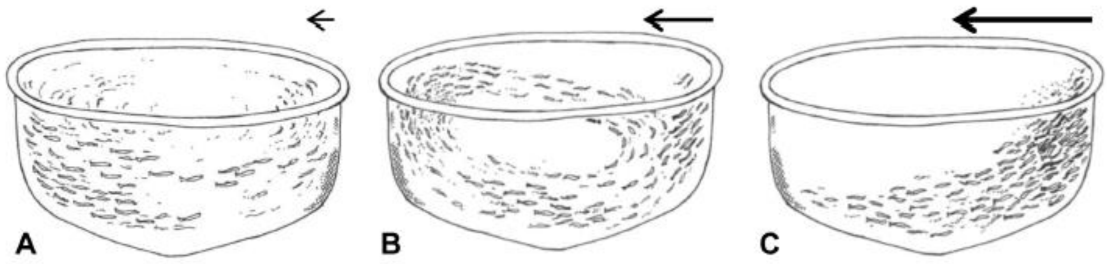

Figure 1: Observed *S.salar* swimming structures circle (A, circular movement), mixed (B, Circle and On Current) or on current (C, standing on current). The arrows indicate strength and direction of the water current during the different group structures, *(Reported from Hvas et al., 2017)*.

At an exposed commercial farm in the Faroe Island, the salmon swimming pattern changed from circular to a mixture of circular and standing on current, and then all standing on current at low, rapid and fast water currents respectively (Johannson et al., 2014). Salmon swimming performance was observed and measured in a cage of 41 Ø with a density of 6.2 kg/m^3; 1.54 kg as fish average weight and 50 cm as fish fork length. Swimming behaviours were observed during 48h using two cameras at two different points. One was positioned next to the net and the other approximately 15 m from the net at the opposite side of the cage at approximately 6 m depth to give a good representation of behaviours both upward- and downwards. The observed water current velocities varied in a tidal pattern between 0 and 69 cm.s^{-1} at the reference point, and between 0 and 42 cm.s^{-1} at the single point measured inside the cage.

The reduced current velocity inside the cage was related to dampening by the net and the fish inside the cage and the other cages sheltering the observed cage (Johansson et al., 2007; Gansel et al., 2012; Klebert et al., 2013). Swimming behaviours was as shown in Figure 1.

Swimming structure could be divided into 3 categories:

- Circle : polarized swimming in a circular movement;
- On Current : swimming towards the current with no forward movement;
- Mixed : both circle and on current in the same time.

Circle structure was associated with low current velocities ≈ 20 cm.s^{-1}; **Mixed** with increased current velocities ≈ 35 cm.s^{-1} and **On current** with an even stronger current velocities ≈ 46 cm.s^{-1}.

At low current velocities the fish swam in circle (Fig. 2A) and occupied most of the cage volume. This normal schooling structure can be identified as the fishes' preferred speed. With increasing current velocities, a shift occurred with some fish seeking a new position facing the net towards the current while other fish continued to swim in elliptic-shaped circles behind the stationary fish at the net (Fig. 2B).

When the circling fish came to a position where they were exposed to the current on their sides they turned inwards toward the centre of the cage and drifted with the current to the leeward side of the cage. With high current velocity, fish switched from schooling to swimming towards the current next to the net wall, until all fish stood in a dense group along the side of the cage with no circling fish net (Fig. 2C). Swimming behind others against the current in a group has been reported to save energy and could reflect energetic optimization as a response to the increased current velocities (Herskin et al., 1998).

Since strong currents disrupt the circular schooling behaviour and force the fish to swim at speeds dictated by the environment within the sea cages, this could severely compromise animal welfare where the magnitude and duration of water currents exceeds the swimming capacities of the fish (Hvas et al., 2017).

The same swimming pattern (Figure 1) was also observed in the study of Hvas et al. (2017). Salmon in an offshore cage were exposed to strong currents to assess their swimming behaviour. Current velocities were generated by a ship that was tied to a rigid docking bay on the downstream side of the fish cage, which allowed for strong controlled current generation by pushing the cage system. The ship generated a current of 14.9 meter long and 6.3 meter wide. Currents speeds were measured from 1.4-3.4 m depth upstream and downstream the sea cage. The current speed at 1.4 m of depth was 0.7-0.9 m.s^{-1} and increased above 140-154 cm. s^{-1} at greater depth.

Here the average weight of the fish was 3.4 kg, fork length was 63.5 cm and stocking density was 11.3 kg m^{-3}. At the lowest current velocities (15-30 cm.s^{-1}) fish were swimming in a homogenous circular pattern and voluntary swimming was 0.76 BL.s^{-1}. As the speed increased, the circular structure became more skewed and elliptical-shaped, while some fish began to stand on the current at 30-35 cm.s^{-1}. Above 45-60 cm.s^{-1} the circular structure was completely abolished and all fish were standing on the current. At ≈ 65 cm.s^{-1} ram ventilation was observed in the fish swimming and was the dominating mode of ventilation for all fish swimming above 100 cm.s-1.

Ram ventilation thus marks an adaptation to more effective sustained swimming when oxygen requirements are higher. The onset of ram ventilation in S. salar was at higher flow speeds than the speed at which complete disrupting of circular voluntary swimming occurred***. Since ram ventilation is an easily observable trait, it can be used to assess welfare status, where it would indicate that the fish are aerobically challenged. Prolonged swimming with ram ventilation would increase the risk of physiological fatigue and certainly impair growth.***

At 125 cm.s^{-1} (1.97 BL.s^{-1}) fish would start to be fatigued, meaning that short durations of currents at or above this magnitude in an exposed setting would be detrimental to animal welfare. When the current velocity had returned to its initial value, a circular schooling pattern was re-established.

To define the water current thresholds that secure salmon welfare in exposed aquaculture, it was been proposed that **the critical swimming speed (U_{crit})** (Remen et al., 2016) be used as the limiting value. **U_{crit}** is obtained in swim trials by an incremental increase in water velocity until the fish fatigues (Brett, 1964), and theoretically provides a good estimate of swimming capabilities in fish that experience strong currents (Plaut, 2001). Prolonged exposure at or above U_{crit} will result in physiological exhaustion (Wood, 1991; Burnett et al., 2014). Exhaustion was defined as the point where fish were unable to remove themselves from the posterior retaining grid. Exhaustion is associated with:

- loss of locomotion control
- depletion of muscle glycogen reserves
- accumulation of lactate
- release of catecholamines and even death

U_{crit} is size dependent. Although U_{crit} in salmonids has been reported in several swimming tunnel studies, few exist on large adult fish. In reared *S. salar* the U_{crit} in adults (1.75 kg, L_f = 51.3 cm, 14°C) was 100 cm.s^{-1} (Remen et al., 2016). In mature sockeye salmon (*Oncorhynchus nerka*) (2.41 kg, L_f = 61.4 cm, 19–21°C) the U_{crit} was 97 cm s^{-1} (Jain et al., 1998). U_{crit} of 1.25 m.s^{-1} in farmed *S.salar* (3.4 kg, L_f = 63 cm, 7-7.5°C) was found in Hvas et al. (2017). In wild caught adult *S. salar* (L_f = 55-60 cm, body weight was not reported) U_{crit} was an impressive 2.16 m.s^{-1} and 1.76 m.s^{-1} at 18°C and 13°C respectively (Booth et al., 1997).

Remen et al. (2016), demonstrated that U_{crit} shift with size from 80.6 cm.s^{-1} in small post-smolts (≈80 g) to 90.9 cm.s^{-1} in large post-smolts (≈289 g) and 99.5 cm.s^{-1} in adults (≈1750 g). U_{crit} when expressed as BL/sec, is inversely correlated to fork lengths, i.e., ***it is higher in smaller fish.***

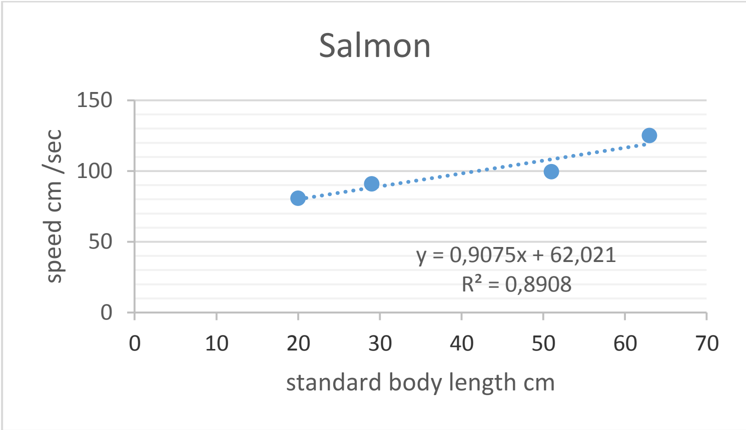

Figure 2: Linear interpolating function describing relationship between U_{crit} and fork length in Atlantic salmon (Remen et al., 2016; and Hvas et al., 2017)

No data were found on the swimming performance of gilthead seabream (*Sparus aurata*) and seabass (*Dicentrarchus labrax*) farmed in offshore cages.

Basaran et al. (2007) studied the swimming performances of wild and farmed **seabream** in a current channel. Biometric parameters (total average weight and total lenght) of both fish are given in Table 1. Results demonstrated that ***absolute*** $\mathbf{U_{crit}}$ performance of both wild and farmed fish increased with fish length (Figure 3) and the mean U_{crit} of wild fish was significantly higher (0.86 $m.s^{-1}$) than that of farmed fish (0.79 $m.s^{-1}$). They demonstrated that the ***relative*** $\mathbf{U_{crit}}$ decreased with the fish length (Figure 2) and was significantly higher in wild fish (4.52 $BL.s^{-1}$) than the farmed fish (4.21 $BL.s^{-1}$), (Table 1).

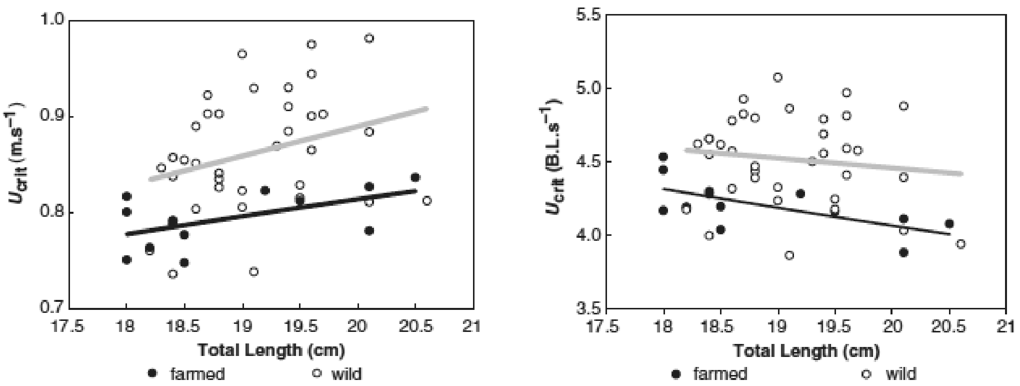

Figure 3: Total length (cm), absolute (m.s^{-1}) and relative U_{crit} (BL.s^{-1}) of wild and farmed seabream at 17°C. *(Basaran et al., 2007).*

Table 2: Absolute (m.s^{-1}) and relative (BL.s^{-1}) U_{crit} of wild and farmed seabream. *(Basaran et al., 2007).*

Classes (W–F)	N	Mean ± SE Total lengths (cm)	Total weights (g)	U_{crit} (m s^{-1})	U_{crit} (BL s^{-1})
Wild	36	19.10 ± 0.10	99.33 ± 1.56	0.86 ± 0.01	4.52 ± 0.05
Farmed	13	18.88 ± 0.25	95.92 ± 4.30	0.79 ± 0.01	4.20 ± 0.04
Statistics		NS	NS	S	S

Seabass critical speed was observed in a few studies. Carbonara et al. (2006), observed that **$U_{crit,}$** measured in tunnel, is lower than in seabream, being at a value of absolute U_{crit} in the range of 0,97-1,27 m.s^{-1} and relative U_{crit} in the range of 3.6 - 4.1 BL.s^{-1}. Different values are reported in the review of Luna-Acosta et al. (2011), ranging from 2,4 to 2,7 BL.s$^{-1,}$ as standard length.

In **Atlantic Salmon** *Salmo salar*, Johansson et al. (2014) inferred that a speed of 0,7 BL/sec can be kept as a limit for disruption of circle swimming pattern. They proposed setting up at twice this speed (1,4 BL/sec, approximately 0,66 **U_{crit}**) the upper limit of water speed that may be considered as within the range of water velocity that salmon can normally manage and withstand without impairing its welfare and growing capability under normal farming conditions.

The same assessment of the disruption of swimming pattern with an increase in water speed is not available within the scientific literature for Seabream and Seabass.

Here, making an arbitrary assumption, we propose to keep the same criterion used for Salmon (0,66 **U_{crit}**), given the lack of any experimental evidence, as threshold for water velocity suitable for Seabream and Seabass under farming conditions, with the aim of maintaining an acceptable standard of fish welfare. Therefore, the values would be 2,7 BL.s-1 for seabream and 2,5 BL.s-1 for seabass, considering their **U**crit of 4,2 and 3,85 respectively (Basaran et al., 2007 ; Carbonara et al., 2006) .

U_{crit} values are experimentally derived in tunnel experiments and for salmon in cages under an unidirectional current. No references in the scientific literature exist reporting fish endurance under wave movements. Several authors (including our personal observations) reported that under severe wave action, fish disrupt their schooling behaviour, shifting to a pattern in cage characterized by the following.

1. They dive down to a position where they can apparently minimize the movements induced by the waves;
2. They head towards the direction of the wave, swimming in an attempts to mantain their relative position, and avoid hitting the net walls. When wave motion moves them backwards, fish swim against the wave movement to minimize the shift in the wave direction; and when the wave motion carry them forward, they passively re-gain their primitive position.

Therefore, within each wave cycle, fish display an active swimming phase the length of which is similar to the wavelength at the depth where the fish stay, and the duration of movement is close to half of the wave period, at that depth. Thus, during wave episodes, fish experience a number of cycles of swim-and-resting, that we argue it can be compared to the effort sustained under continuous exercise of rather short duration (from 20 min to 1,5 h), being a storm duration from several hours to several days, and thus not less energy-consuming.

To assess a fish sustainable wave motion, we take into account the water speed leading to the active swimming phase within the wave cycle, and its corresponding horizontal velocity U, given by the mathematical decomposition of wave orbit at the fish's preferential depth.

$U = Hs/2 * gT/\lambda * \cosh(2\pi(z+d)/\lambda) / \cosh(2\pi d/\lambda)$,

Where:

Hs: Significant wave height, m

T: Period, sec.

λ: Wavelength, m

z: Depth, m

d: Bottom depth, m

As a first approach, we propose that the wave motion cyclical speed ***U*** should not have to exceed the **U_{crit},** therefore not leading to fish exhaustion under a prolonged storm peak.

When considering an ideal wave, it is well known that a negative exponential law governs the wave attenuation with depth, by a factor of e^{-z}.

Hence, within a cage, the space available for sheltering during a storm is restricted to its deepest volume, at least for the duration of most intense wave motion.

Several authors observed a cage volume reduction under strong current episodes (Figs 4, 5)

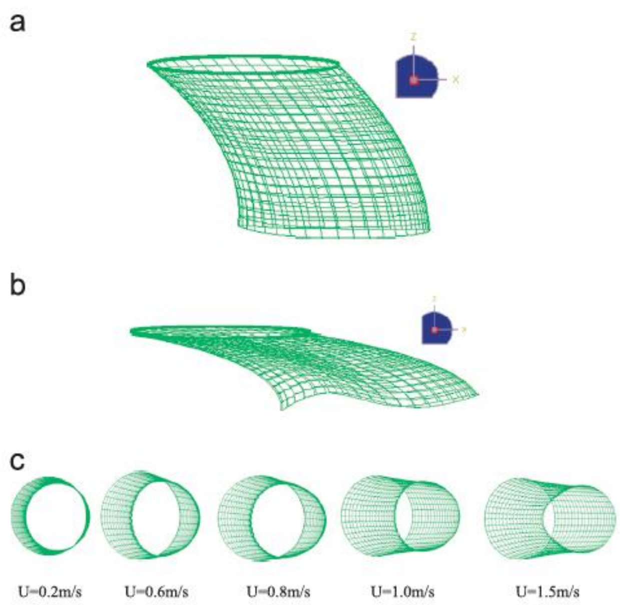

Figure 4: Net deformations in different currents (a) net deformations in current velocity of 0.6 m.s-1; (b) net deformations in current velocity of 1.5 m.s-1; (c) bird's view of net deformation at different current velocity. *(Li et al., 2013)*

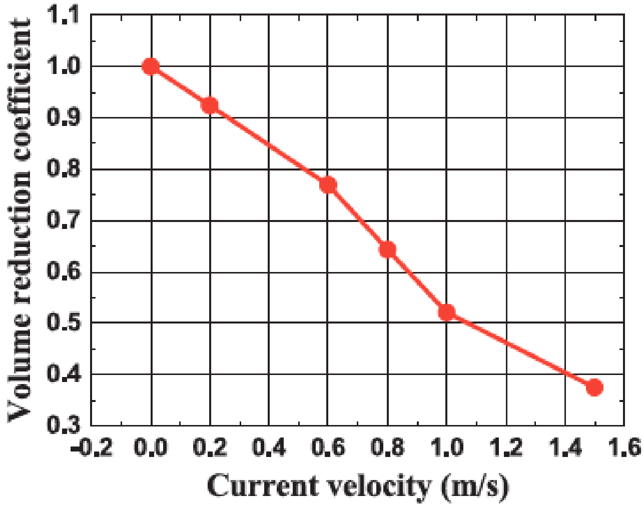

Figure 5: Cage volume under different current velocity. (*Li et al., 2013*).

While fish ideally take advantage of all of the cage volume within normal farming conditions, in the event of a stressing episode they may display a schooling behaviour leading to fish grouping in considerable densities, up to 20 times more than normal (Oppedal et al., 2011). *Here, maintaining a precautionary approach, we propose considering a cage suitable for hosting fish at an acceptable welfare standard under storm conditions, when it is able to offer them a volume where the level of combined current and wave motion does not trespass the threshold of 0,66 **$U_{crit.}$**, as previously stated for unidirectional currents. The above value should take in account both current and wave motion, in the event of their concordance at the selected site. The volume of cage suitable for sheltering should not be smaller than that necessary to maintain a sufficient oxygen level and waste dilution, as the basic conditions for fish welfare. This volume should not lead to exceeding a fish density of 25 kg m^{-3}.*

Table 3: Proposed values ($cm.s^{-1}$) of sustainable environmental speeds (66% $U_{crit.}$) for species and size at 20 °C, derived from equations in Basaran et al. (2007) and in Carbonara et al. (2006).

SPECIES/SIZE (CM)	5	10	20	30
Seabream	20	35	55	58
Seabass	17	32	58	76

Table 4 Proposed limit state wave in open sea for Seabream

Table 4: Proposed limit wave state in open sea for Seabream: Mediterranean wave of Hs 6,5 m; T 8,0 sec; l 100,0 m, _without any shelter from Blue Growth Farm platform_. Depth of acceptable motion for 20 and 35 cm Seabream, dark green; -

horizontal and vertical components of orbital wave velocities																																			
Hs significant heigth	6,5	6,5	6,5	6,5	6,5	6,5	6,5	6,5	6,5	6,5	6,5	6,5	6,5	6,5	6,50	6,5	6,5	6,5	6,5	6,5	6,5	6,5	6,5	6,5	6,5	6,5	6,5	6,5	6,5	6,5	6,5	6,5	6,5	6,5	6,5
Period T sec.	8,0	8,0	8,0	8,0	8,0	8,0	8,0	8,0	8,0	8,0	8,0	8,0	8,0	8,0	8,00	8,0	8,0	8,0	8,0	8,0	8,0	8,0	8,0	8,0	8,0	8,0	8,0	8,0	8,0	8,0	8,0	8,0	8,0	8,0	8,0
Lambda m	100,0	100,0	100,0	100,0	100,0	100,0	100,0	100,0	100,0	100,0	100,0	100,0	100,0	100,0	99,97	100,0	100,0	100,0	100,0	100,0	100,0	100,0	100,0	100,0	100,0	100,0	100,0	100,0	100,0	100,0	100,0	100,0	100,0	100,0	100,0
gravity g	9,8	9,8	9,8	9,8	9,8	9,8	9,8	9,8	9,8	9,8	9,8	9,8	9,8	9,8	9,81	9,8	9,8	9,8	9,8	9,8	9,8	9,8	9,8	9,8	9,8	9,8	9,8	9,8	9,8	9,8	9,8	9,8	9,8	9,8	9,8
wave at depth m	-1,0	-2,0	-3,0	-4,0	-5,0	-6,0	-7,0	-8,0	-9,0	-10,0	-11,0	-12,0	-13,0	-14,0	-15,00	-16,0	-17,0	-18,0	-19,0	-20,0	-21,0	-22,0	-23,0	-24,0	-25,0	-26,0	-27,0	-28,0	-29,0	-30,0	-31,0	-32,0	-33,0	-34,0	-35,0
site depth m	100,0	100,0	100,0	100,0	100,0	100,0	100,0	100,0	100,0	100,0	100,0	100,0	100,0	100,0	100,00	100,0	100,0	100,0	100,0	100,0	100,0	100,0	100,0	100,0	100,0	100,0	100,0	100,0	100,0	100,0	100,0	100,0	100,0	100,0	100,0
horizontal speed m/sec	2,4	2,3	2,1	2,0	1,9	1,8	1,6	1,5	1,4	1,4	1,3	1,2	1,1	1,1	0,99	0,934	0,88	0,8	0,8	0,7	0,7	0,6	0,6	0,6	0,5	0,5	0,5	0,4	0,4	0,4	0,4	0,3	0,3	0,3	0,3
%	100,0	78,4	73,6	69,1	64,9	61,0	57,3	53,8	50,5	47,4	44,5	41,8	39,3	36,9	34,65	32,5	30,6	28,7	26,9	25,3	23,8	22,3	21,0	19,7	18,5	17,4	16,3	15,3	14,4	13,5	12,7	14,3	13,4	12,6	11,8
vertical speed m/sec	-2,4	-2,3	-2,1	-2,0	-1,9	-1,8	-1,6	-1,5	-1,4	-1,4	-1,3	-1,2	-1,1	-1,1	-0,99	-0,9	-0,9	-0,8	-0,8	-0,7	-0,7	-0,6	-0,6	-0,6	-0,5	-0,5	-0,5	-0,4	-0,4	-0,4	-0,4	-0,3	-0,3	-0,3	-0,3
%	100,0	78,4	73,6	69,1	64,9	61,0	57,3	53,8	50,5	47,4	44,5	41,8	39,3	36,9	34,64	32,5	30,6	28,7	26,9	25,3	23,8	22,3	21,0	19,7	18,5	17,4	16,3	15,3	14,4	13,5	12,7	14,3	13,4	12,6	11,8

Table 5. Proposed limit state wave in open sea for Seabass

Table 5: Proposed limit wave state in open sea for Seabass: for a Mediterranean wave of Hs 7,0 m; T 9,0 sec; l 126,5 m; *without any shelter from Blue Growth Farm platform*. Depth of acceptable motion for 20 and 35 cm Seabass, dark green.

horizontal and vertical components of orbital wave velocities																																			
Hs significant heigth	6,5	6,5	6,5	6,5	6,5	6,5	6,5	6,5	6,5	6,5	6,5	6,5	6,5	6,5	6,50	6,5	6,5	6,5	6,5	6,5	6,5	6,5	6,5	6,5	6,5	6,5	6,5	6,5	6,5	6,5	6,5	6,5	6,5	6,5	6,5
Period T sec.	8,0	8,0	8,0	8,0	8,0	8,0	8,0	8,0	8,0	8,0	8,0	8,0	8,0	8,0	8,00	8,0	8,0	8,0	8,0	8,0	8,0	8,0	8,0	8,0	8,0	8,0	8,0	8,0	8,0	8,0	8,0	8,0	8,0	8,0	8,0
Lambda m	100,0	100,0	100,0	100,0	100,0	100,0	100,0	100,0	100,0	100,0	100,0	100,0	100,0	100,0	99,97	100,0	100,0	100,0	100,0	100,0	100,0	100,0	100,0	100,0	100,0	100,0	100,0	100,0	100,0	100,0	100,0	100,0	100,0	100,0	100,0
gravity g	9,8	9,8	9,8	9,8	9,8	9,8	9,8	9,8	9,8	9,8	9,8	9,8	9,8	9,8	9,81	9,8	9,8	9,8	9,8	9,8	9,8	9,8	9,8	9,8	9,8	9,8	9,8	9,8	9,8	9,8	9,8	9,8	9,8	9,8	9,8
wave at depth m	-1,0	-2,0	-3,0	-4,0	-5,0	-6,0	-7,0	-8,0	-9,0	-10,0	-11,0	-12,0	-13,0	-14,0	-15,00	-16,0	-17,0	-18,0	-19,0	-20,0	-21,0	-22,0	-23,0	-24,0	-25,0	-26,0	-27,0	-28,0	-29,0	-30,0	-31,0	-32,0	-33,0	-34,0	-35,0
site depth m	100,0	100,0	100,0	100,0	100,0	100,0	100,0	100,0	100,0	100,0	100,0	100,0	100,0	100,0	100,00	100,0	100,0	100,0	100,0	100,0	100,0	100,0	100,0	100,0	100,0	100,0	100,0	100,0	100,0	100,0	100,0	100,0	100,0	100,0	100,0
horizontal speed m/sec	2,4	2,3	2,1	2,0	1,9	1,8	1,6	1,5	1,4	1,4	1,3	1,2	1,1	1,1	0,99	0,934	0,88	0,8	0,8	0,7	0,7	0,6	0,6	0,6	0,5	0,5	0,5	0,4	0,4	0,4	0,4	0,3	0,3	0,3	0,3
%	100,0	78,4	73,6	69,1	64,9	61,0	57,3	53,8	50,5	47,4	44,5	41,8	39,3	36,9	34,65	32,5	30,6	28,7	26,9	25,3	23,8	22,3	21,0	19,7	18,5	17,4	16,3	15,3	14,4	13,5	12,7	14,3	13,4	12,6	11,8
vertical speed m/sec	-2,4	-2,3	-2,1	-2,0	-1,9	-1,8	-1,6	-1,5	-1,4	-1,4	-1,3	-1,2	-1,1	-1,1	-0,99	-0,9	-0,9	-0,8	-0,8	-0,7	-0,7	-0,6	-0,6	-0,6	-0,5	-0,5	-0,5	-0,4	-0,4	-0,4	-0,4	-0,3	-0,3	-0,3	-0,3
%	100,0	78,4	73,6	69,1	64,9	61,0	57,3	53,8	50,5	47,4	44,5	41,8	39,3	36,9	34,64	32,5	30,6	28,7	26,9	25,3	23,8	22,3	21,0	19,7	18,5	17,4	16,3	15,3	14,4	13,5	12,7	14,3	13,4	12,6	11,8

Table 6:Proposed values (cm.s-1) of sustainable environmental speeds (66% $U_{crit.}$) for Salmon for smolt (small and large) and adult at 14°C and 7°C, derived from data in Remen et al., 2016; and Hvas et al., 2017.

Size (cm)	10	20	30	50	60
Smolt small	47	53			
Smol large			59		
Adult				71	77

Table 7. Proposed limit state wave in open sea for Salmon

Table 7: Proposed limit wave state in open sea for Salmon: Atlantic wave of Hs 6,5m; T 10,9 sec; l 184,3 m ; *<u>without any shelter from Blue Growth Farm platform.</u>* Depth of acceptable motion for 30 and 50 cm Salmon, dark green.

horizontal and vertical components of orbital wave velocities																	
Hs significant heigth	6,5	6,5	6,5	6,5	6,5	6,5	6,5	6,5	6,5	6,5	6,5	6,5	6,5	6,5	6,50	6,5	6,5
Period T sec.	10,9	10,9	10,9	10,9	10,9	10,9	10,9	10,9	10,9	10,9	10,9	10,9	10,9	10,9	10,86	10,9	10,9
Lambda m	184,3	184,3	184,3	184,3	184,3	184,3	184,3	184,3	184,3	184,3	184,3	184,3	184,3	184,3	184,33	184,3	184,3
gravity g	9,8	9,8	9,8	9,8	9,8	9,8	9,8	9,8	9,8	9,8	9,8	9,8	9,8	9,8	9,81	9,8	9,8
wave at depth m	-1,0	-2,0	-3,0	-4,0	-5,0	-6,0	-7,0	-8,0	-9,0	-10,0	-11,0	-12,0	-13,0	-14,0	-15,00	-16,0	-17,0
site depth m	100,0	100,0	100,0	100,0	100,0	100,0	100,0	100,0	100,0	100,0	100,0	100,0	100,0	100,0	100,00	100,0	100,0
horizontal speed m/sec	1,8	1,8	1,7	1,6	1,6	1,5	1,5	1,4	1,4	1,3	1,3	1,3	1,2	1,2	1,13	1,092	1,06
%	100,0	96,7	93,4	90,3	87,3	84,4	81,6	78,8	76,2	73,7	71,2	68,8	66,5	64,3	62,18	60,1	58,1
vertical speed m/sec	-1,8	-1,8	-1,7	-1,6	-1,6	-1,5	-1,5	-1,4	-1,4	-1,3	-1,3	-1,2	-1,2	-1,2	-1,12	-1,1	-1,0
%	100,0	96,6	93,4	90,3	87,2	84,3	81,5	78,7	76,1	73,5	71,0	68,7	66,3	64,1	61,95	59,9	57,8

Hs significant heigth	6,5	6,5	6,5	6,5	6,5	6,5	6,5	6,5	6,5	6,5	6,5	6,5	6,5	6,5	6,5	6,5	6,5	6,5
Period T sec.	10,9	10,9	10,9	10,9	10,9	10,9	10,9	10,9	10,9	10,9	10,9	10,9	10,9	10,9	10,9	10,9	10,9	10,9
Lambda m	184,3	184,3	184,3	184,3	184,3	184,3	184,3	184,3	184,3	184,3	184,3	184,3	184,3	184,3	184,3	184,3	184,3	184,3
gravity g	9,8	9,8	9,8	9,8	9,8	9,8	9,8	9,8	9,8	9,8	9,8	9,8	9,8	9,8	9,8	9,8	9,8	9,8
wave at depth m	-18,0	-19,0	-20,0	-21,0	-22,0	-23,0	-24,0	-25,0	-26,0	-27,0	-28,0	-29,0	-30,0	-31,0	-32,0	-33,0	-34,0	-35,0
site depth m	100,0	100,0	100,0	100,0	100,0	100,0	100,0	100,0	100,0	100,0	100,0	100,0	100,0	100,0	100,0	100,0	100,0	100,0
horizontal speed m/sec	1,0	1,0	1,0	0,9	0,9	0,9	0,8	0,8	0,8	0,8	0,7	0,7	0,7	0,7	0,6	0,6	0,6	0,6
%	56,2	54,3	52,5	50,8	49,1	47,5	45,9	44,4	42,9	41,5	40,1	38,8	37,5	36,3	35,1	33,9	32,8	31,7
vertical speed m/sec	-1,0	-1,0	-0,9	-0,9	-0,9	-0,9	-0,8	-0,8	-0,8	-0,7	-0,7	-0,7	-0,7	-0,6	-0,6	-0,6	-0,6	-0,6
%	55,9	54,0	52,2	50,4	48,7	47,1	45,5	43,9	42,4	41,0	39,6	38,3	37,0	35,7	34,5	33,3	32,2	31,1

3 MEDITERRANEAN SEA

3.1 Farming species

The species selected for fish farming within the Blue Growth Platform facilities located within the Mediterranean Sea is the seabass Dicentrarchus labrax (Linnaeus, 1758). This species is one of the most farmed within Mediterranean waters, showing an annual gross production of 157.698 tonnes (FEAP, 2017) in 2016.

Seabass is farmed both in coastal and offshore waters at a weight of 5 to 10g, to attain a final weight of 350-400 g, at a length of 35 cm at the end of a 18-20 months growing period.

While Seabass is spread from the North Sea to the whole Mediterranean Sea to Cape Verde (FAO, 2018; Fishbase.org, 2018), its optimal temperature range lies between 12 and 24 °C, with suboptimal temperature from 10°C up to 28 °C

Its optimal growing range is here considered between the 12 °C and the 24°C, as experienced within most Seabass farms in Mediterranean.

Figure 6: Seabass areal distribution. (*www.iucnredlist.org*).

3.2 Pre-screening process

A list of excluding criteria to be considered when selecting a new potential site was given in Section 2.2.1.

With the aim of identifying the area of the Mediterranean sea where the best growing conditions are to be found, a series of large-scale maps showing the average daily sea temperature in surface at day 15 and 30 of each month from April 2014 to March 2018 were produced. The use of these maps, at a resolution of

0,25 x 025 degree, see paragraph 2.1., enables a very large area to be surveyed, for a consistent period of time, and offers the significant advantage, with respect to punctual temperature time series, of the comprehensive view of the evolution of temperature at a basin scale.

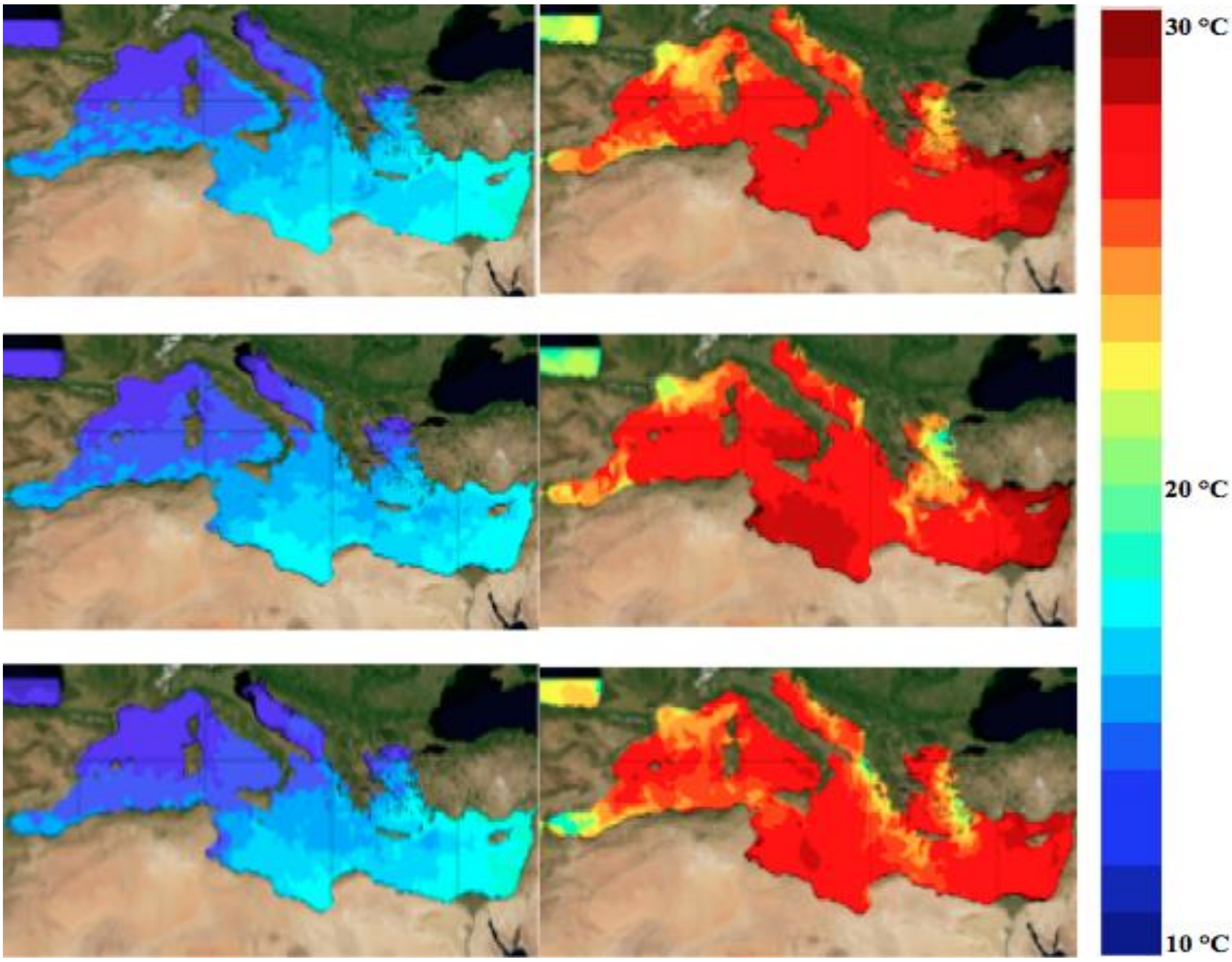

Figure 7: Maps of Mediterranean Sea water superficial temperature; displayed the three coldest months and the three warmest, year 2016-2017-2018. Colour scale: 10 – 30 °C. *(Source, Marine.copernicus.eu).*

Unfortunately, the time series available on the Copernicus Service server is spread over only three years, but is sufficient to exclude some areas from farming activities, based on the appearance of extreme values over a moderate time window. These maps are shown in Fig. 7.

From the maps, it appears that the optimal farming range is comprised between the 45° and the 34° of Latitude, with the possible exclusion for the North Adriatic Sea, which is not considered optimal to bream farming because of its winter peak of low temperatures, and Eastern Mediterranean due to its summer temperature approaching 30°C, not adapted to seabass farming.

Based on existing literature on wind/wave power, a preliminary list of sites, located within the above latitude range, and where energy resources are optimal, was selected.

This list included:

- Marseille
- Alghero

- Portoscuso
- Mazara del Vallo

The list of possible location was then analysed in detail in order to narrow the spatial range of a suitable site.

Each location was analysed in detail in a GIS environment, adding layers of marine traffic, bathymetry, protected areas, sediment/benthos, to support the preliminary exclusion of areas not adapted to platform installation.

3.3 Site 1 – Marseille

The Gulf of Marseille offers a large continental shelf, at a depth below the 200m threshold; some wind farms are installed and some are at still at project level; the deepest areas are assigned to O&G exploitation, and several closed boreholes are present.

The area has several large ports (Marseille, Toulon, Rone, Sete, etc.). Consequently the marine traffic is intense.

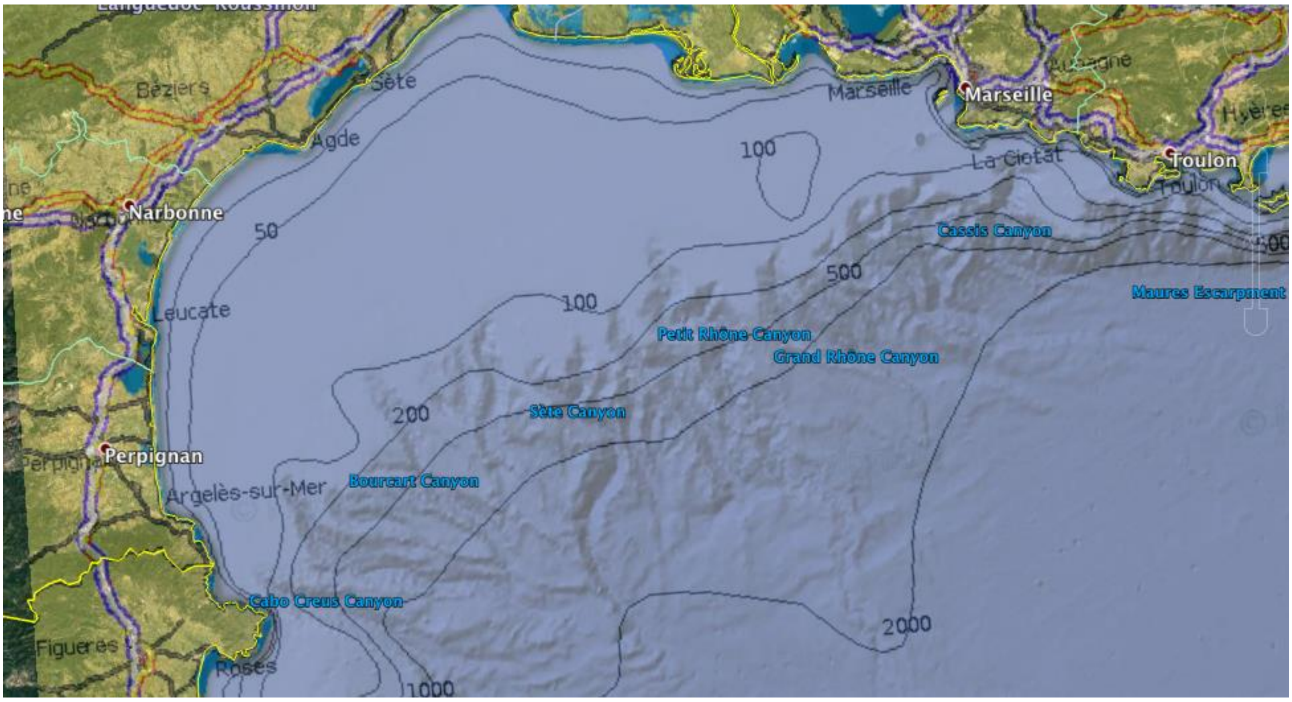

Figure 8: Bathymetry in the Gulf of Lion. ***(Source: Navionics.com)***

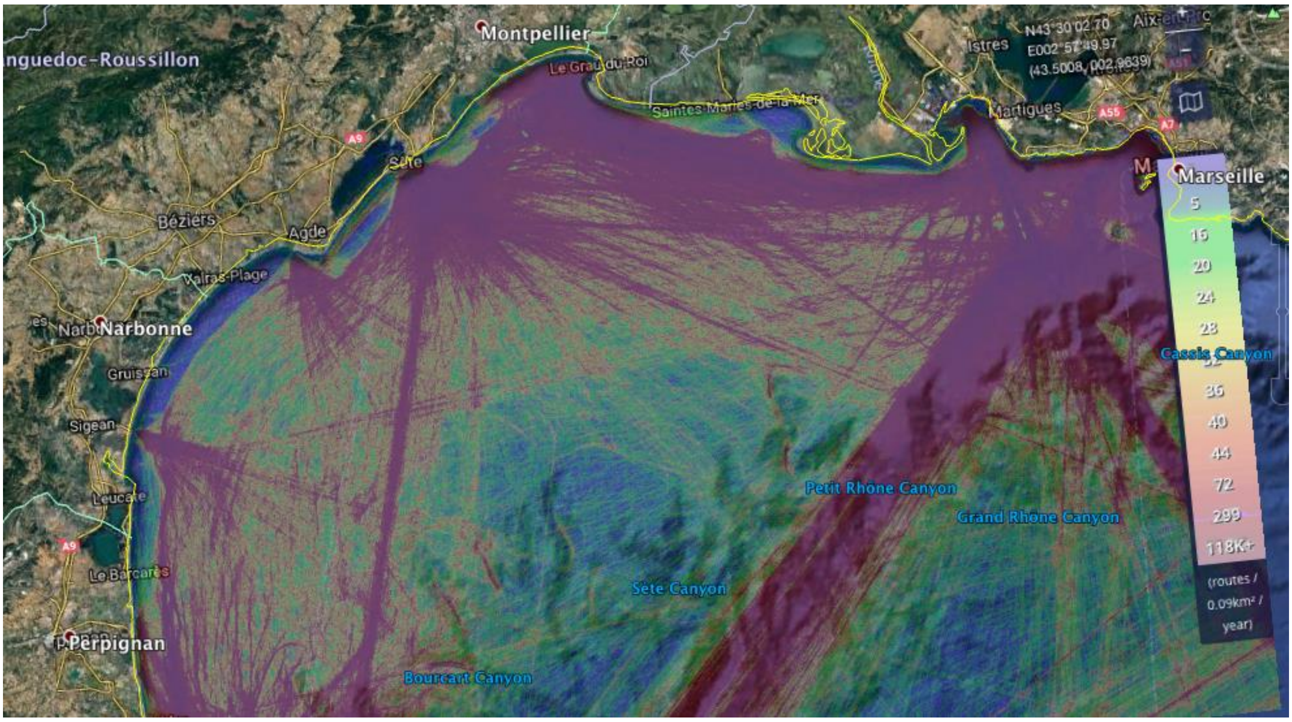

Figure 9: Marine traffic routes in the Gulf of Lion. (*Source, MarineTraffic.com*)

Nevertheless, there are some areas with minor traffic density are present, especially outside the shipping lanes to major ports. These are characterized by several protected areas. Both Natura 2000 sites and nationally designed areas are extending well beyond the coastline into the marine domain.

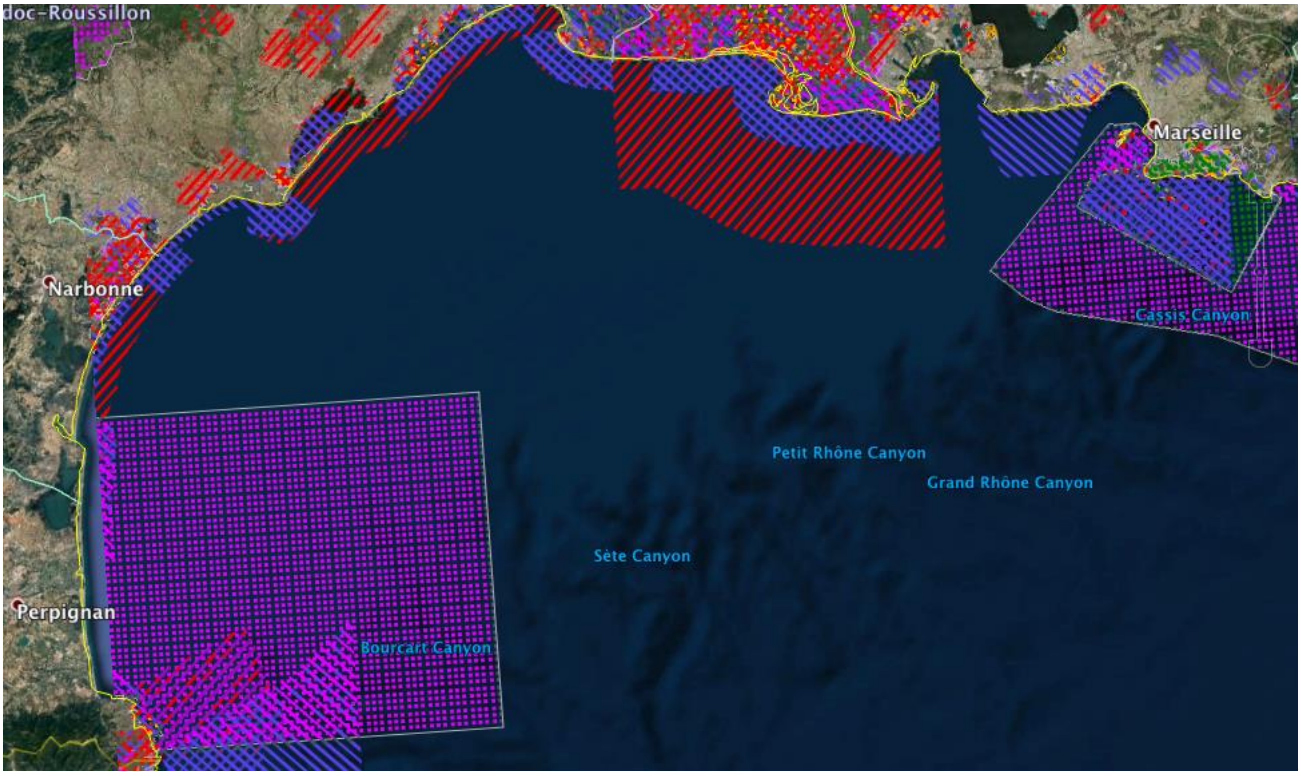

Figure 10: Protected areas in the Gulf of Lion. ***(Sources: EEA, Natura2000 Viewer.)***

A detailed map of benthos distribution is available (EMODnet website) for the Gulf of Marseille. Most of the gulf is characterized by soft bottom biocenosis; the deepest part is covered by Circalittoral and shelf ridge muds (EUNIS classification A5.37), the sign of a mobile seabed.

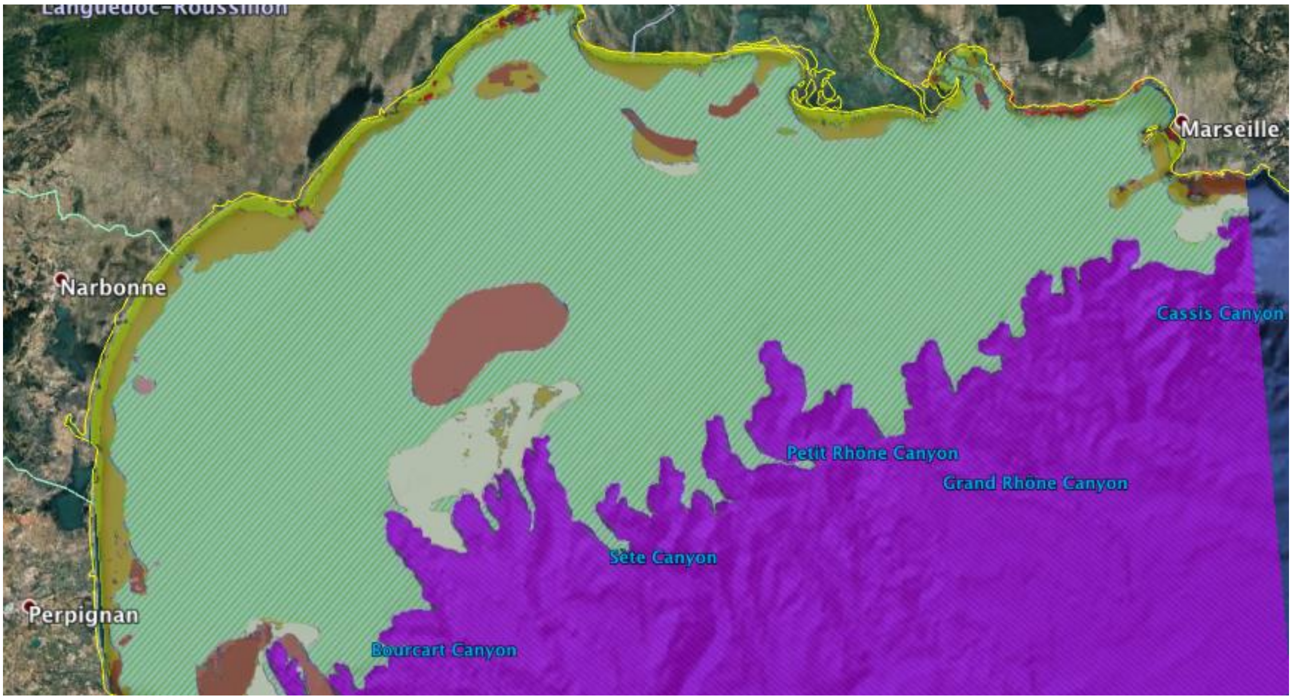

Figure 11: Benthos distribution in the Gulf of Lion. ***(Sources: EMODnet-seabedhabitat.eu)***

Based on all the above maps, a point within the Gulf has been selected, that fulfil all the basic conditionsof section 2.2.1. The selected location is shown in the last map, where protected areas, bathymetry, and marine traffic are condensed.

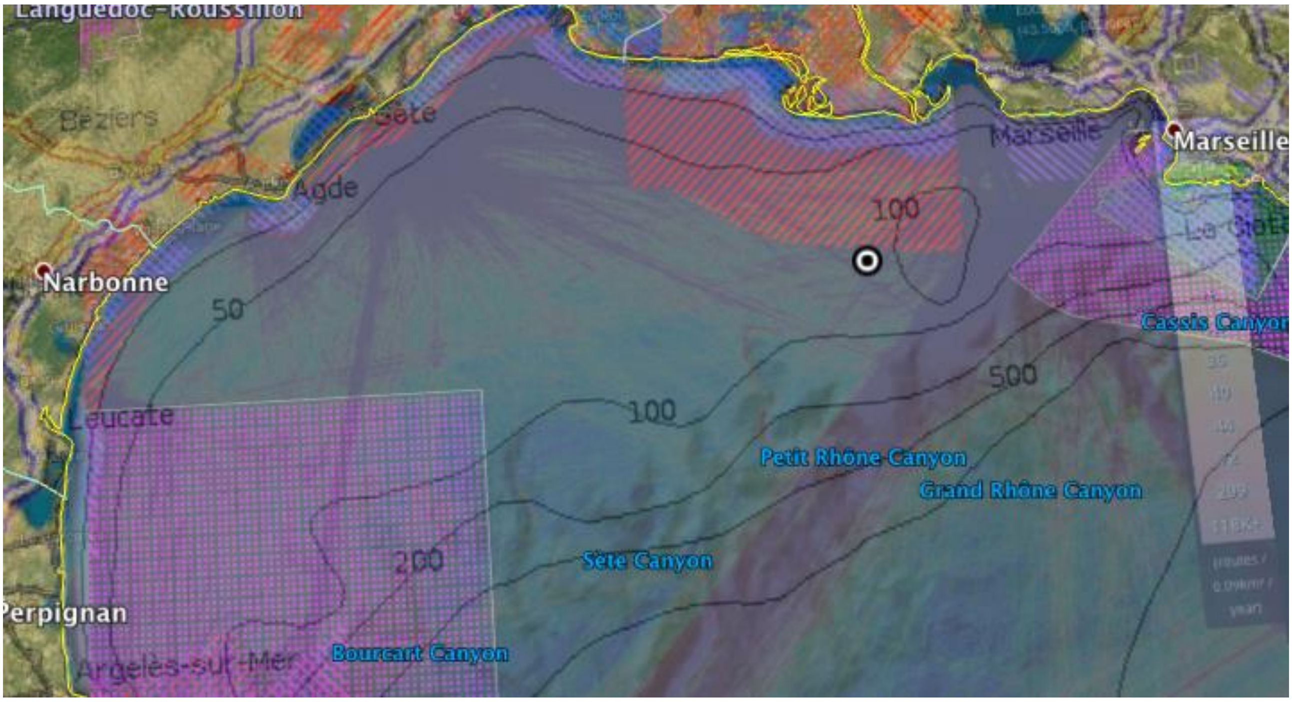

Figure 12: The selected site in the Gulf of Lion compared to the protected areas; naval and shipping routes traffic and bathymetry.

The selected site has the following characteristics, as shown in Table 8.

Table 8: Marseille site characteristics

SITE NAME: MARSEILLE	POSITION: λ 43,127718° φ 4,709296°
Port distance	13,7 nm
Land distance	13,2 nm
Depth	90 m
Seabottom	Mud
Protected areas distance	1,5 nm
Minimum temperature	13
Maximum temperature	24
Tide amplitude	30 cm
Annual wave power	4,5 kW/m
Annual wind power	1,2 kW/m^2
Maximum Hs 2016-2018	6,8 m

3.4 Site 2 – Alghero

The Bay of Alghero faces a large moderately deep continental shelf. The area is free of any industrial activity or exploitation at sea besides the traditional ones such as fisheries and aquaculture, since O&G exploitation is forbidden within Italian territorial waters within 12 miles from the coast and at the same distance from protected areas. Moreover, the Regional Authority of Sardinia has in the past forbidden the installation of any offshore wind farm within its waters. However, this resolution has since then been rejected by the Italian authorities, which claimed that the Central Government held the decision power over offshore waters.

Marine traffic in the area is rather limited, mainly costal and directed to the Ports of Alghero and Bosa. A shipping route to Genova runs at a fair distance from coast.

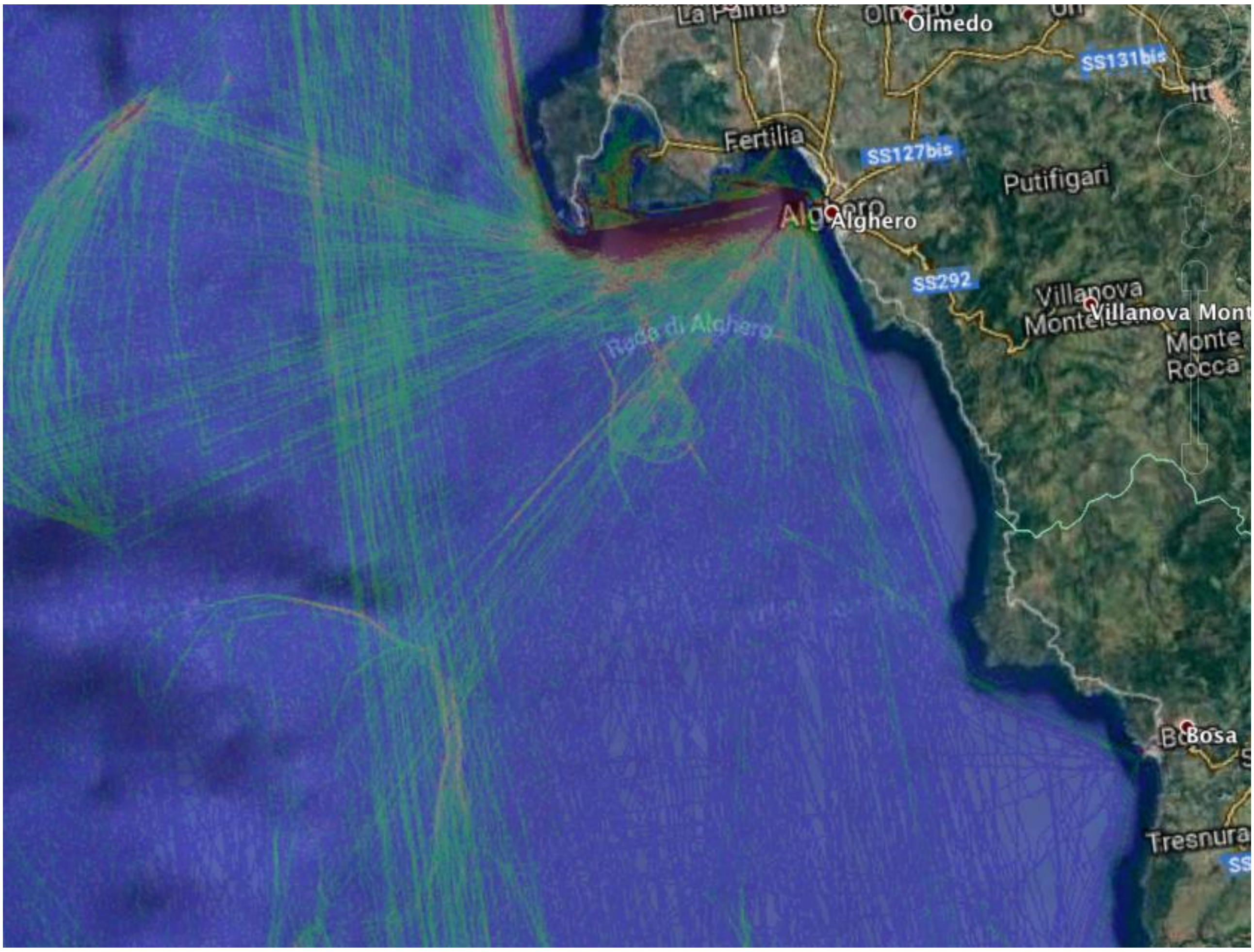

Figure 13: Naval and shipping routes traffic in the Bay of Alghero. (*Source: Marinetraffic.com*).

There is a marine protected area is present at Capo Caccia, close to the town of Alghero.

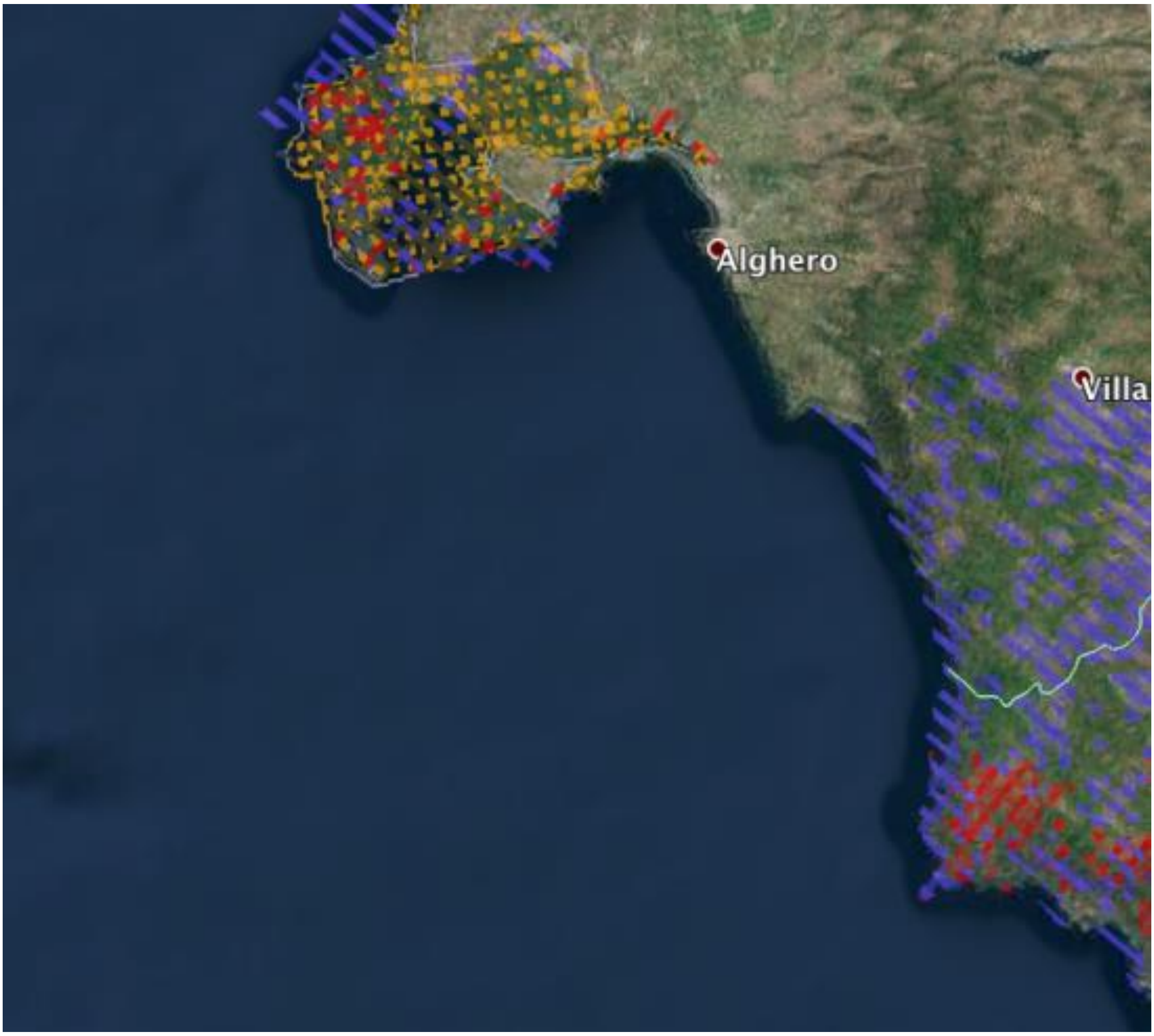

Figure 14: Protected areas near Alghero site. (*Source: EEA, Natura2000 Viewer).*

The seabed is characterized by the biocenosis of Detritic bottoms (EUNIS A 5.24) a soft-bottom community living on mixed sediments.

In accordance with the previous features, a suitable point fulfilling all the condition of section 2.2.1. has been identified.

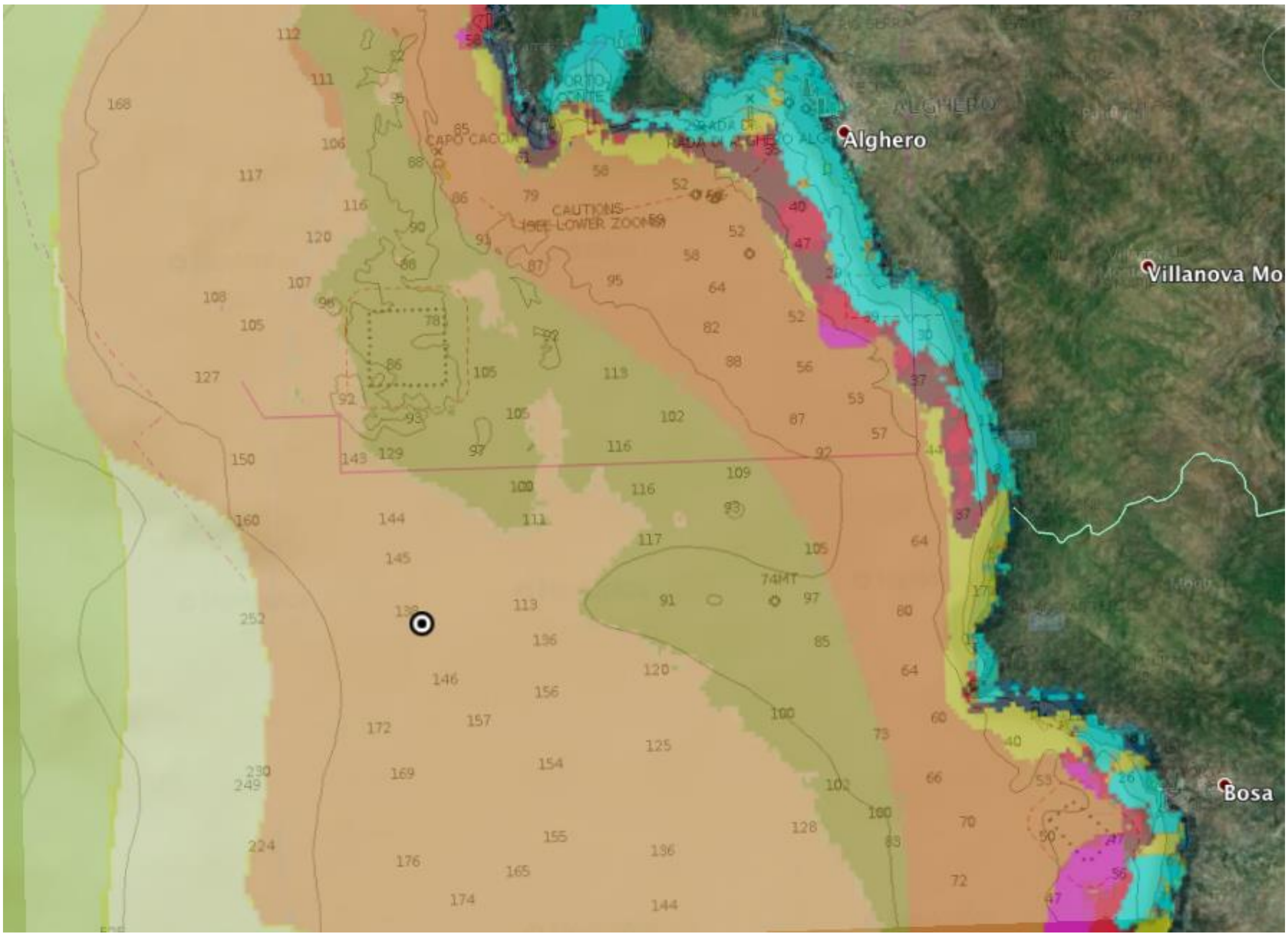

Figure 15: Biocenosis distribution near the Alghero site. *(Source: EMODnet-seabedhabitat.eu).*

The characteristics of the Alghero site are shown in Table 9.

Table 9: Alghero site characteristics

SITE NAME: ALGHERO	POSITION: λ 40,370004° φ 8,092971°
Port distance	15 nm
Land distance	13 nm
Depth	138 m
Seabottom	Detritic
Protected areas distance	11,7 nm
Minimum temperature	13,8
Maximum temperature	27
Tide amplitude	33 cm
Annual wave power	9,5 kW/m
Annual wind power	0,7 kW/m^2
Maximum Hs 2016-2018	7,9 m

3.5 Site 3 – Portoscuso

The area, located northern of the island of San Pietro, is characterized by a moderately deep and large continental shelf, and is completely exposed to wind and waves from N-NW. Two industrial ports are present (Portoscuso and Portovesme), working in the past as service ports for mines and for an alloy factory, the only industrial activity in the area.

Naval traffic is rather limited and local, while there are shipping lanes offshore at a fair distance from coast.

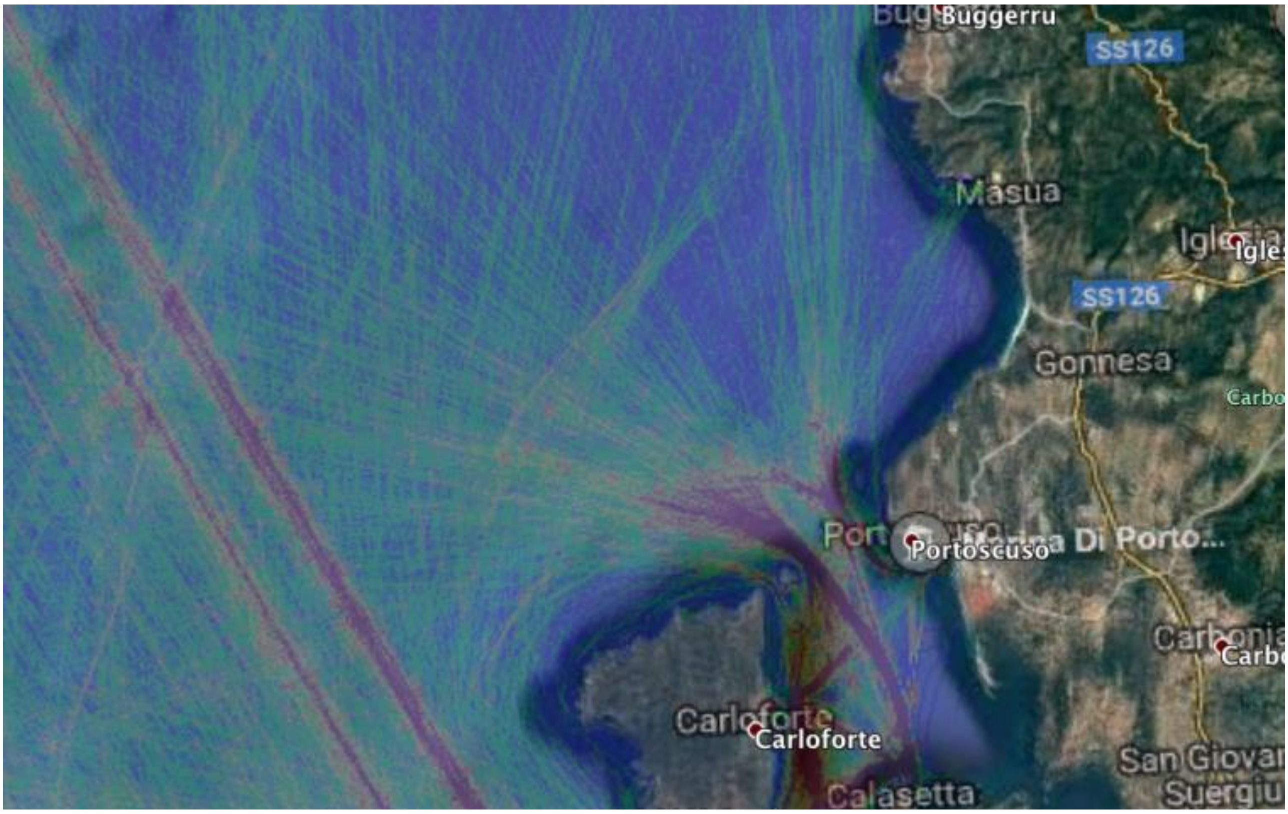

Figure 16: Naval and shipping traffic routes near the Portoscuso site. (Sources, *Marinetraffic.com*).

There is a network of protected areas (Natura 2000 sites) is present along the coast and a marine park surrounds the coast of the island San Pietro.

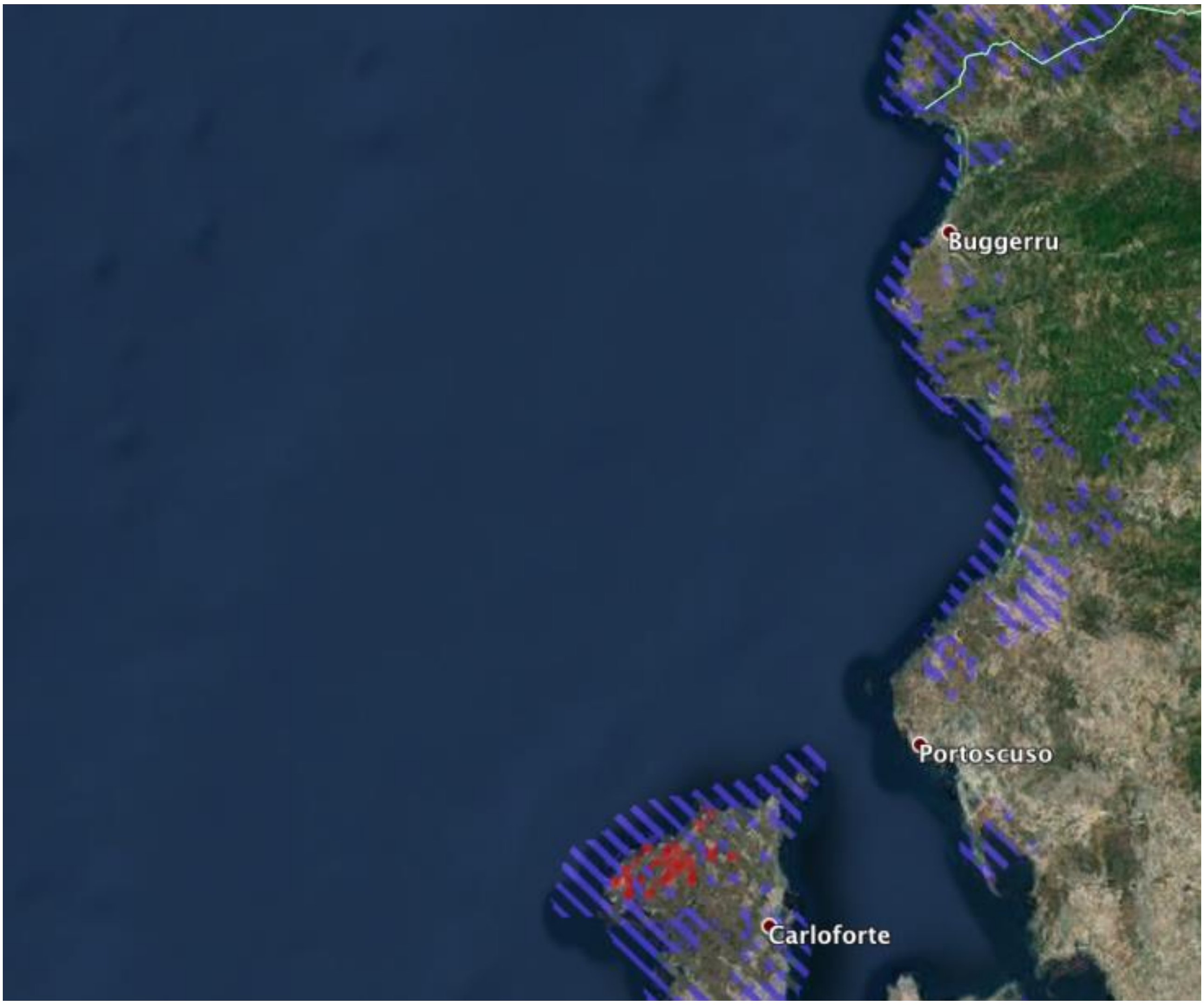

Figure 17: Protected areas near the Portoscuso site. (*Sources, EEA, Natura2000 Viewer).*

Since the area is free of any activity, a suitable installation point for the platform has been selected, and its position has then been superimposed over maps with depth and benthos features.

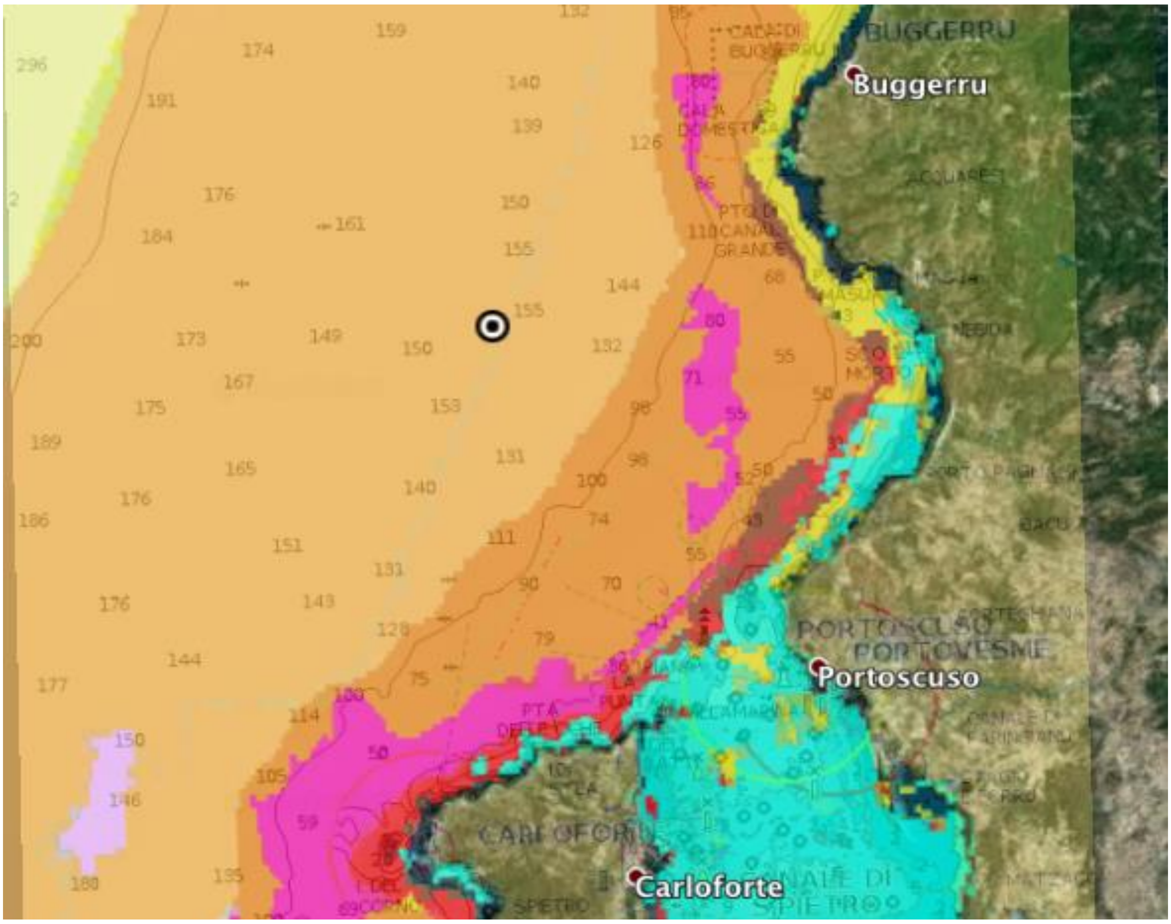

Figure 18: Biocenosis distribution near the Portoscuso site. (*Sources, EMODnet-seabedhabitat.eu; Navionics.com).*

The selected site has the following features:

Table 10: Portoscuso site characteristics.

SITE NAME: PORTOSCUSO	POSITION: λ 39,321745° φ 8,254050°
Port distance	9,9 nm
Land distance	6,3 nm
Depth	155 m
Sea bottom	Detritic
Protected areas distance	6 nm
Minimum temperature	13,8
Maximum temperature	26,5
Tide amplitude	32 cm
Annual wave power	10,2 kW/m
Annual wind power	0,75 kW/m^2
Maximum Hs 2016-2018	7,2 m

3.6 Site 4 – Mazara del Vallo

The fishing port of Mazara del Vallo is located in an area of intense marine traffic, where several other uses of the sea coexists, such as pipelines, power and transmission cables. The area has also been opened in the past to O&G exploitation, and several wind farms have been requested within its offshore area.

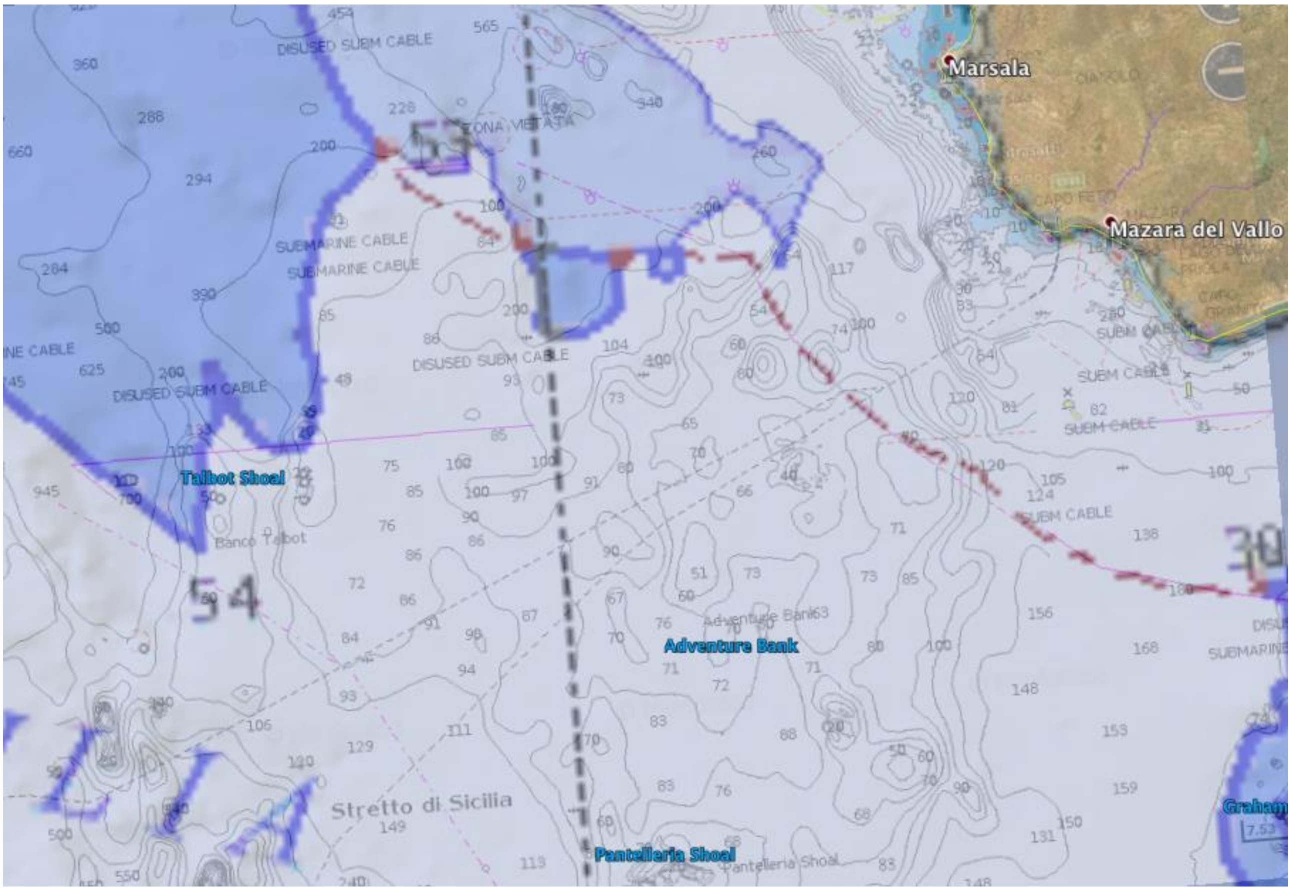

Figure 19: Bathymetry, co-existing infrastructures and O&G exploratory blocks in the area of Mazara del Vallo site. ***(Source: Navionics.com; unmig.sviluppoeconomico.gov.it).***

A protected area is located around the Favignana Island, and the Sicilian Channel hosts one of the most intense marine traffic routes within the Mediterranean Sea.

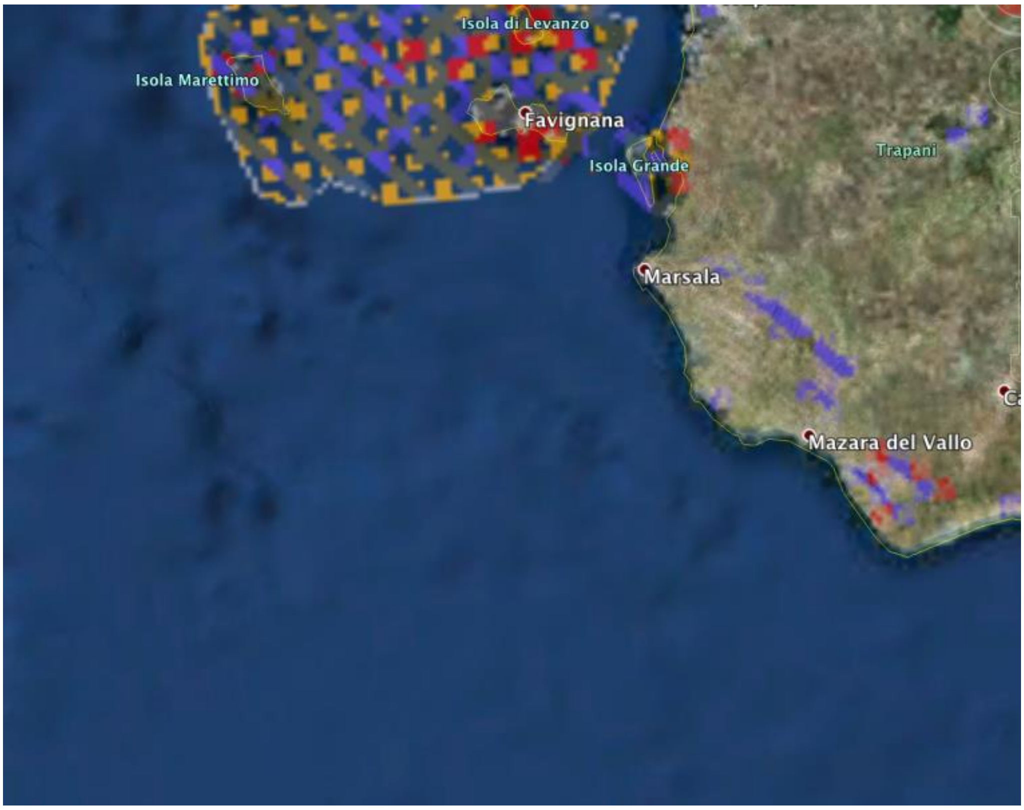

Figure 20: The protected area near the Mazara del Vallo site. *(Source: EEA, Natura2000 Viewer).*

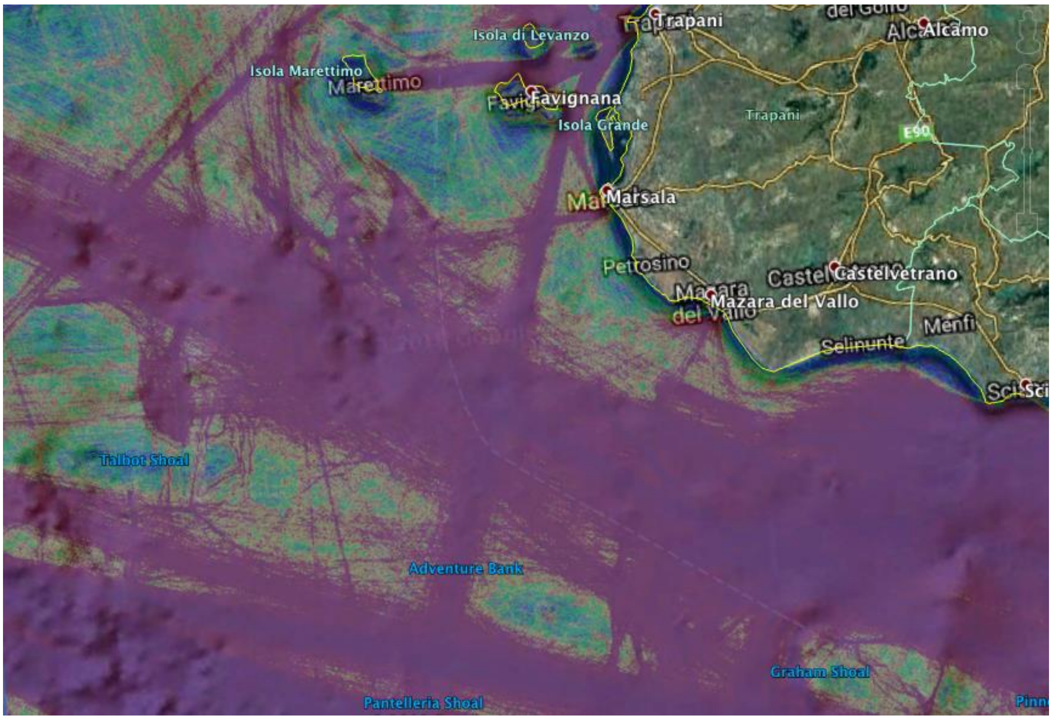

Figure 21: Naval and shipping routes traffic in the Mazara del Vallo area. *(Source, Marinetraffic.com).*

Based on previous maps, a suitable site has been identified, as shown in Figure 22. The point lies over a soft bottom biocenosis, belonging to the Mediterranean communities of muddy detritic bottoms (EUNIS A5.38).

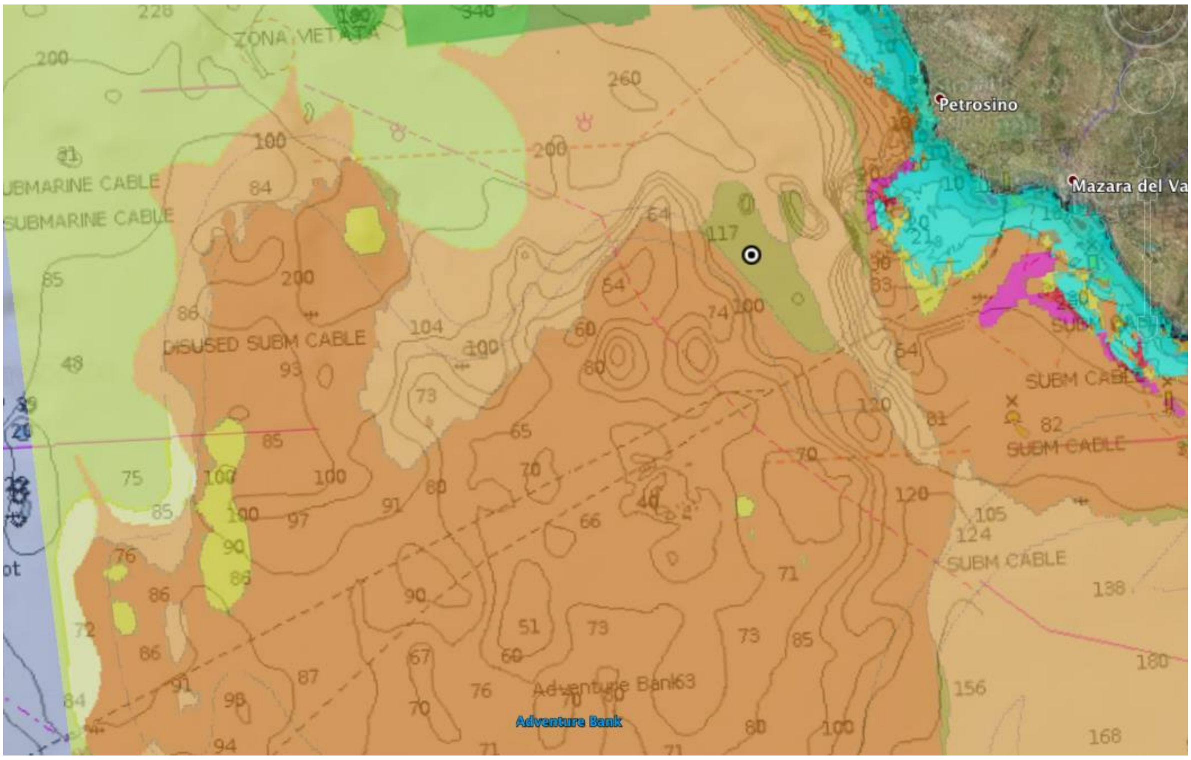

Figure 22: Benthic biocenosis distribution in the Mazara del Vallo site area. ***(Source, EMODnet-seabedhabitat.eu, Navionics.com).***

Table 11 summarize the data available for this site.

Table 11: Mazara del Vallo site characteristics

SITE NAME: MAZARA DEL VALLO	POSITION: λ 37,620106° φ 12,332056°
Port distance	12,2 nm
Land distance	8,2 nm
Depth	110 m
Seabottom	Detritic mud
Protected areas distance	15,3 nm
Minimum temperature	14,5
Maximum temperature	27
Tide amplitude	20 cm
Annual wave power	5,6 kW/m
Annual wind power	0,78 kW/m^2
Maximum Hs 2016-2018	5 m

3.7 Site selection matrix

Using values derived from the literature and web portals on selected sites, a decision matrix based on the TOPSIS methods (see section 2.2.1.) has been calculated. For the final site decision, a different rank value has been assigned to the criteria of the significant wave Hs, giving the lowest value to extreme environmental energy, thereby taking into greatest account the fish resistance to water motion.

Table 12: Criteria Vs. Sites matrix of Mediterranean sites

	Attributes/ Criteria	Port distance	Land distance	Depth	Soft seabottom	Protected areas distance	Minimal temp 12-15°	Maximum temperature 24-28°	Tide amplitude	Annual wave power	Annual wind power	Max recorded Hs
Solutions/Options												
m =												
1	Marseille	14	13	90	5	1,5	13	23	30	4,5	12	6,8
2	Alghero	15	13	138	4	11,7	13,8	27	33	9,49	9,5	7,9
3	Portoscuso	10	6	155	4	6	13,8	26,5	32	10,2	7,5	7,2
4	Mazara	12	8	110	2	15,3	14,5	27	20	5,6	7,8	5
5												

Table 13: TOPSIS selection matrix – All criteria are ranked 1, but Hs ranked (-3) to give weight to sites with lower extreme waves.

Attributes / Criteria		Port distance	Land distance	Depth	Soft seabottom	Protected areas distance	Minimal temp 12-15°	Maximum temperature 24-28°	Tide amplitude	Annual wave power	Annual wind power	Maximum recorded Hs	SUM	Closeness to the ideal POSITIVE solution
WEIGHTS		1	1	1	1	1	1	1	1	1	1	-3		
Ideal Positive Solutions	A+	0,58	0,00	0,00	0,64	0,00	0,00	0,52	0,00	0,00	0,00	0,00		
Ideal Negative Solutions	A-	0,00	0,62	0,62	0,00	0,76	0,53	0,00	0,56	0,65	0,64	-1,72		
Solutions/Options														
Distances from the ideal POSITIVE solution														
Marseille	8	0,003	0,387	0,128	0,000	0,005	0,222	0,006	0,264	0,082	0,410	2,182	0,863	56%
Alghero	10	0,000	0,375	0,301	0,016	0,335	0,251	0,000	0,319	0,367	0,257	2,945	1,130	41%
Portoscuso	9	0,039	0,088	0,380	0,016	0,088	0,251	0,000	0,300	0,423	0,160	2,446	0,929	48%
Mazara	11	0,012	0,149	0,191	0,148	0,572	0,277	0,000	0,117	0,128	0,173	1,427	1,161	35%

The best closeness to the ideal positive solution has been recorded at the Marseille site,. This will therefore be considered as the best site solution within the Mediterranean Sea for the Blue Growth Farm operation, at least at the current design level.

3.8 Platform motion sheltering capability

The following tables show the maximum allowable sea state for farmed Mediterranean species, considering the internal platform basin as a confined volume where the wave motion is transmitted from the adjacent sea waves to the pool. *This approach should be regarded as a first degree approximation, because within the design development, the full assessment of water pool motion is expected; at the present stage, this approximation may be useful indicate the likely range of platform utilization, with regard to fish resistance to motion and engineering features.*

A wave of Hs = 3,0 m and T = 7,4 sec., as derived from a JONSWAP spectrum, that is oscillating within the platform internal basin, lead to a water motion at a horizontal speed within the range of $\boldsymbol{U_{crit}}$ for seabass and seabream, and for a depth range of several metres, even within the Welfare $\boldsymbol{U_{crit}}$. This wave motion state enables for a safe basin depth exploitation by Mediterranean species. Data are summarized in Table 14.

Table 14. Summary of welfare water velocities (cm.s^{-1}) for Mediterranean farmed species, seabass.

	Welfare $\boldsymbol{U_{crit}}$
Seabass 20 cm	58
Seabass 35 cm	83

Table 15: Horizontal speed within a depth of 12m, for a wave of Hs = 3,0 m, T = 7,4 sec.

horizontal and vertical components of orbital wave velocities												
Hs significant heigth	3,0	3,0	3,0	3,0	3,0	3,0	3,0	3,0	3,0	3,0	3,0	3,0
Period T sec.	7,4	7,4	7,4	7,4	7,4	7,4	7,4	7,4	7,4	7,4	7,4	7,4
Lambda m	85,1	85,1	85,1	85,1	85,1	85,1	85,1	85,1	85,1	85,1	85,1	85,1
gravity g	9,8	9,8	9,8	9,8	9,8	9,8	9,8	9,8	9,8	9,8	9,8	9,8
wave at depth m	-1,0	-2,0	-3,0	-4,0	-5,0	-6,0	-7,0	-8,0	-9,0	-10,0	-11,0	-12,0
site depth m	100,0	100,0	100,0	100,0	100,0	100,0	100,0	100,0	100,0	100,0	100,0	100,0
horizontal speed m/sec	1,2	1,1	1,0	1,0	0,9	0,8	0,8	0,7	0,7	0,6	0,6	0,5
%	100,0	92,9	86,3	80,1	74,4	69,1	64,2	59,6	55,4	51,5	47,8	44,4
vertical speed m/sec	-1,2	-1,1	-1,0	-1,0	-0,9	-0,8	-0,8	-0,7	-0,7	-0,6	-0,6	-0,5
%	100,0	92,9	86,3	80,1	74,4	69,1	64,2	59,6	55,4	51,5	47,8	44,4

Increasing Hs and T, the horizontal velocity within the pool increases beyond $\boldsymbol{U_{crit}}$ **,** and the extent of the safe zone decreases to negligible values, therefore becoming unsuitable for fish farming.

The above wave parameters have been used to calculate a wave power (in kW/m) associated to this wave condition within the pool, using the formula

$W_p = 0{,}55\,(H_s)^2\,T_z$, (Twiddel and Weir, 2006; kW/m)

Where Hs= Significant wave; m

T_z = zero crossing period, sec.

Here we consider the $T_z \equiv T_p$,

where T_p is calculated as:

$T_p = 8{,}5\pi(H_s/4g)^{0{,}5}$ (Boccotti, 2004)

The result is:

$0{,}55*(3{,}0)^2*7{,}4 = 37{,}0$ kW/m

Under the hypothesis that the WEC system would lead to a conversion of a significant percentage of wave incident power, the maximum allowable sea states in the surrounding marine waters that provide an acceptable fish welfare inside the platform basin, under different wave power absorption, are:

- for a storm of Hs 6,5 m, T= 10,86 sec, leading to a WP of 252 kW/m, the wave power absorption hasto be close to 80 %, in order to provide a safe fish shelter;
- for a storm of Hs 8,5 m, T= 12,4 sec, leading to a WP of 493 kW/m, the wave power absorption has to be close to 90 %, in order to provide a safe fish shelter;

The maximum recorded sea state for the selected site, Marseille, within the time series (2016-2018) available on Copernicus website as hourly means, is relative to a storm occurred the 1st march 2018, with a Hs = 6,8 m, at a Period = 9,7 sec, although with a duration of some hours.

This storm gave raise to a WP of 242 kW/m; these wave horizontal speeds can be susteined by the selected aquaculture species, seabass, diving to a depth between 22 to 35 m within the cage net, or, within the 12 m shelter wall of the platform, in case this is able to provide a wave power shelter of 85 % of the external incident wave power.

The second ranked site, Alghero, has experienced a maximum recorded storm of Hs = 7,9 m, at a T = 9.5 sec. Within this condition, the platform has to provide an incidence wave power reduction of 88 % in order to offer a safe shelter to fish within the platform pool.

4 NORTH ATLANTIC

4.1 Farming species

The species selected for fish farming within the Blue Growth platform facilities located within the North Atlantic Sea is the Atlantic Salmon *Salmo salar (*Linnaeus, 1758). This species is one of the most farmed in temperate waters around the world, with an annual gross production of 1.488.434 tons in year 2016 (FEAP, 2017).

Atlantic Salmon has a singular life cycle, consisting of fresh water egg to juvenile “parr” stage at the end of which the fish undergoes a metabolic adaptation to the seawater environment; is then termed a “smolt”at which point in nature migrates to sea. In farming practice, smolts can be transferred to sea cages, where they enter the growing phase experiencing fully marine conditions. Atlantic salmon are usually grown to sizes of 0,5 – 0,8 m, for a weight up to 5 kg.

While Atlantic salmon is spread from nearly arctic waters down to Britain on the European coast (FAO, 2018; Fishbase.org, 2018), its temperature range lies between 8 and 18 °C, with suboptimal temperature from 4 °C up to 20 °C, tolerable for short periods.

Its optimal growing range is here considered between the 6 °C and the 18°C, as experienced within most salmon farms in Scotland.

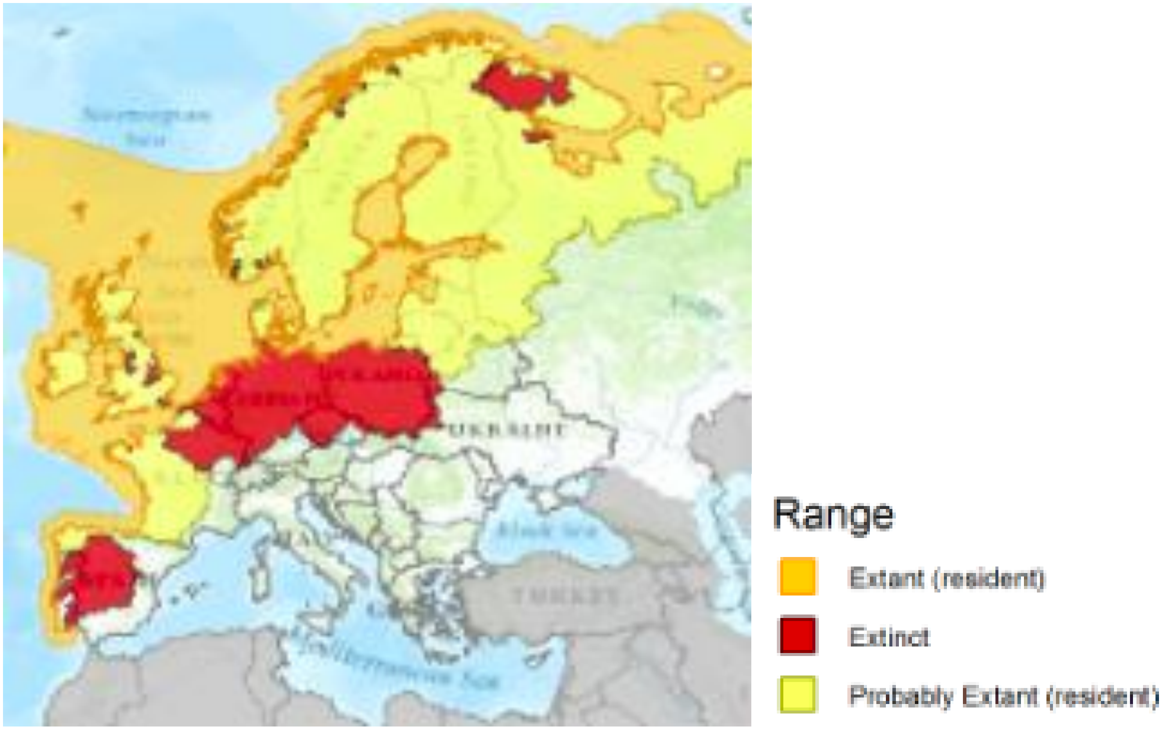

Figure 23: Atlantic salmon areal distribution *(Source: IUCN, 2015)*

4.2 Pre-screening process

With the aim of identifying the area of North Sea where the best salmon growing conditions are to be found, a series of large-scale maps, showing the average surface daily sea temperature at day 15 and 30 of each month from April 2014 to March 2018, have been produced. The use of these maps, at a resolution of 0,25 x 025 degree (see section 2.1), enables the surveying of a very large area, for a consistent period of time, and offers the significant advantage, with regard to punctual temperature time series, of the comprehensive view of evolution of temperature on a basin scale. Unfortunately the time series available on the Copernicus Service server covers only a four years period, but is sufficient to exclude some areas from farming activities based on the appearance of extreme values over a moderate time window.

These maps are shown in Fig. 24, colour scale from 6 to 20 °C.

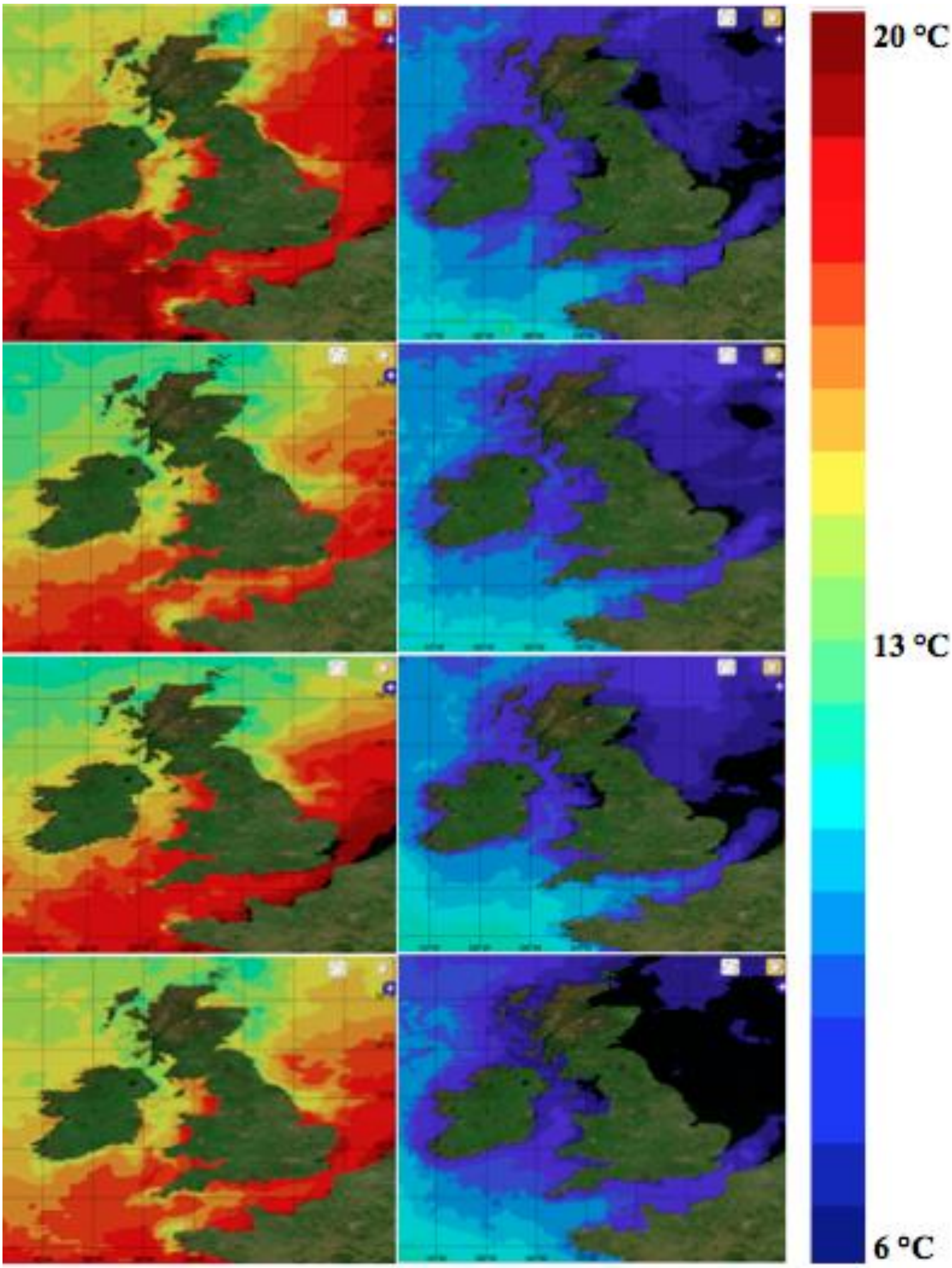

Figure 24: Maps of extreme temperatures values in years 2016-2018. (*Source, marine.copernicus.eu).*

Visual examination of the maps indicates that the optimal farming range is between 52° and 60° of Latitude. While the southern coast of England experiences some high temperature peaks, the North Sea and the Norwegian coast are generally colder than the English coast and in particular the west coast. During summer, the Welsh waters temperature approaches 20 °C, a limit for optimal salmon farming.

In section 2.2.1., a list of excluding criteria to be considered when selecting a new potential site, has been given.
Based on existing literature on wind/wave power, a preliminary list of sites, laying within the above latitude range, and where energy resources are optimal was selected.
This list includes:

- Aberdeen area
- The Irish Sea
- The North Channel

This list of possible location was subsequently analysed in detail in order to narrow the spatial range of a suitable site.

Each location was analysed in detail in a GIS environment, adding layers of marine traffic, bathymetry, protected areas, sediment/benthos, to support the preliminary exclusion of areas not suitable for platform installation.

4.3 Site 1- Aberdeen

The shelf facing Aberdeen is extremely large, at shallow depth, and is also characterized by the presence of various human activities. Marine traffic is intense, but shipping lanes are easily recognizable and some areas remains have very low shipping density.

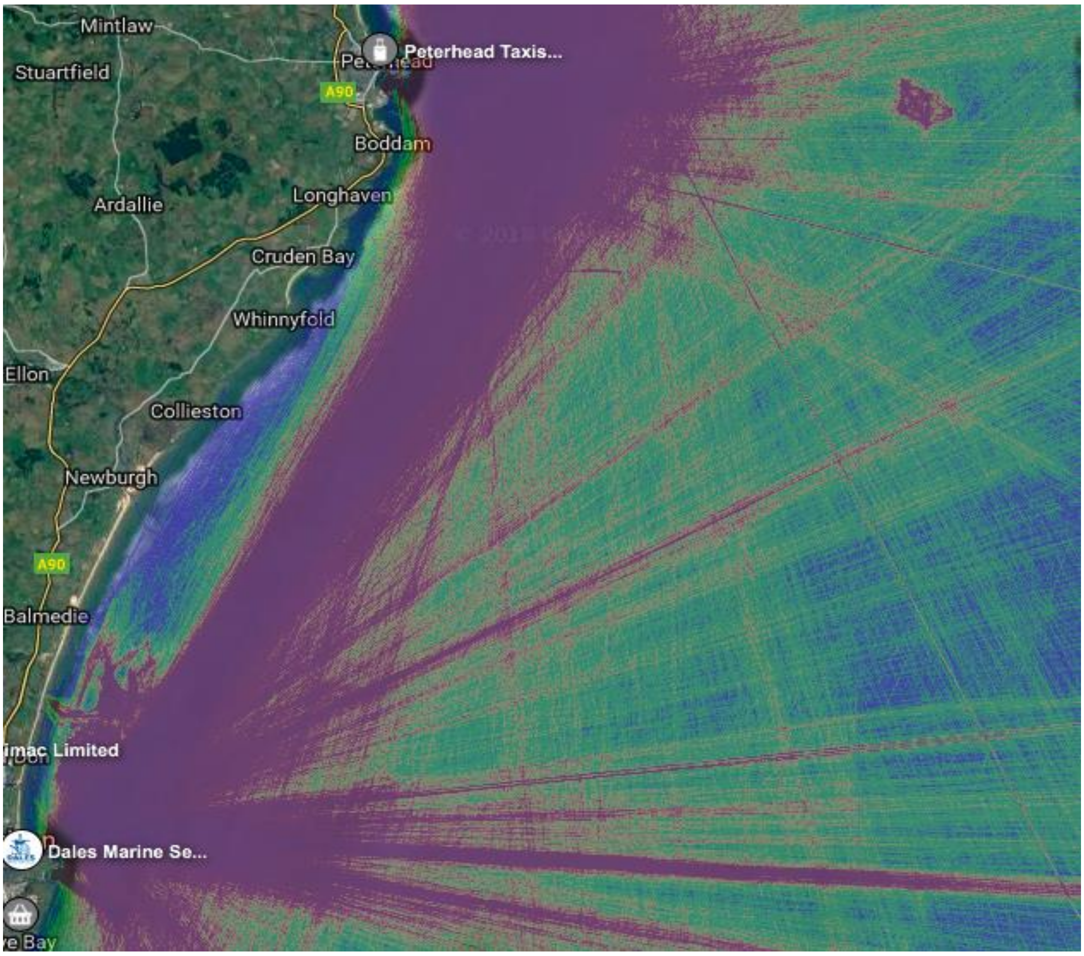

Figure 25: Naval and shipping routes traffic near the Aberdeen shelf. (Source: Marinetraffic.com)

Protected areas are limited to a shallow area, protected under the Birds Directive that covers a coastal area northern of Aberdeen.

Figure 26: Protected areas near the Aberdeen site. *(Source, EEA, Natura2000 Viewer).*

Close to the port of Aberdeen, a depth of 70 m is reached outside the territorial waters, over a seabed that belongs to the deep circa-littoral coarse sediments, and is classified as EUNIS A5.15.

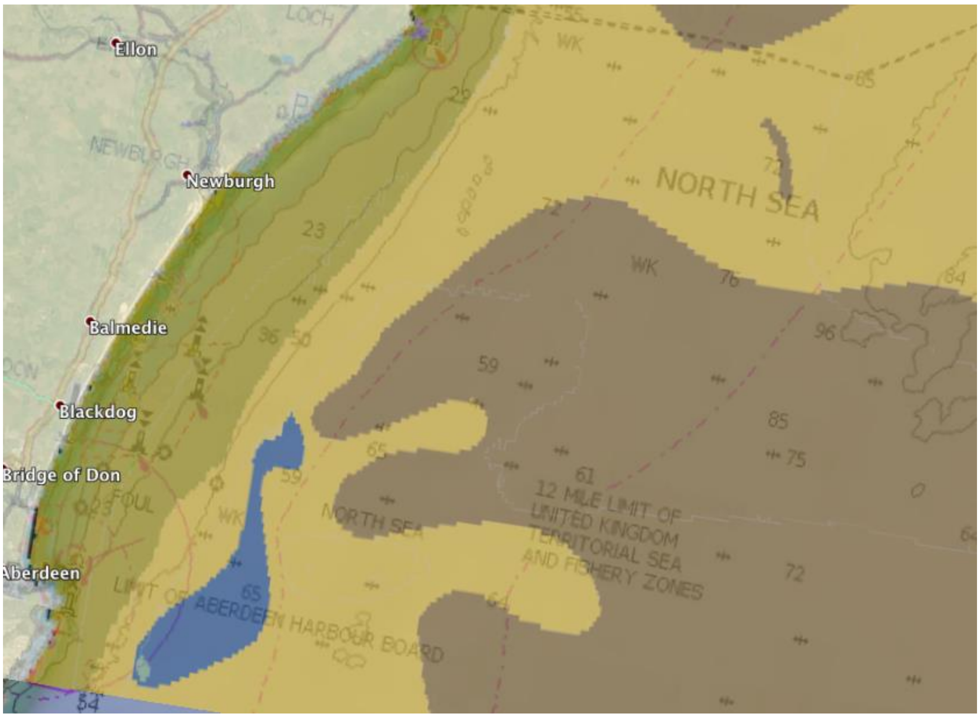

Figure 27: Benthic biocenosis distribution near the Aberdeen site. (Source: *EMODnet-seabedhabitat.eu*).

Based on previous elements, a suitable installation point for the Blue Growth Platform has been identified. It lies over a 70 m- deep sedimentary coarse seabed, at a distance of 15 nm from the port of Aberdeen. The point is included within an area already identified by the national authority as dedicated to wind farm operation.

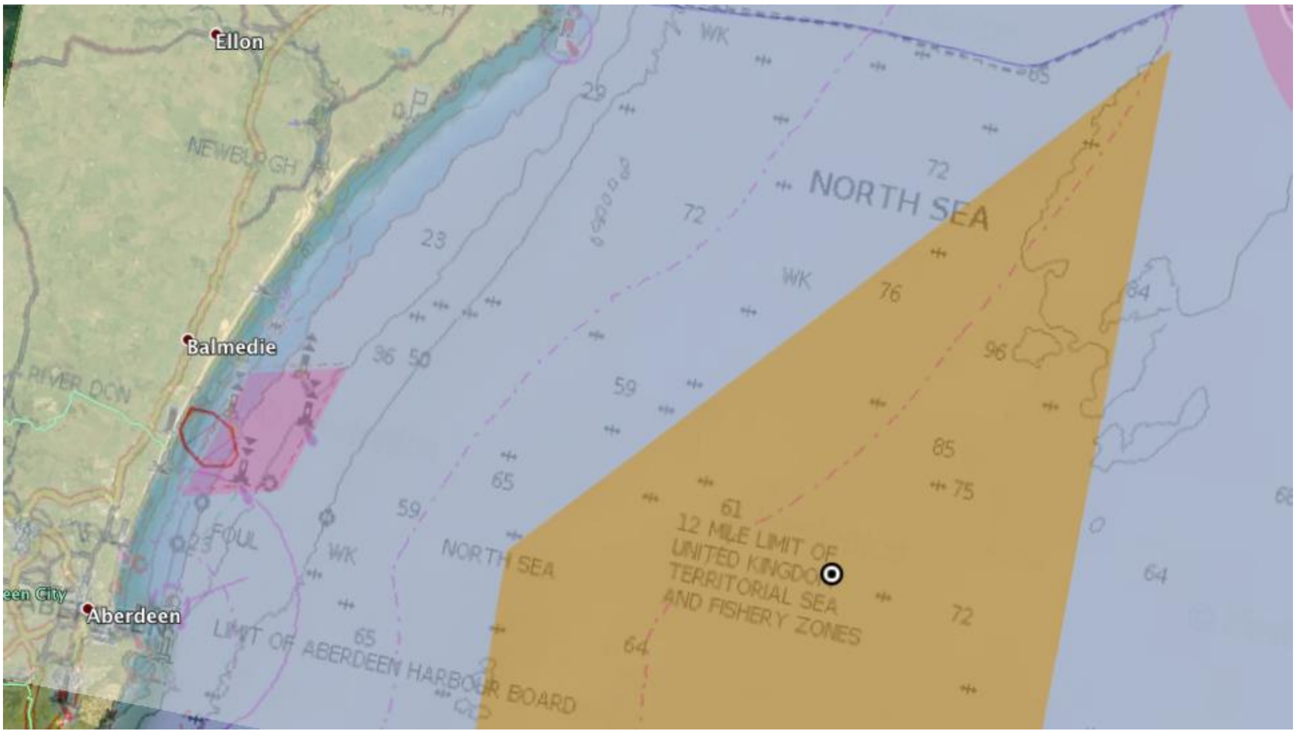

Figure 28: Aberdeen site compared to the authorized area for wind farms operation. *(Source: marinescotland.atkinsgeospatial.com).*

The selected site has the following features:

Table 16: Aberdeen site characteristics

SITE NAME: ABERDEEN	POSITION: λ 57,206937° φ -1,602185°
Port distance	15,0 nm
Land distance	13,8 nm
Depth	70 m
Seabottom	Detritic
Protected areas distance	13 nm
Minimum temperature	5,2
Maximum temperature	16,3
Tide amplitude	3,0 m
Annual wave power	12,5 kW/m
Annual wind power	1,2 kW/m^2
Maximum Hs 2016-2018	7,2 m

4.4 Site 2 – Greenore

The port of Greenore, in the Irish Sea, faces a large sound with a huge shelf of low to moderate depth. The port has a large quay, currently used for containers, which may be diverted to other uses. Commercial traffic is limited, with a shipping lane directed to the port and a shipping lane passing way offshore from the coast.

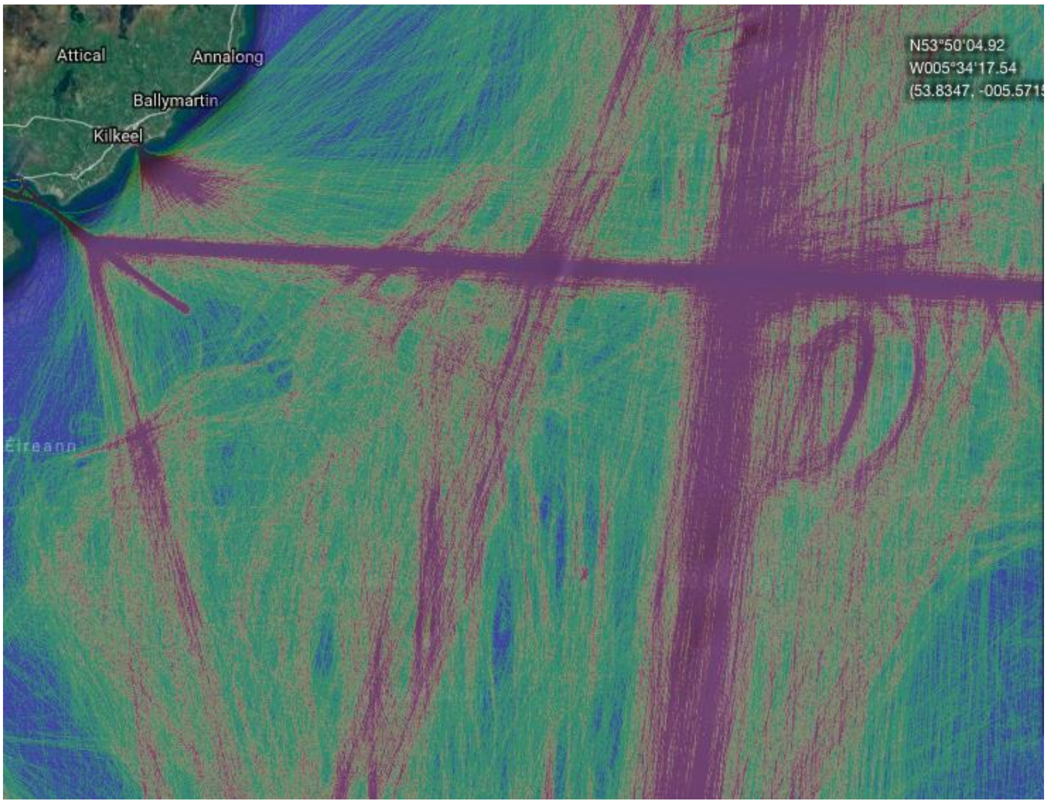

Figure 29: Naval and shipping routes traffic near the Greenore site. (*Source:* Marinetraffic.com*).*

The marine area has several protected zones along the coast and offshore, the first close to the town of Newcastle, a second located some miles offshore. There is a nationally protected area is located beside the Carlingford port area.

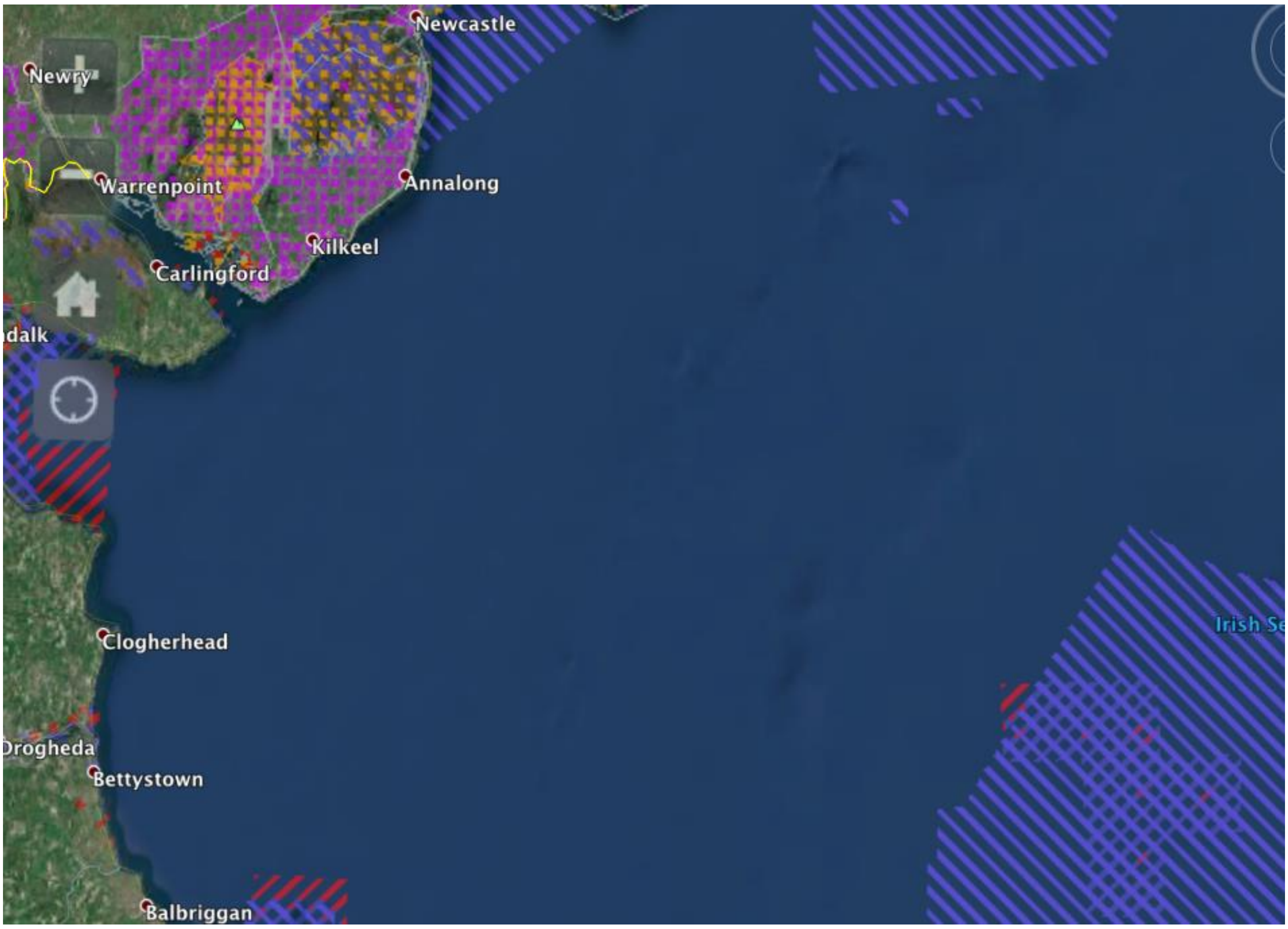

Figure 30: Protected areas near th Greenore site. (*Source: EEA, Natura2000 Viewer).*

The results from previous maps have been matched with a bathymetric map and a biocenosis map. This enables the identification of a possible installation site, as shown in the following map.

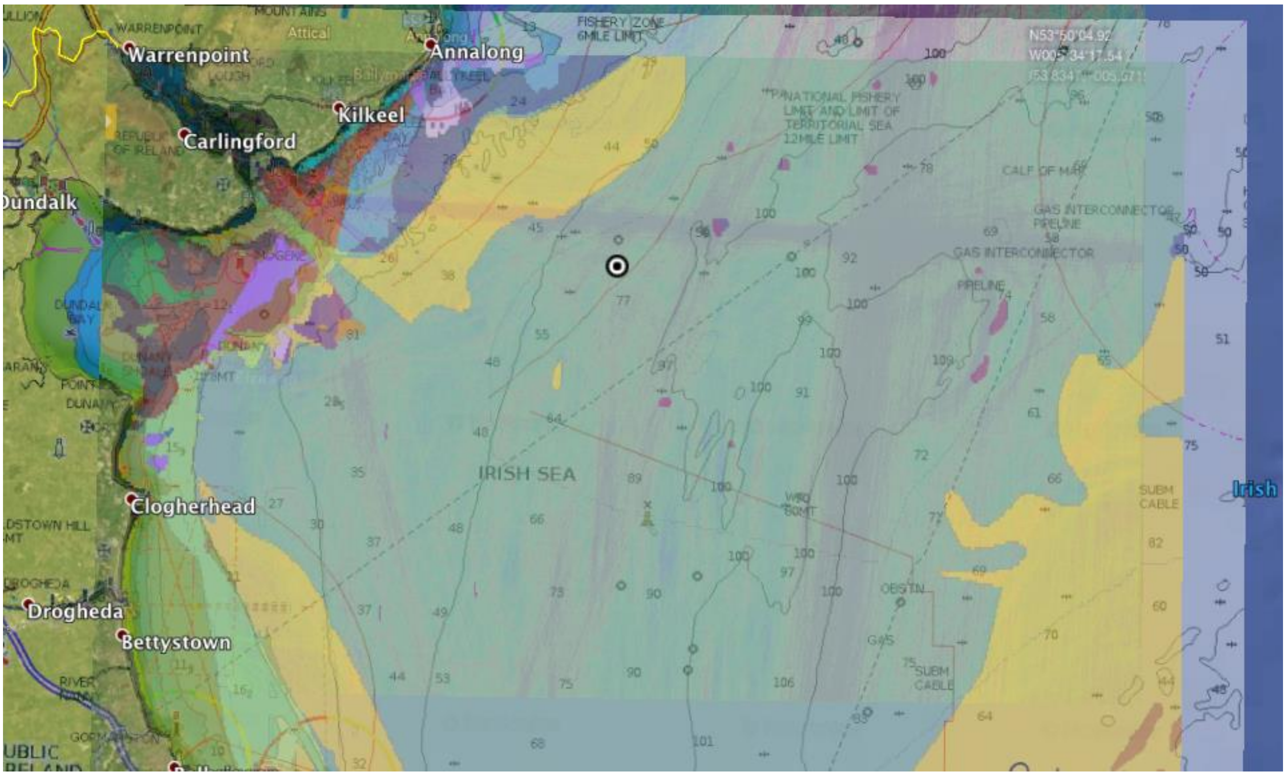

Figure 31: The Greenore site compared to the biocenosis distribution, naval and shipping routes traffic and bathymetry. ***(Source: EMODnet-seabedhabitat.eu; Navionics.com, Marinetraffic.com).***

The site is located over a shallow shelf, on a deep circa littoral mud (Eunis A5.37). The location does not intercept any shipping lane. The site characteristics are shown in Table 17.

Table 17: Greenore site characteristics.

SITE NAME: GREENORE	POSITION: λ 53,958885° φ -5,677144°
Port distance	15,0 nm
Land distance	11,6
Depth	70 m
Seabottom	Mud
Protected areas distance	12 nm
Minimum temperature	6,5
Maximum temperature	16,5
Tide amplitude	3,7 m
Annual wave power	5,35 kW/m
Annual wind power	0,875 kW/m^2
Maximum Hs 2016-2018	7,2 m

4.5 Site 3 – Port Ellen

On the Atlantic side of Scotland, the Sound of Jura, beside the island of Islay, has a deep sea bottom with a moderate shelter for oceanic waves, together with major exposure to wind. Moreover, the area is characterized by the lowest tide oscillation around the UK, and water temperatures are subject to the beneficial influence of the Gulf Stream. The UK's Navy uses all the surrounding areas for exercises so any infrastructure development would have to be discussed with the Ministry of Defence at early stages. Nevertheless, an offshore wind farm located opposite Islay is also in adjacent waters with the same kind of possible restriction.

The sound remains outside from the great shipping lanes that run offshore, and has only a moderate local ferry passing through.

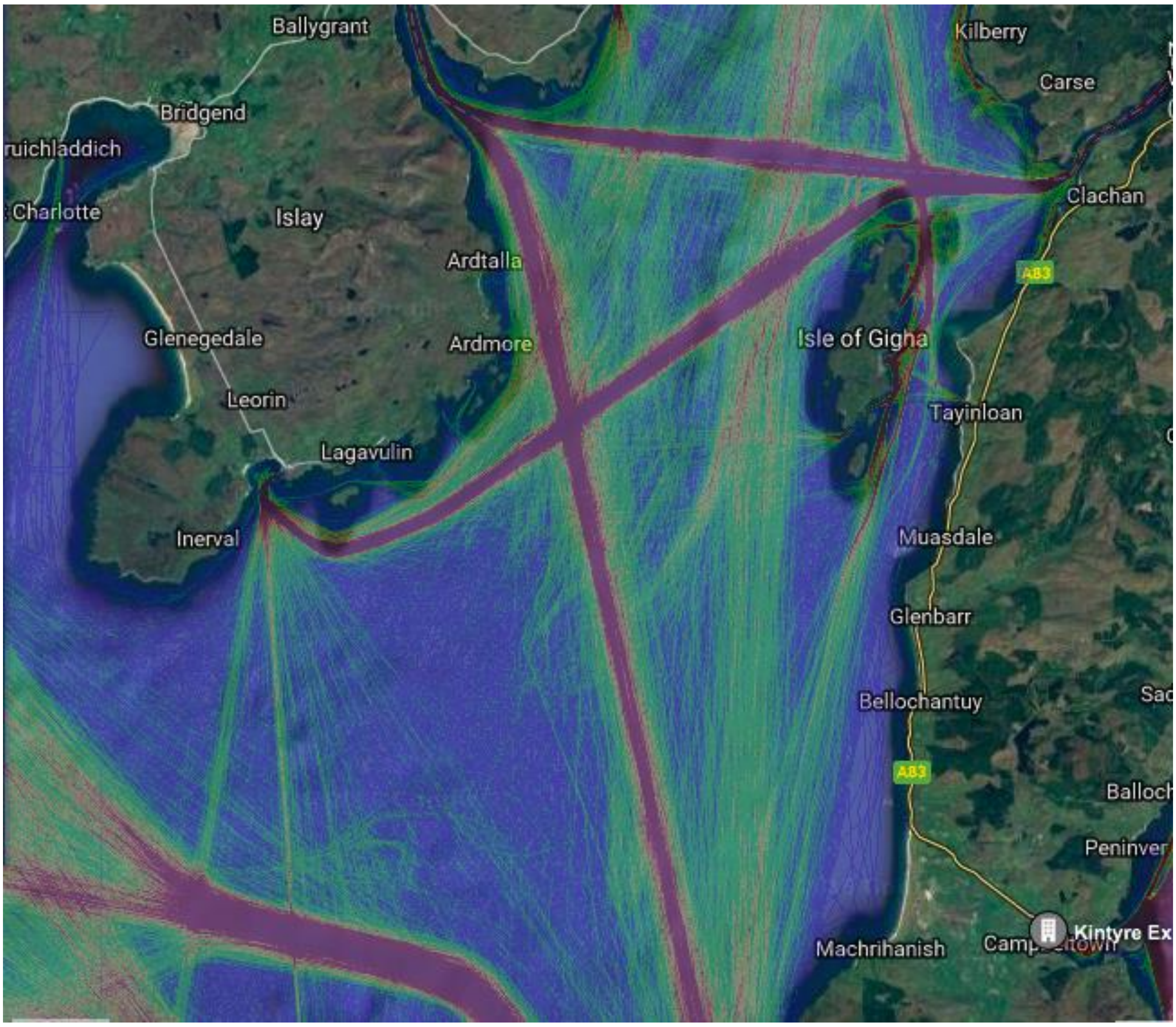

Figure 32: Naval and shipping routes traffic near the Port Ellen site. ***(Source, Marinetraffic.com).***

The North Channel is widely integrated within the Natura2000 network, but the Sound mouth is free, through its extensive width, from protected areas. Two Natura 2000 sites of limited sixze are on the coast of the Islay Island.

Figure 33: Protected areas around Port Ellen. *(Source: EEA, Natura2000 Viewer).*

Based on previous elements, a suitable installation point for the Blue Growth Platform has been identified. It lies over an 80 m- deep sedimentary seabed, at a distance of 7,1 nm from Port Ellen. A Deep circa littoral fine sand, as in EUNIS A5.27, composes the sea bottom.

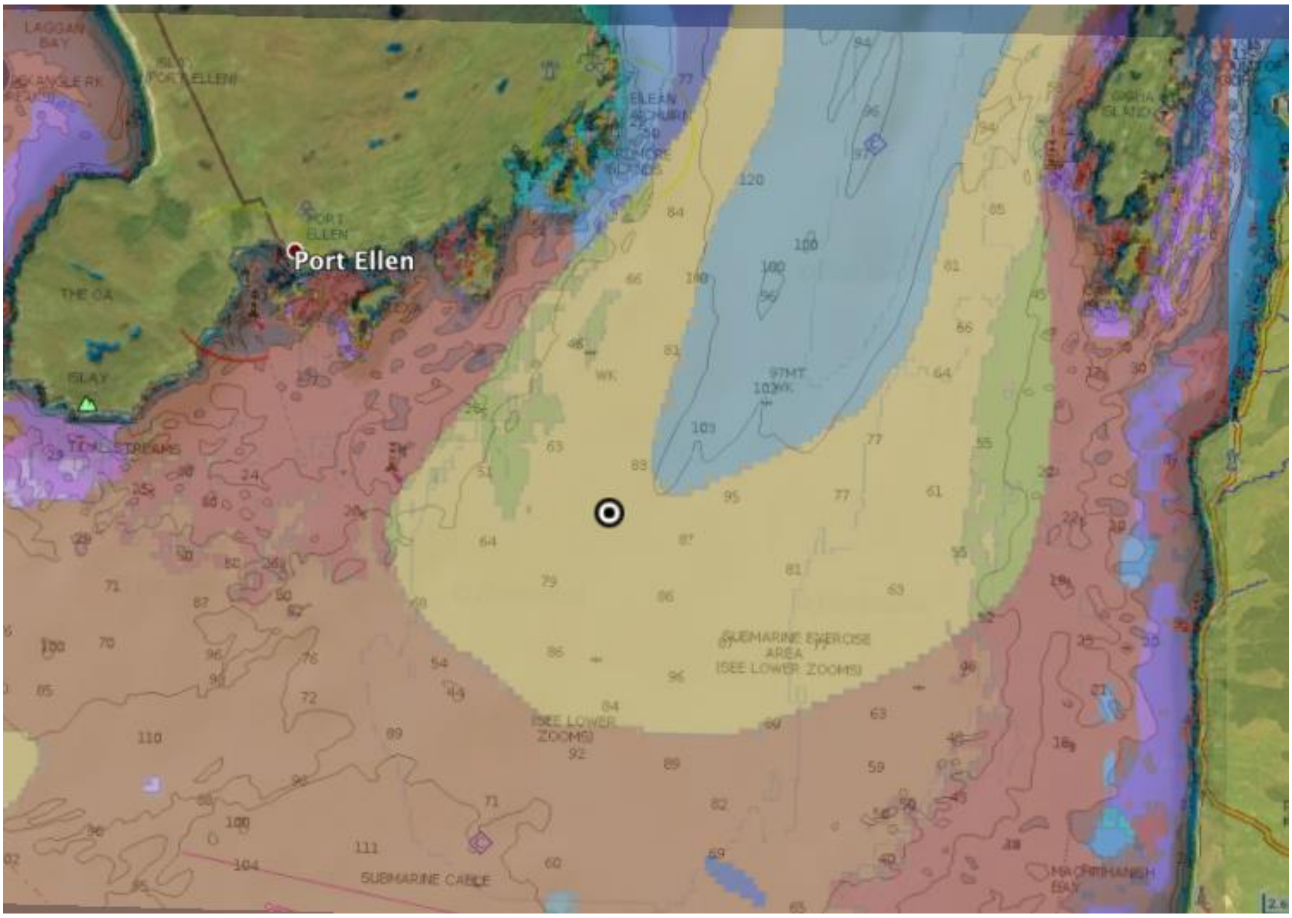

Figure 34: Site location over depth and biocenosis distribution maps near Port Ellen. ***(Source: EMODnet-seabedhabitat.eu; Navionics.com,).***

The site features are shown in Table 18.

Table 18: Port Ellen site characteristics

SITE NAME: PORT ELLEN	POSITION: λ 55,555297° φ -6,019110°
Port distance	7,1 nm
Land distance	5,7 nm
Depth	80 m
Sea bottom	Sand
Protected areas distance	5,7 nm
Minimum temperature	6,1
Maximum temperature	15,6
Tide amplitude	1,2 m
Annual wave power	11,9 kW/m
Annual wind power	0,892 kW/m^2
Maximum Hs 2016-2018	6,2 m

4.6 Site selection matrix

Based on values derived from the literature on the selected sites, a decision matrix using the TOPSIS method (see section 2.2.1.) has been calculated. For the final site decision, a different rank value has again been assigned to the criteria, giving the lowest negative value to tide amplitude and to Hs, directly influencing the fish welfare through water motion.

Table 19: Criteria Vs. Sites matrix of North Atlantic sites.

	Attributes/ Criteria	Port distance	Land distance	Depth	Soft seabottom	Protected areas distance	Minimal temp 4-8°	Maximum temperature 15-18°	Tide amplitude	Annual wave power	Annual wind power	Max recorded Hs
Solutions/Options												
m =												
1	Aberdeen	15	14	70	4	13	5,2	16,3	3	12,5	1,2	7,2
2	Greenor	15	12	70	5	12	6,5	16,5	3,7	5,4	0,87	7,2
3	Port Ellen	7	6	80	4	5,7	6,1	15,6	1,2	11,9	0,89	6,2

Table 20: TOPSIS selection matrix – All criteria are ranked 1, but Hs ranked (-3) to give weight to sites with lower extreme waves.

Attributes / Criteria		Port distance	Land distance	Depth	Soft seabottom	Protected areas distance	Minimal temp 12-15°	Maximum temperature 24-28°	Tide amplitude	Annual wave power	Annual wind power	Maximum recorded Hs	SUM	Closeness to the ideal POSITIVE solution
WEIGHTS		1	1	1	1	1	1	1	-3	1	1	-3		
Ideal Positive Solutions	A+	0,67	0,00	0,00	0,66	0,00	0,00	0,59	-2,26	0,00	0,00	0,00		
Ideal Negative Solutions	A-	0,00	0,73	0,63	0,00	0,70	0,63	0,00	0,00	0,69	0,69	-1,81		
Solutions/Options														
Distances from the ideal POSITIVE solution														
Aberdeen	11	0,000	0,533	0,302	0,018	0,489	0,254	0,000	0,183	0,478	0,482	3,283	1,263	40%
Greenor	10	0,000	0,376	0,302	0,000	0,417	0,397	0,000	0,000	0,089	0,253	3,283	1,222	44%
Port Ellen	9	0,125	0,091	0,395	0,018	0,094	0,349	0,001	2,331	0,433	0,265	2,434	1,035	45%

The best closeness to the ideal positive solution was recorded at the Port Ellen site. This therefore will be considered as the best site solution within the northern waters for the Blue Growth Farm operations.

4.7 Platform motion sheltering capability

The following tables show the maximum allowable sea state for the Atlantic salmon, considering the internal platform basin as a confined volume where the wave motion is transmitted from the adjacent sea waves to the pool. *This approach should be regarded as a first degree approximation, because within the design development, the full assessment of water pool motion is expected; at the present stage, this* *approximation may be useful to identify the likely range of platform utilization, with concern to fish resistance to motion and engineering features.*

Based on critical water speed for salmon, it is possible to calculate the wave state inside the platform basin that enables for an acceptable level of welfare concerning water motion. A wave of Hs 3,3 m and T 7,4 sec oscillating within the platform internal basin, leads to a water motion whit a horizontal speed within the range of $\boldsymbol{U_{crit}}$ for salmon, and for several metres even within the Welfare $\boldsymbol{U_{crit}}$, thereby allowing for a safe basin volume exploitation for the Atlantic species. Data are summarized in Table 21.

Table 21: Summary of welfare water velocities cm.s^{-1} for Atlantic Salmon.

	WELFARE UCRIT
Salmon smolt large	53
Salmon 50 cm	71

Table 22: Horizontal speed within a depth of 12m, for a wave of Hs = 3,4 m, T = 7,9 sec.

horizontal and vertical components of orbital wave velocities												
Hs significant heigth	3,3	3,3	3,3	3,3	3,3	3,3	3,3	3,3	3,3	3,3	3,3	3,3
Period T sec.	7,7	7,7	7,7	7,7	7,7	7,7	7,7	7,7	7,7	7,7	7,7	7,7
Lambda m	93,6	93,6	93,6	93,6	93,6	93,6	93,6	93,6	93,6	93,6	93,6	93,6
gravity g	9,8	9,8	9,8	9,8	9,8	9,8	9,8	9,8	9,8	9,8	9,8	9,8
wave at depth m	-1,0	-2,0	-3,0	-4,0	-5,0	-6,0	-7,0	-8,0	-9,0	-10,0	-11,0	-12,0
site depth m	100,0	100,0	100,0	100,0	100,0	100,0	100,0	100,0	100,0	100,0	100,0	100,0
horizontal speed m/sec	1,3	1,2	1,1	1,0	1,0	0,9	0,8	0,8	0,7	0,7	0,6	0,6
%	100,0	93,5	87,4	81,8	76,5	71,5	66,9	62,5	58,5	54,7	51,1	47,8
vertical speed m/sec	-1,3	-1,2	-1,1	-1,0	-1,0	-0,9	-0,8	-0,8	-0,7	-0,7	-0,6	-0,6
%	100,0	93,5	87,4	81,8	76,5	71,5	66,9	62,5	58,5	54,7	51,1	47,8

Increasing Hs and T, the horizontal velocity within the pool increases beyond $\boldsymbol{U_{crit}}$ **,** and the extent of safe zone decreases to negligible values.

These wave parameters have been used to calculate a wave power (in kW/m) associated to this wave condition within the pool, by the formulas as per section 3.8.,

Wp= 0,55 $(H_s)^2 T_z$, (kW/m)

The result is:

$0{,}55*(3{,}3)^2*7{,}4 = 46{,}3$ kW/m

Hypothesizing that the WEC system will lead to a conversion of a significant percentage of wave incident power, the maximum allowable sea states in the surrounding marine waters, that permits an acceptable fish welfare inside the platform basin, under different wave power absorption, are:

- for a storm of Hs 6,5 m, T= 10,8 sec, leading to a WP of 252 kW/m, the Wave Power absorption has to be close to 80 %, in order to provide a safe fish shelter;
- for a storm of Hs 8,5 m, T= 12,4 sec, leading to a WP of 278 kW/m, the Wave Power absorption has to be close to 90 %, in order to provide a safe fish shelter;

The platform location within the North Atlantic, will then be selected considering the above sea states as limits for an acceptable fish welfare inside the platform basin.

The maximum recorded sea state for the selected site, Port Ellen, within the time series (2016-2018) available on the Copernicus website as hourly means, is related to a storm that occurred on 30 December 2017, with an Hs = 6,2 m, at a Period = 10,6 sec, although with a duration of several hours.

This storm gave rise to a WP of 224 kW/m; these wave horizontal speeds can be sustained by the Atlantic salmon, diving to a depth between 24 and 35 m within the cage net, or, within the 12 m shelter wall of the platform, where this is able to provide a wave power absorption of at least 78 % of the external incident wave power.

The second ranked site, Greenore, has experienced a maximum recorded storm of Hs = 7,9 m, at a T = 9.5 sec. Within this condition, the platform has to provide an incidence wave power reduction of 88 % to offer a safe shelter to fish within the platform pool.

5 ATLANTIC OCEAN, SUBTROPICAL

5.1 Farming species

The species selected for fish farming within the Blue Growth Platform facilities located within the Atlantic Ocean, the Canary Islands, is the seabream *Sparus aurata (*Linnaeus, 1758). This species is one of the most farmed within the Mediterranean and adjacent waters, with an annual gross production in the Mediterranean of 160.563 tonnes (FEAP, 2017) in 2016.

Seabream is farmed both in coastal and offshore waters from a weight of 5 to 10g, to attain a final weight of 350-400 g, and a length of 35 cm at the end of a 16-18 month growth cycle.

Whilst seabream areal extends from the UK to the whole Mediterranean Sea, and down to Cape Verde (ref. FAO, 2018; Fishbase.org, 2018), its temperature range lies between 13 and 26 °C, with suboptimal temperature from 10°C up to 28 °C tolerable for short periods.

Its optimal growing range is here considered to be between 15 °C and 26°C, as experienced within most bream farms in the Mediterranean Sea.

Figure 35: Seabream areal distribution *(Source:www.iucnredlist.org)*

5.2 Pre-screening process

A list of excluding criteria to be considered when selecting a new potential site was given In section 2.2.1.

With the aim of identifying the area of the European Atlantic Ocean where the best growing conditions are to be found, a series of large-scale maps, showing the average surface daily sea temperature at day 15 and 30 of each month from April 2014 to March 2018 have been produced. The use of these maps, at a resolution of 0,25 x 025 degree, (see section 2.1.), enables a very large area to be surveyed for a consistent period of time, and offers the significant advantage, with regard to punctual temperature time series, of the comprehensive view of evolution of temperature on a basin scale. Unfortunately the time series available on the Copernicus Service server is spread over four years only, but is sufficient to exclude some areas from farming activities on the basis of appearance of extreme values over a moderate time window.

These maps are shown in Fig. 36, colour scale from 10 to 30 °C.

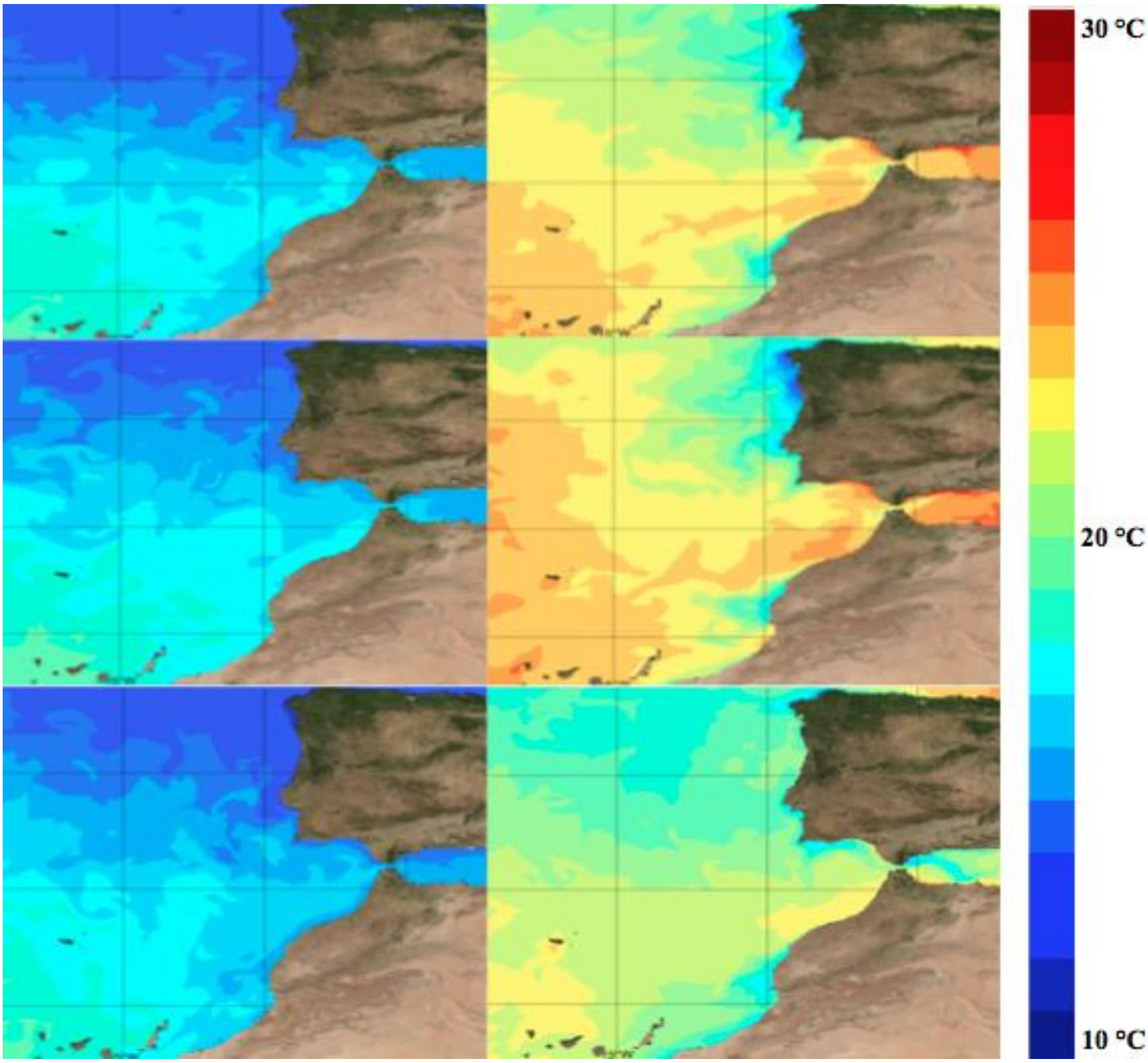

Figure 36: Maps of extreme temperatures values in 2016-2018 years. (*Source, marine.copernicus.eu).*

Examination of the maps revealed a good temperature range for seabream farming around the Canary Islands, with a warm minimum and a mild temperate maximum. The Canary Island are also reknowed for their wind resources, even being outside the path of great Atlantic low pressure systems.

The pre-screening process on the Canary Islands area has led to the identification of a single area suitable for the Blue Growth Farm Platform deployment. In fact, the only areas with a flat seabed within the suitable depth range are around the Tenerife Island. Unfortunately, this is part of a Natura 2000 site, and has thus been discarded. Therefore, within the selection process, it has been possible to identify a single suitable site.

The possible location has been analysed in detail in a GIS environment, adding layers of marine traffic, bathymetry, protected areas, sediment/benthos, to support the preliminary exclusion of areas not adapted to platform installation.

5.3 Site 1 – Gran Canaria: Arinaga

The island of Gran Canaria is a Volcanoe structure, of approximately circular shape, surrounded for the most part of its perimeter by very deep waters down to 3500 m.

Figure 37: Canary Islands

Its southeast side faces an area within a suitable depth range of approximately 50 km2. The zone is free from any protection regime and from any other constraints, and is included within the blocks where offshore wind farming is allowed, under Spanish Crown law 1028/2008. Two areas Natura 2000 areas are present at different distances.

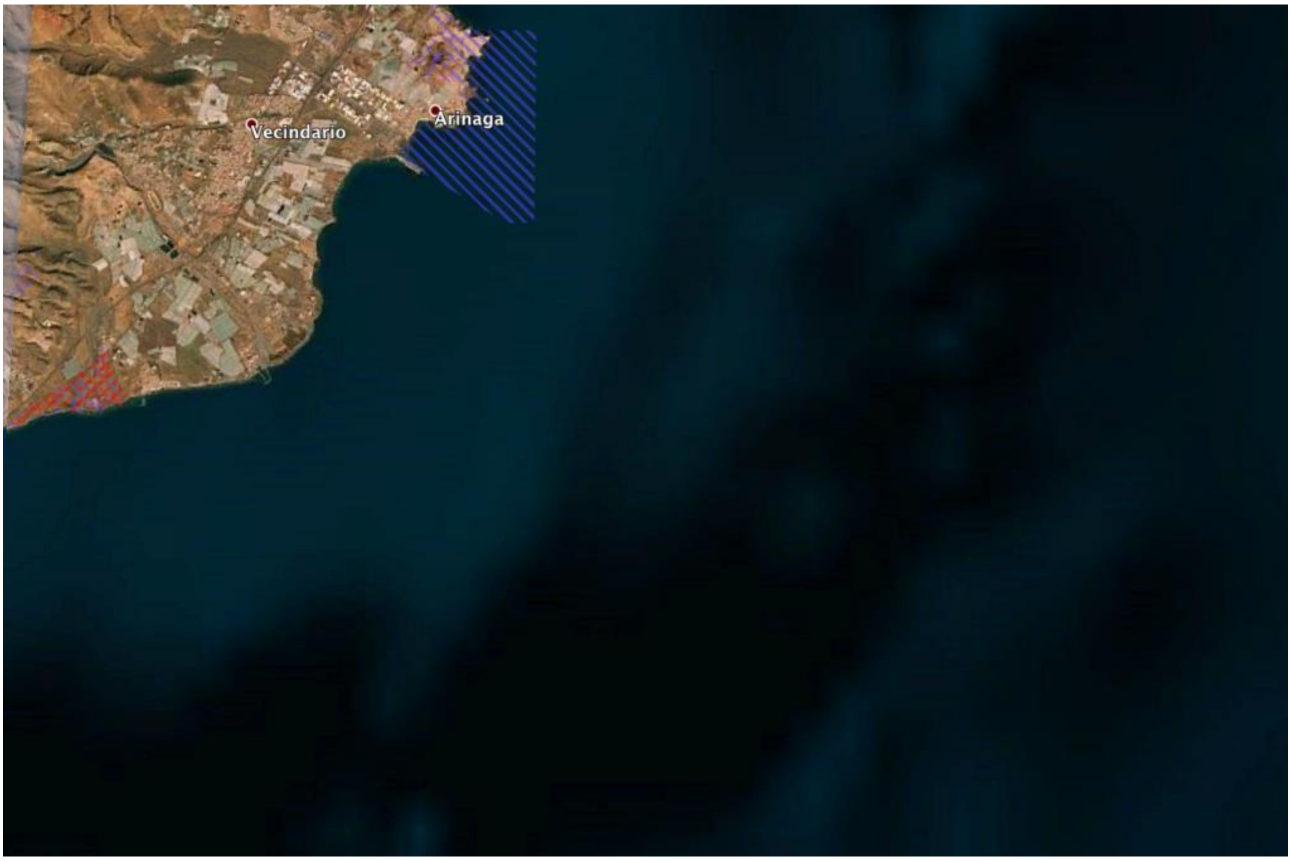

Figure 38: Protected areas near Arinaga. *(Source: EEA, Natura2000 Viewer).*

The whole area is notably free of any significant marine traffic. The shipping lane directed to Las Palmas runs offshore. There is a port serving the Arinaga industrial complex.

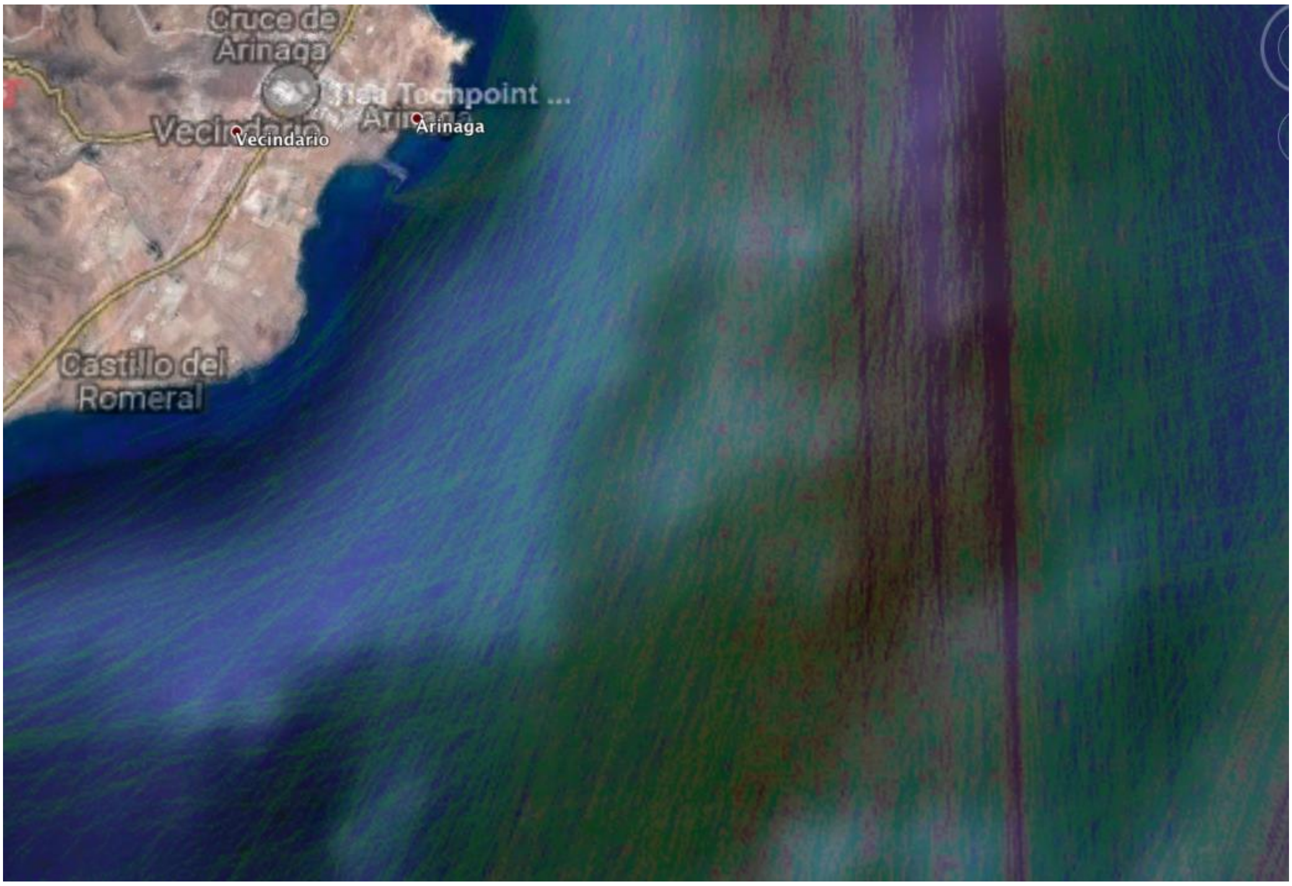

Figure 39: Naval routes traffic and shipping near the Arinaga site. ***(Source, Marinetraffic.com).***

The area selected for a possible Blue Growth Farm Platform installation is located eastward of the port, over a sea bottom with a slight slope, and a depth is in the range of 70-95 m.

The seabed is presumably rocky, given the island's geological nature. It is not described in detail in the EMODnet seabed cartography. The selected site is shown in the following map, with depth contours and the seabed features.

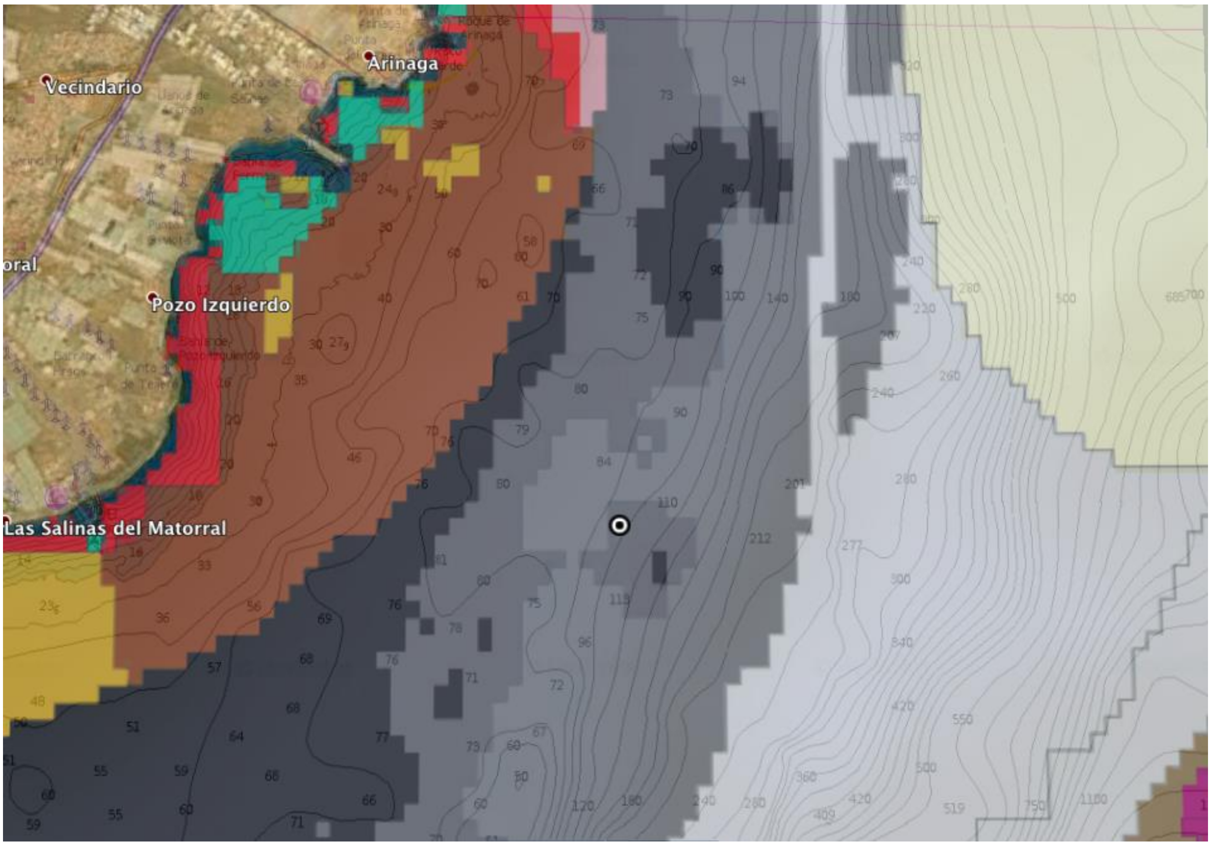

Figure 40: Site location over depth and biocenosis distribution maps at the proximity of Arinaga. ***(Source: EMODnet-seabedhabitat.eu; Navionics.com,).***

Several wind farms are present in the area onshore; close to the selected site, the PLOCAN platform has been installed, although in a more sheltered position; an offshore wind farm (FLOCAN 5) is in operation three miles southward, in shallow waters.

Table 23: Arinaga site characteristics

SITE NAME: ARINAGA	POSITION: λ 27,79986° φ -15,359552°
Port distance	3,5 nm
Land distance	3,5 nm
Depth	95 m
Seabottom	Rock
Protected areas distance	2,1 nm
Minimum temperature	18
Maximum temperature	23,5
Tide amplitude	3,2 m
Annual wave power	12,1 kW/m
Annual wind power	0,892 kW/m^2
Maximum Hs 2016-2018	4,5 m

5.4 Platform motion sheltering capability

The following tables report the maximum allowable sea state for farmed species in temperate waters, considering the internal platform basin as a confined volume where the wave motion is transmitted from the adjacent sea waves to the pool. *This approach should be regarded as a first degree approximation, because within the design development, the full assessment of water pool motion is expected; at the present stage, this approximation may be useful to indicate the likely range of platform utilization, with concern to fish resistance to motion and engineering features.*

A wave of Hs = 3,0 m and T = 7,4 sec., as derived from a JONSWAP spectrum, that is oscillating within the platform internal basin, leads to a water motion at a horizontal speed within the range of U_{crit} for seabass and seabream, and for a depth range of several metres, even within the Welfare U_{crit}. This wave motion state enables a safe basin depth exploitation for the Mediterranean species. Data are summarized below.

Table 24: Summary of welfare water velocities (cm.s^{-1}) for seabream.

	WELFARE UCRIT
Seabream20 cm	55
Seabream 35 cm	54

Table 25: Horizontal speed within a depth of 12m, for a wave of Hs = 3,0 m, T = 7,4 sec.

horizontal and vertical components of orbital wave velocities												
Hs significant heigth	3,0	3,0	3,0	3,0	3,0	3,0	3,0	3,0	3,0	3,0	3,0	3,0
Period T sec.	7,4	7,4	7,4	7,4	7,4	7,4	7,4	7,4	7,4	7,4	7,4	7,4
Lambda m	85,1	85,1	85,1	85,1	85,1	85,1	85,1	85,1	85,1	85,1	85,1	85,1
gravity g	9,8	9,8	9,8	9,8	9,8	9,8	9,8	9,8	9,8	9,8	9,8	9,8
wave at depth m	-1,0	-2,0	-3,0	-4,0	-5,0	-6,0	-7,0	-8,0	-9,0	-10,0	-11,0	-12,0
site depth m	100,0	100,0	100,0	100,0	100,0	100,0	100,0	100,0	100,0	100,0	100,0	100,0
horizontal speed m/sec	1,2	1,1	1,0	1,0	0,9	0,8	0,8	0,7	0,7	0,6	0,6	0,5
%	100,0	92,9	86,3	80,1	74,4	69,1	64,2	59,6	55,4	51,5	47,8	44,4
vertical speed m/sec	-1,2	-1,1	-1,0	-1,0	-0,9	-0,8	-0,8	-0,7	-0,7	-0,6	-0,6	-0,5
%	100,0	92,9	86,3	80,1	74,4	69,1	64,2	59,6	55,4	51,5	47,8	44,4

Increasing Hs and T, the horizontal velocity within the pool increases beyond U_{crit} , and the extent of the safe zone decreases to negligible values, therefore becoming unsuitable for fish farming.

The above wave parameters have been used to calculate a wave power (in kW/m) associated with wave condition within the pool, using the formulas given in section 3.8.;

$Wp = 0,55\ (H_s)^2\ T_z$,

The result is:

$0,55*(3,0)^2*7,4 = 37,0$ kW/m

Under the hypothesis that the WEC system would lead to a conversion of a significant percentage of wave incident power, the maximum allowable sea states in the surrounding marine waters that provide an acceptable fish welfare inside the platform basin, under different wave power absorption, are:

- for a storm of Hs 5,5 m, T= 10,0 sec, leading to a WP of 166 kW/m, the wave power absorption has to be close to 72 %, to provide a safe fish shelter;

The maximum recorded sea state for the selected site, Arinaga, within the time series (2016-2018) available on the Copernicus website as hourly means, refers to a storm that occurred the on 10 February 2016, with a Hs = 4,0 m, at a Period = 11 sec, although with a duration of several hours.

This storm has gave rise to a WP of 97 kW/m; these wave horizontal speeds can be sustained by the selected aquaculture species, seabream, diving to a depth between 20 to 35 m within the cage net, or, within the 12 m shelter wall of the platform, where this is able to provide a wave power shelter of 62 % of the external incident wave power.

6 CONCLUSIONS

In the following pages, a number of tables and figures have been added, reporting the climatological features of the three selected sites. Data have been retrieved from the Copernicus website, selecting the appropriate product for the area of interest and for the time series, and from scientific literature on the topic.

This report has been produced based on only some of the possible criteria that can be taken in account during site identification: landscape, cultural heritage, social acceptance and protected/vulnerable species presence, to mention just a few, have not yet been considered. At the current platform design stage, the overall picture still lacks all the details necessary to provide a definitive platform location on the one hand and, on the other, to insert the apparatus and its operational life harmoniously into the surrounding environment.

During the site selection process, particular attention was given to the fish farming included into the platform, and to its possibility to cope with extreme environmental conditions, since farmed fish the “weakest link” within the platform’s operational chain.

Other environmental data will be retrieved and added to this deliverable in the future, as and when necessary to support the platform’s technological development.

Annex I: MEDITERRANEAN SEA

Table 26: Mediterranean site characteristics

MEDITERRANEAN SITE	
Geographical location	λ 43,127°, φ 4,709°
Surface area of study site	5 x 5 km
Offshore distance	13,2 nm
Depth	90 m
Substrate	Soft seabed
Substrate properties	Mud, Folk 1
Water temperature	13-24 °C
Salinity	36-38 PSU
Tidal range	0,30 m
Mean Wave height	1,02 m
Expected annual wave power	4,48 kW/m
Average wind speed	7,6 m/sec
Expected annual wind power	1200 W/m^2

Table 27: Main characteristics of the selected site for fish production

DATA FOR FISH PRODUCTION	
Temperature range	13-24 ° C
Oxygen range	Saturation
Salinity	36-38 PSU
Turbidity	0,15 KD490
Selected species for farm production	Seabass

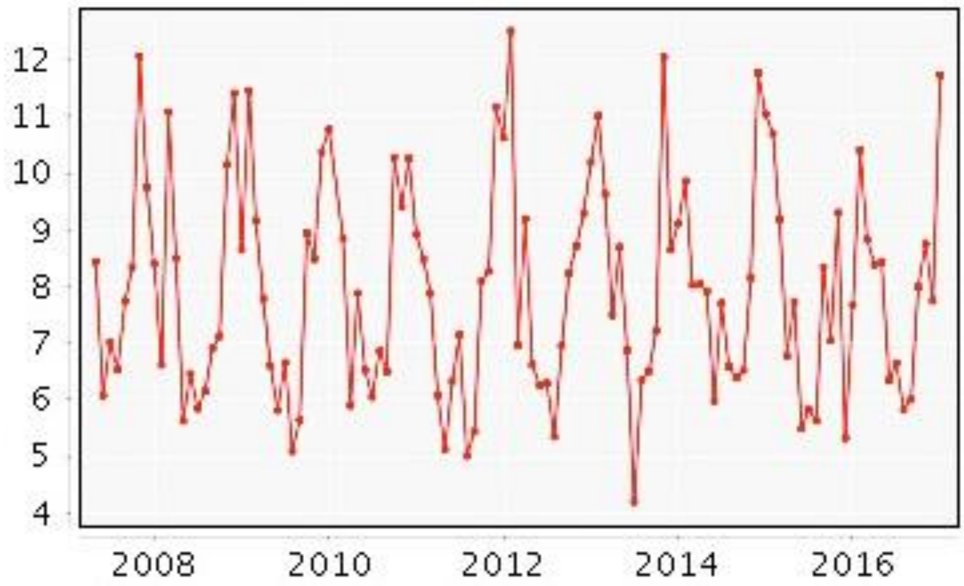

Figure 41: Wind speeds (m/sec) at Marseille site; years 2007-2017, monthly means (*Source, marine.copernicus.eu*).

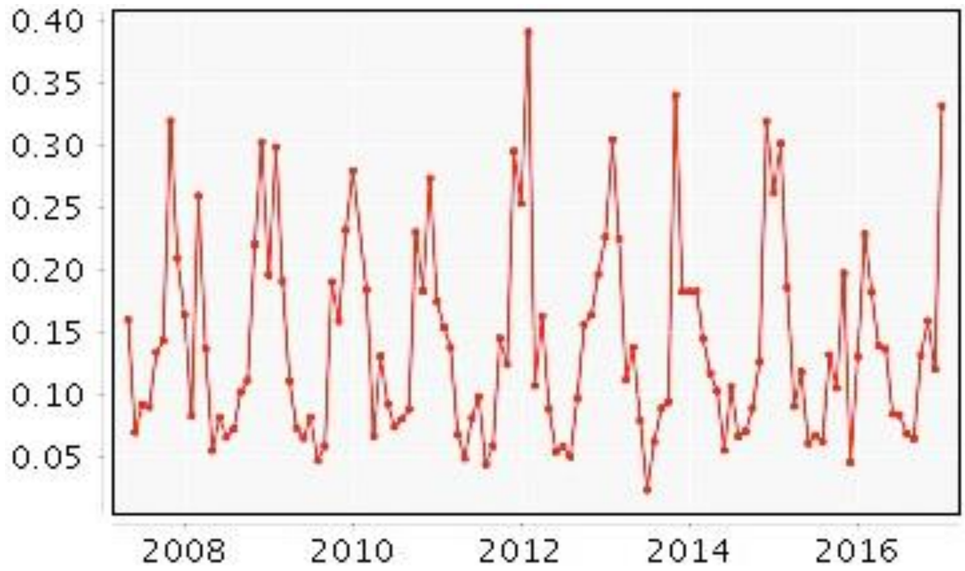

Figure 42: Wind stress (Pa) at Marseille site; years 2007-2017, monthly means (*Source, marine.copernicus.eu*).

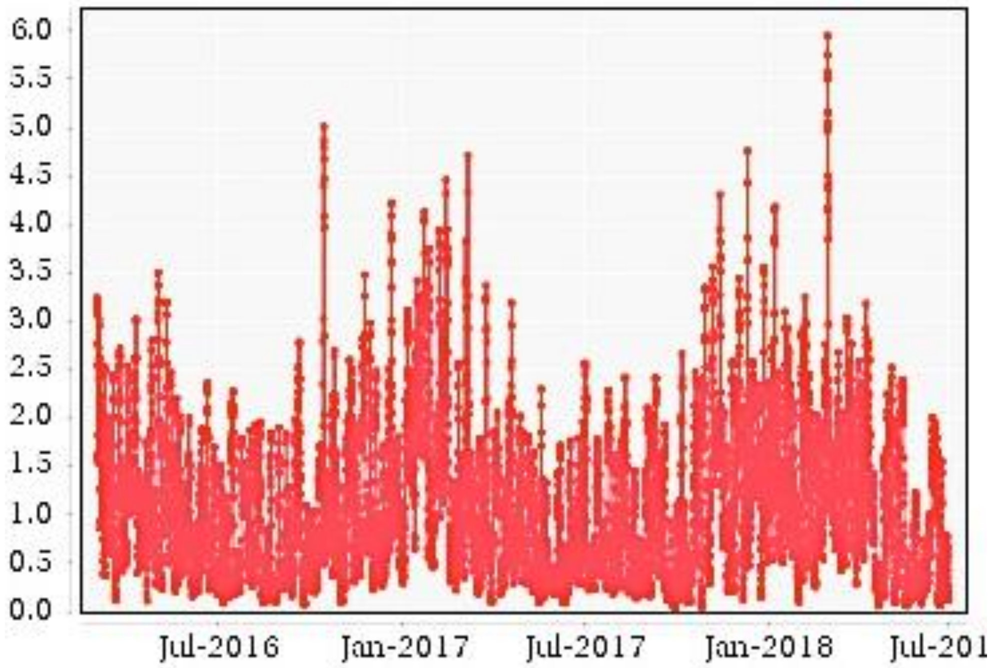

Figure 43: Significant waves (m) at Marseille site; years 2016-2018, hourly means (*Source, marine.copernicus.eu).*

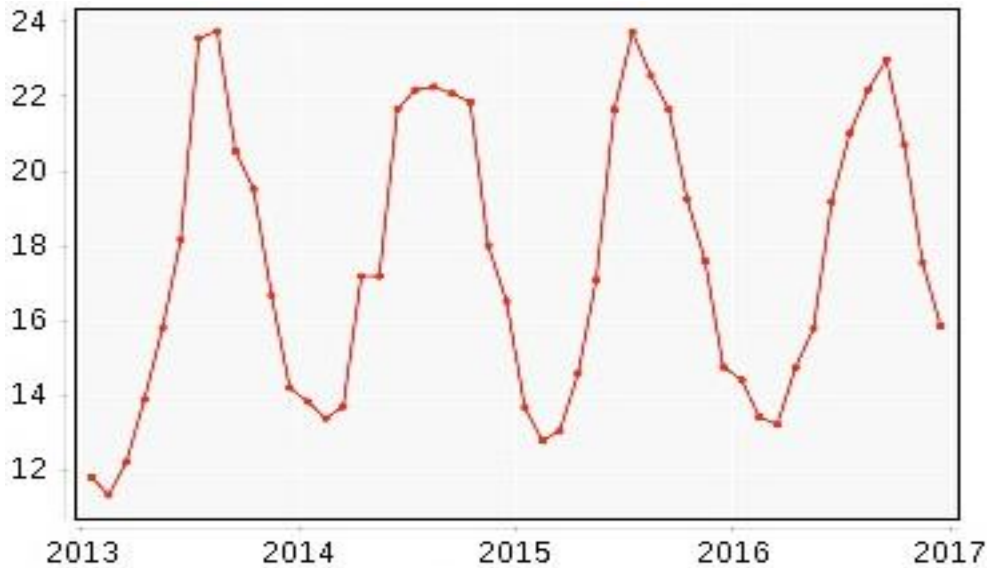

Figure 44: Seawater potential temperature (°C) at Marseille site; years 2013-2017, monthly means (*Source, marine.copernicus.eu).*

Figure 45: Seawater velocity (m/sec) at Marseille site; years 2014-2016, monthly means (*Source, marine.copernicus.eu).*

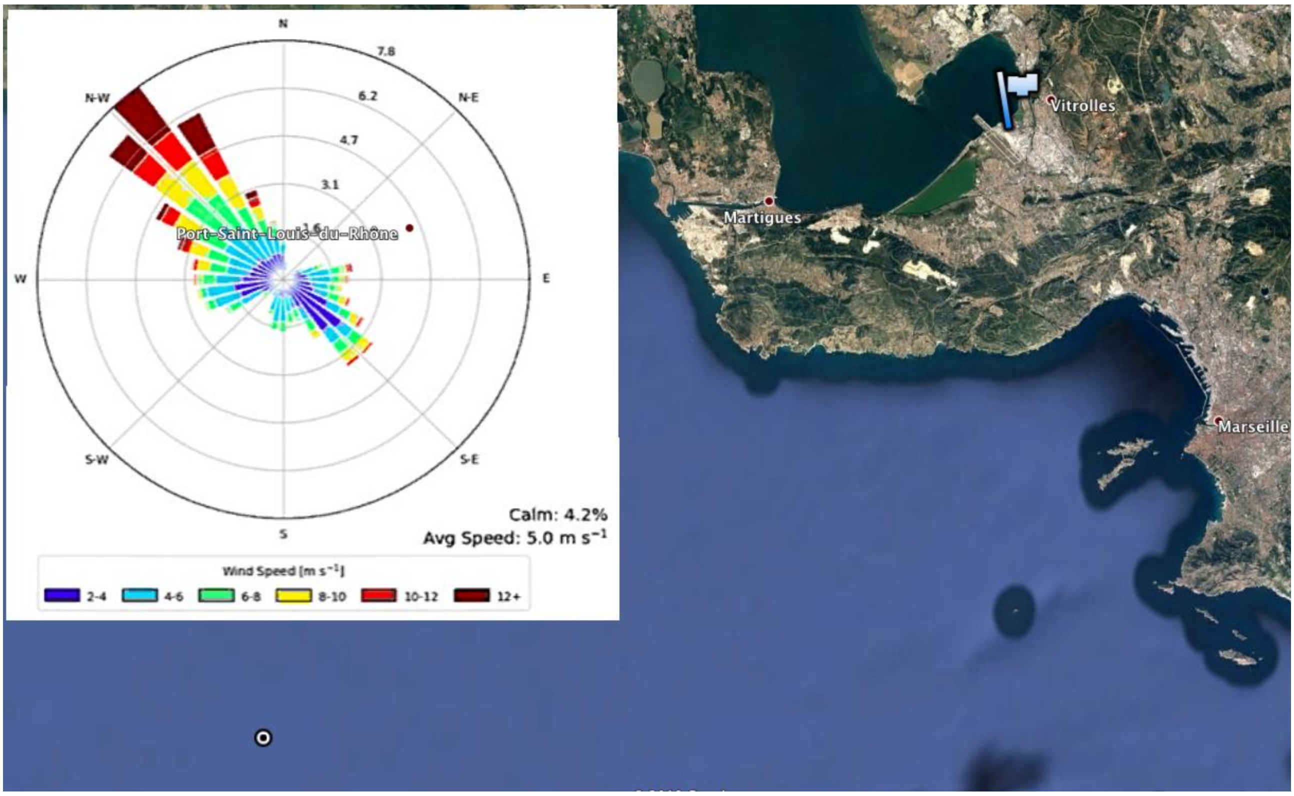

Figure 46: Windrose plot for Marseille, period 01 Jan 2008 to 14 July 2018 ;

Flag: Recorder position; Point: selected site. (Source : [https://mesonet.agron.iastate.edu)](https://mesonet.agron.iastate.edu)

Table 28: Marseille, windrose data ; latitude : 43.44167 ; longitude : 5.22667 ; elevation (m) = 36.

\# Windrose Data Table (Percent Frequency) for MARSEILLE/MARIGN (LFML)
\# Observations Used/Missing/Total: 167562/14316/181878
\# Period: 1 Jan 2008 - 14 Jul 2018
\# Hour Limiter: All included
\# Month Limiter: All included
\# Wind Speed Units: meters per second
\# Generated 26 Jul 2018 09:17 UTC, contact: akrherz@iastate.edu
\# First value in table is CALM

,	0.0- 1.9,	2.0- 3.9,	4.0- 5.9,	6.0- 7.9,	8.0- 9.9,	10.0-11.9,	12.0- inf,
355-005,	4.466,	0.797,	0.359,	0.085,	0.031,	0.008,	0.004,
005-015,	0.206,	0.439,	0.130,	0.017,	0.004,	0.000,	0.001,
015-025,	0.178,	0.246,	0.050,	0.011,	0.001,	0.000,	0.000,
025-035,	0.150,	0.179,	0.026,	0.010,	0.001,	0.001,	0.000,
035-045,	0.132,	0.168,	0.036,	0.011,	0.003,	0.000,	0.001,
045-055,	0.143,	0.217,	0.059,	0.028,	0.016,	0.003,	0.001,
055-065,	0.167,	0.423,	0.184,	0.099,	0.033,	0.017,	0.007,
065-075,	0.160,	0.610,	0.399,	0.199,	0.110,	0.051,	0.038,
075-085,	0.202,	0.766,	0.705,	0.362,	0.208,	0.101,	0.087,
085-095,	0.264,	0.828,	0.667,	0.309,	0.168,	0.080,	0.048,
095-105,	0.351,	0.889,	0.553,	0.257,	0.132,	0.057,	0.016,
105-115,	0.587,	1.003,	0.508,	0.381,	0.243,	0.093,	0.033,
115-125,	0.955,	1.567,	0.471,	0.397,	0.312,	0.104,	0.048,
125-135,	1.198,	2.299,	0.449,	0.394,	0.302,	0.096,	0.024,
135-145,	1.346,	2.087,	0.521,	0.430,	0.356,	0.127,	0.022,
145-155,	1.041,	1.012,	0.464,	0.445,	0.201,	0.055,	0.017,
155-165,	0.699,	0.586,	0.408,	0.332,	0.133,	0.020,	0.004,
165-175,	0.463,	0.494,	0.579,	0.351,	0.071,	0.004,	0.001,
175-185,	0.358,	0.602,	0.772,	0.352,	0.047,	0.007,	0.000,
185-195,	0.301,	0.566,	0.834,	0.271,	0.014,	0.001,	0.000,
195-205,	0.260,	0.428,	0.643,	0.135,	0.002,	0.001,	0.000,
205-215,	0.190,	0.310,	0.317,	0.039,	0.002,	0.000,	0.001,
215-225,	0.138,	0.269,	0.147,	0.020,	0.002,	0.000,	0.001,
225-235,	0.165,	0.346,	0.275,	0.159,	0.064,	0.007,	0.001,
235-245,	0.204,	0.750,	0.743,	0.442,	0.149,	0.021,	0.002,
245-255,	0.295,	1.415,	0.857,	0.255,	0.094,	0.014,	0.005,
255-265,	0.408,	1.558,	0.874,	0.226,	0.093,	0.027,	0.007,
265-275,	0.418,	1.296,	0.846,	0.420,	0.205,	0.077,	0.014,
275-285,	0.338,	1.088,	0.726,	0.559,	0.378,	0.131,	0.053,
285-295,	0.352,	1.050,	0.776,	0.704,	0.594,	0.277,	0.112,
295-305,	0.257,	0.928,	1.148,	0.974,	0.829,	0.465,	0.182,
305-315,	0.193,	0.920,	1.630,	1.339,	1.209,	0.851,	0.912,
315-325,	0.184,	0.820,	1.330,	1.356,	1.359,	1.156,	1.789,
325-335,	0.187,	0.812,	0.873,	0.999,	1.162,	0.981,	1.253,
335-345,	0.202,	0.861,	0.679,	0.532,	0.454,	0.303,	0.236,
345-355,	0.269,	0.865,	0.542,	0.298,	0.171,	0.061,	0.039,

Annex II: NORTH SEA

Table 29: North Sea site characteristics

NORTH SEA SITE	
Geographical location	λ 55,555°, φ -6,019°
Surface area of study site	5 x 5 km
Offshore distance	5,7 nm
Depth	80 m
Substrate	Soft seabed
Substrate properties	Sand, Folk 2
Water temperature	6,1-15,6 °C
Salinity	33,7-34,2 PSU
Tidal range	1,2 m
Mean wave height	1,20 m
Expected annual wave power	11,9 kW/m
Average wind speed	9,2 m/sec
Expected annual wind power	890 W/m_2

Table 30: Main characteristics of the selected site for fish production

DATA FOR FISH PRODUCTION	
Temperature range	6,1-15,6 °C
Oxygen range	Saturation
Salinity	33,7-34,2 PSU
Turbidity	0,13-0,17 KD490
Selected species for farm production	Atlantic salmon

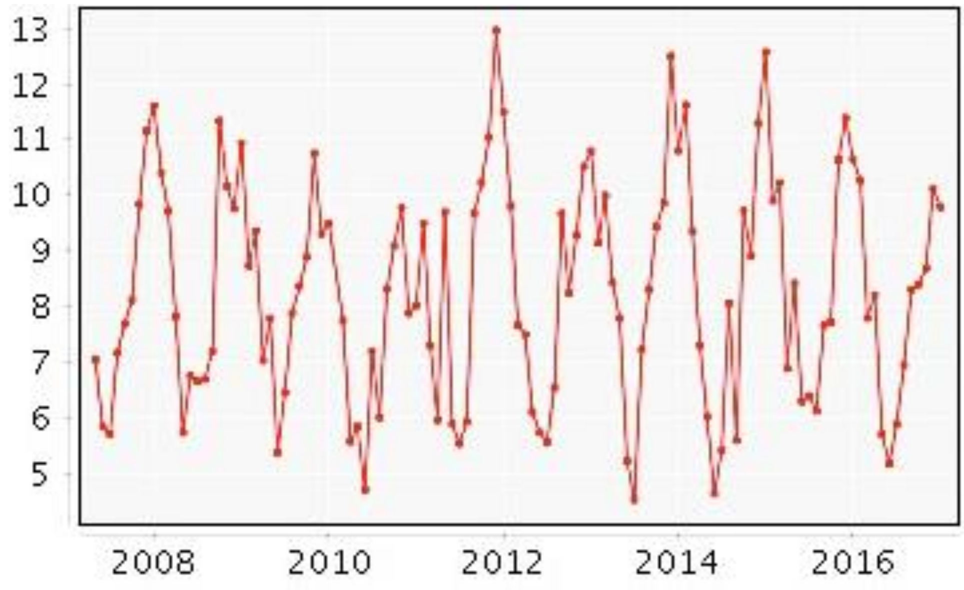

Figure 47: Wind speeds (m/sec) at Port Ellen site; years 2007-2017, monthly means (*Source, marine.copernicus.eu).*

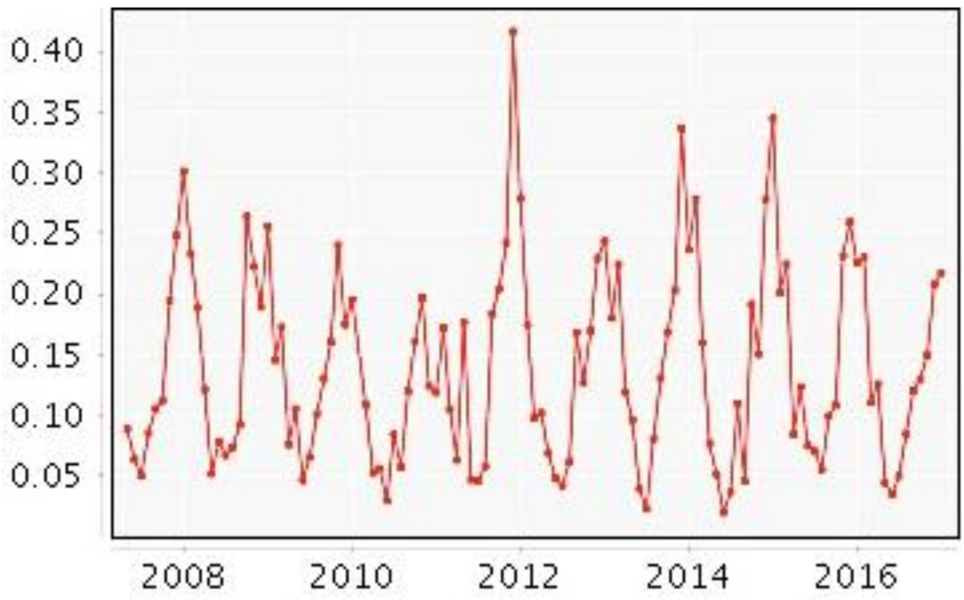

Figure 48: Wind stress (Pa) at Port Ellen site; years 2007-2017, monthly means (*Source, marine.copernicus.eu).*

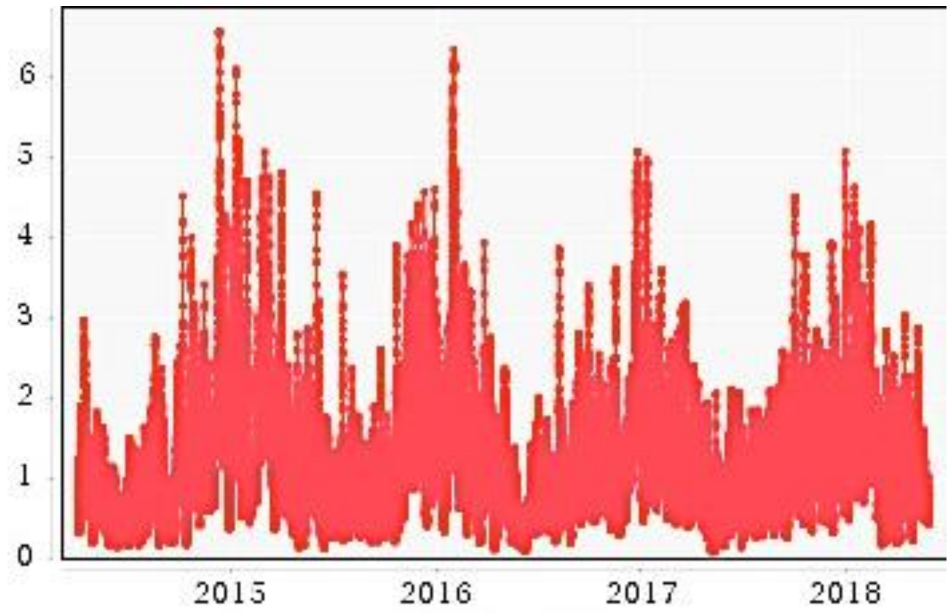

Figure 49: Significant waves (m) at Port Ellen site; years 2014-2018, hourly means (*Source, marine.copernicus.eu).*

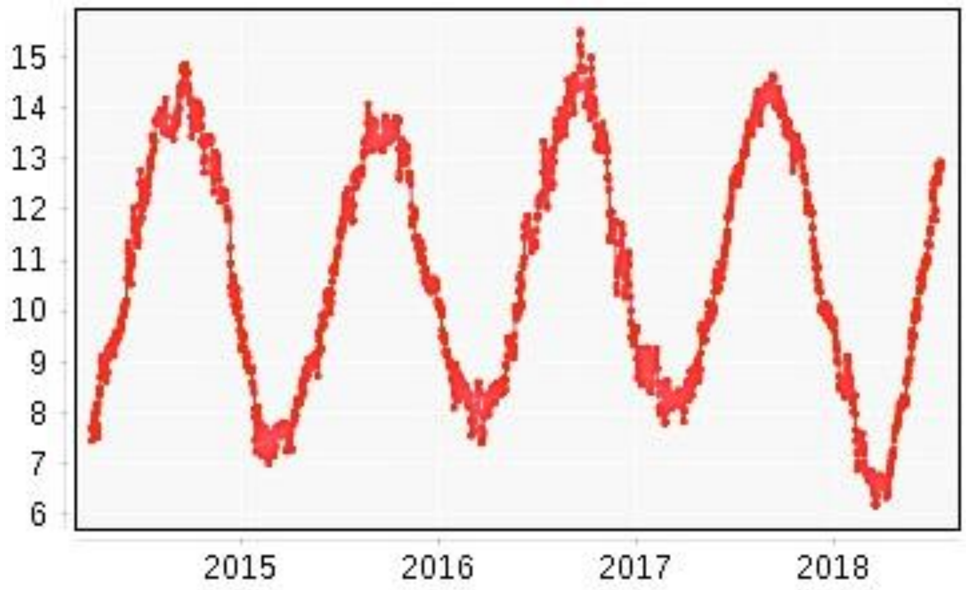

Figure 50: Seawater potential temperature (°C) at Port Ellen site; years 2014-2018, hourly means (*Source, marine.copernicus.eu).*

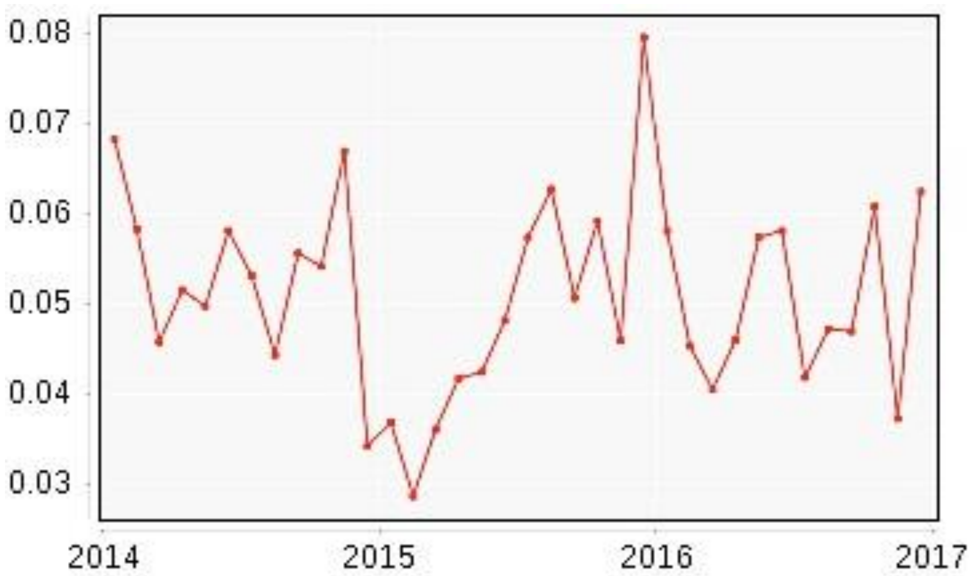

Figure 51: Graph of Seawater Velocity (m/sec) at Port Ellen site; years 2014-2016, monthly means (*Source, marine.copernicus.eu).*

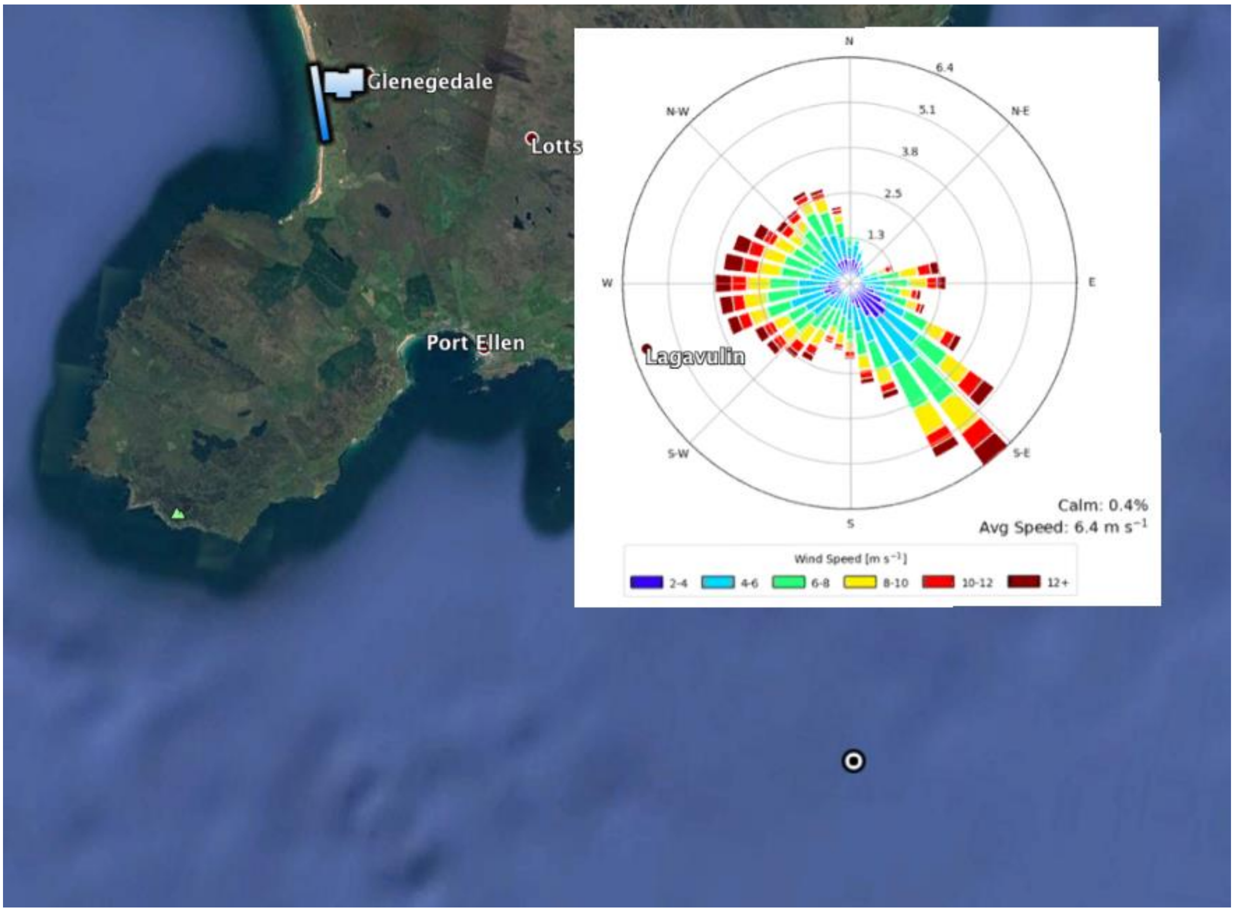

Figure 52: Windrose plot for Port Ellen, period 01 Jan 2008 to 14 July 2018 ;

Flag: Recorder position; Point: selected site. (Source : https://mesonet.agron.iastate.edu)

Table 31: Port Ellen, windrose data ; latitude : 55.68194 ; longitude : -6.25667 ; elevation (m) = 18.

```
# Windrose Data Table (Percent Frequency) for ISLAY/PORT ELLEN (EGPI)
# Observations Used/Missing/Total: 151235/5832/157067
# Period: 1 Jan 2008 - 14 Jul 2018
# Hour Limiter: All included
# Month Limiter: All included
# Wind Speed Units: meters per second
# Generated 26 Jul 2018 09:23 UTC, contact: akrherz@iastate.edu
# First value in table is CALM
```

	0.0- 1.9	2.0- 3.9	4.0- 5.9	6.0- 7.9	8.0- 9.9	10.0-11.9	12.0- inf
355-005	0.571	0.652	0.377	0.198	0.095	0.034	0.013
005-015	0.186	0.706	0.387	0.124	0.036	0.009	0.003
015-025	0.175	0.616	0.277	0.073	0.041	0.016	0.004
025-035	0.175	0.510	0.182	0.050	0.023	0.007	0.000
035-045	0.195	0.448	0.142	0.036	0.012	0.003	0.000
045-055	0.189	0.389	0.129	0.036	0.019	0.004	0.000
055-065	0.179	0.278	0.129	0.079	0.045	0.011	0.002
065-075	0.199	0.288	0.285	0.256	0.227	0.155	0.058
075-085	0.177	0.284	0.531	0.596	0.525	0.365	0.232
085-095	0.190	0.407	0.614	0.610	0.527	0.306	0.237
095-105	0.216	0.484	0.506	0.455	0.302	0.163	0.111
105-115	0.286	0.724	0.557	0.411	0.285	0.130	0.092
115-125	0.244	1.028	0.713	0.714	0.558	0.288	0.193
125-135	0.277	1.271	1.155	0.971	0.766	0.477	0.384
135-145	0.235	1.236	1.564	1.428	1.037	0.573	0.532
145-155	0.214	1.053	1.533	1.383	0.838	0.386	0.298
155-165	0.127	0.752	0.978	0.805	0.469	0.228	0.182
165-175	0.086	0.601	0.776	0.667	0.448	0.233	0.140
175-185	0.073	0.425	0.631	0.544	0.321	0.155	0.065
185-195	0.052	0.321	0.597	0.512	0.295	0.123	0.064
195-205	0.042	0.268	0.506	0.510	0.299	0.123	0.063
205-215	0.058	0.247	0.578	0.679	0.512	0.266	0.179
215-225	0.058	0.276	0.584	0.731	0.549	0.304	0.176
225-235	0.079	0.467	0.841	0.650	0.464	0.276	0.214
235-245	0.069	0.629	0.772	0.547	0.462	0.300	0.274
245-255	0.091	0.768	0.963	0.704	0.516	0.322	0.319
255-265	0.097	0.655	0.797	0.885	0.655	0.336	0.361
265-275	0.103	0.604	0.834	0.828	0.631	0.420	0.473
275-285	0.099	0.440	0.688	0.819	0.657	0.439	0.531
285-295	0.072	0.385	0.697	0.848	0.662	0.396	0.436
295-305	0.063	0.289	0.686	0.820	0.596	0.321	0.310
305-315	0.098	0.344	0.593	0.750	0.435	0.262	0.181
315-325	0.084	0.434	0.764	0.670	0.401	0.207	0.106
325-335	0.110	0.657	0.848	0.721	0.371	0.167	0.131
335-345	0.160	0.678	0.754	0.681	0.383	0.167	0.112
345-355	0.210	0.704	0.546	0.472	0.255	0.114	0.086

Annex III: ATLANTIC OCEAN SUBTROPICAL

Table 32: Subtropical Atlantic site characteristics

ATLANTIC SUBTROPICAL SITE	
Geographical location	λ 27,799° φ -15,359°
Surface area of study site	5 x5 km
Offshore distance	2,8 nm
Depth	80 m
Substrate	Hard
Substrate properties	Rock, Folk 5
Water temperature	18,0-23,5 °C
Salinity	39 PSU
Tidal range	3,2 m
Mean wave height	1,68 m
Expected annual wave power	12,1 kW/m
Average wind speed	8,3 m/sec
Expected annual wind power	520 W/m_2

Table 33: Main characteristics of the selected site for fish production

DATA FOR FISH PRODUCTION	
Temperature range	18,3-23,5 °C
Oxygen range	Saturation
Salinity	39 PSU
Turbidity	< 0,01 KD490
Selected species for farm production	Seabream

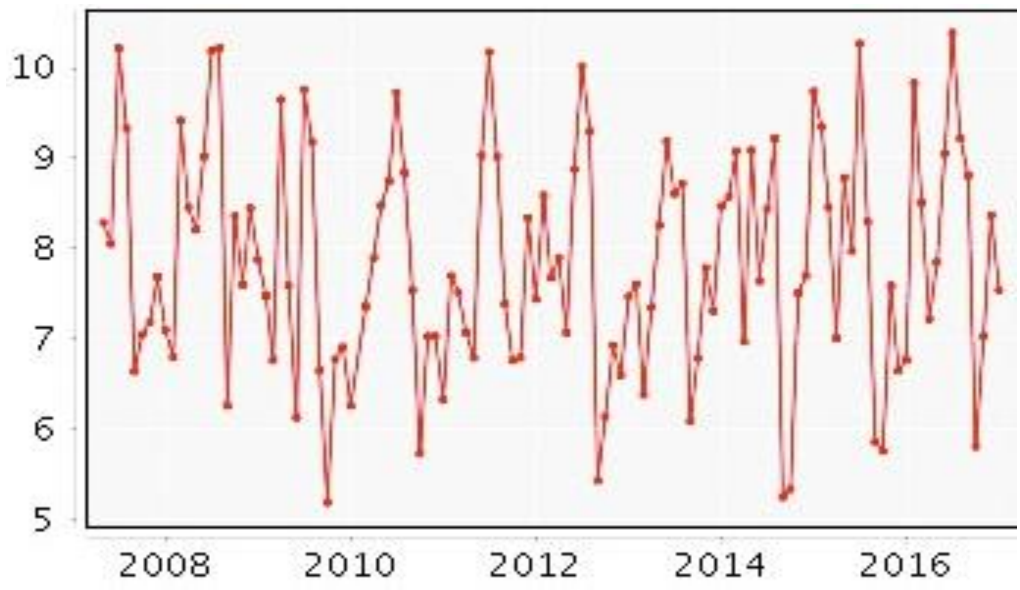

Figure 53: Wind speeds (m/sec) at Arinaga (G. Canaria) site; years 2007-2017, monthly means (*Source: marine.copernicus.eu).*

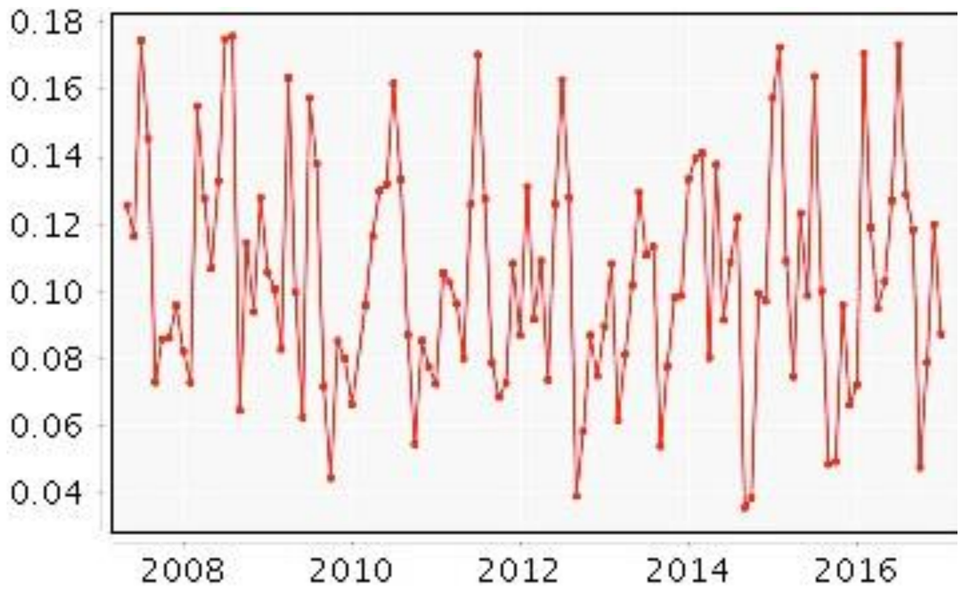

Figure 54: Wind stress (Pa) at Arinaga (G. Canaria) site; years 2007-2017, monthly means (*Source: marine.copernicus.eu).*

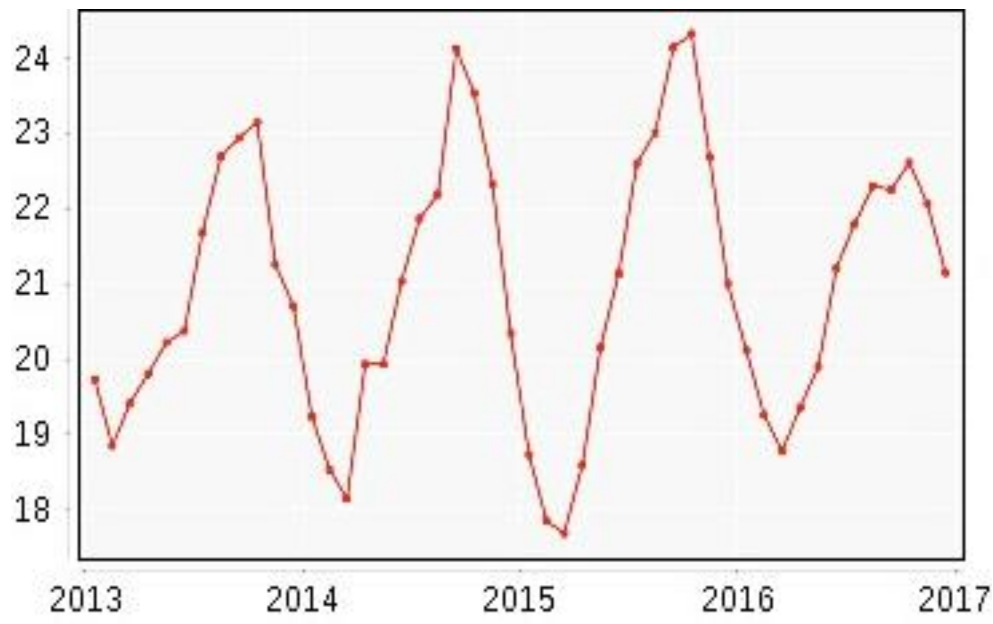

Figure 55: Seawater potential temperature (°C) at Arinaga (G. Canaria) site; years 2013-2017, monthly means (*Source: marine.copernicus.eu*).

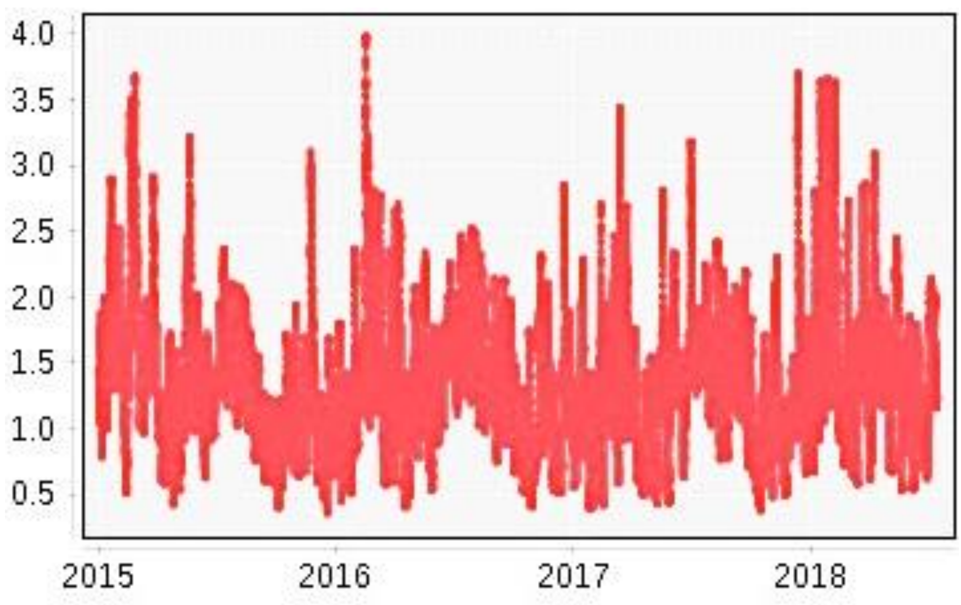

Figure 56: Significant waves (m) at Arinaga (G. Canaria); years 2015-2018, hourly means (*Source: marine.copernicus.eu*).

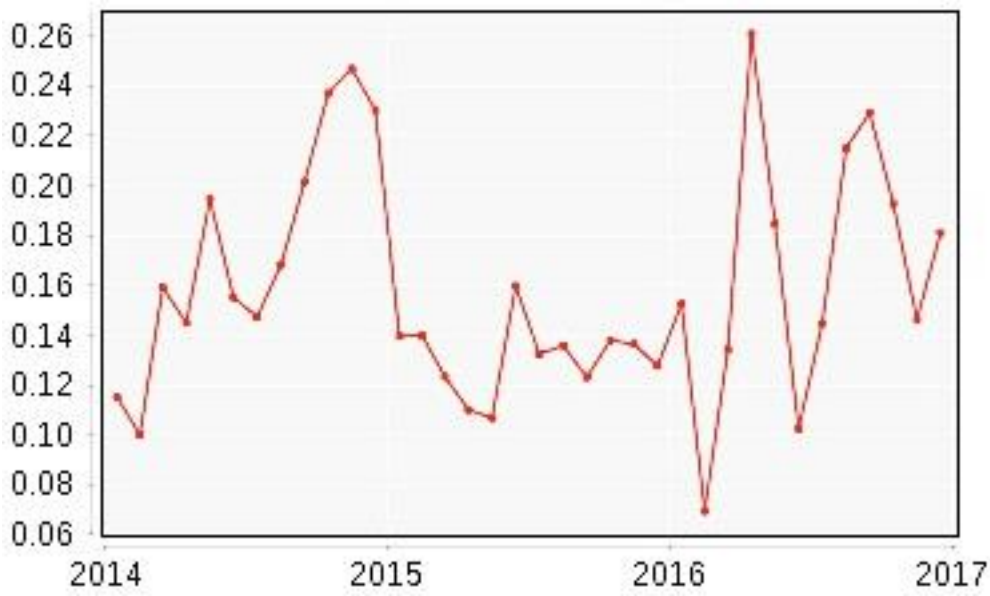

Figure 57: Seawater velocity (m/sec) at Arinaga (G. Canaria) site; years 2014-2016, monthly means (*Source: marine.copernicus.eu).*

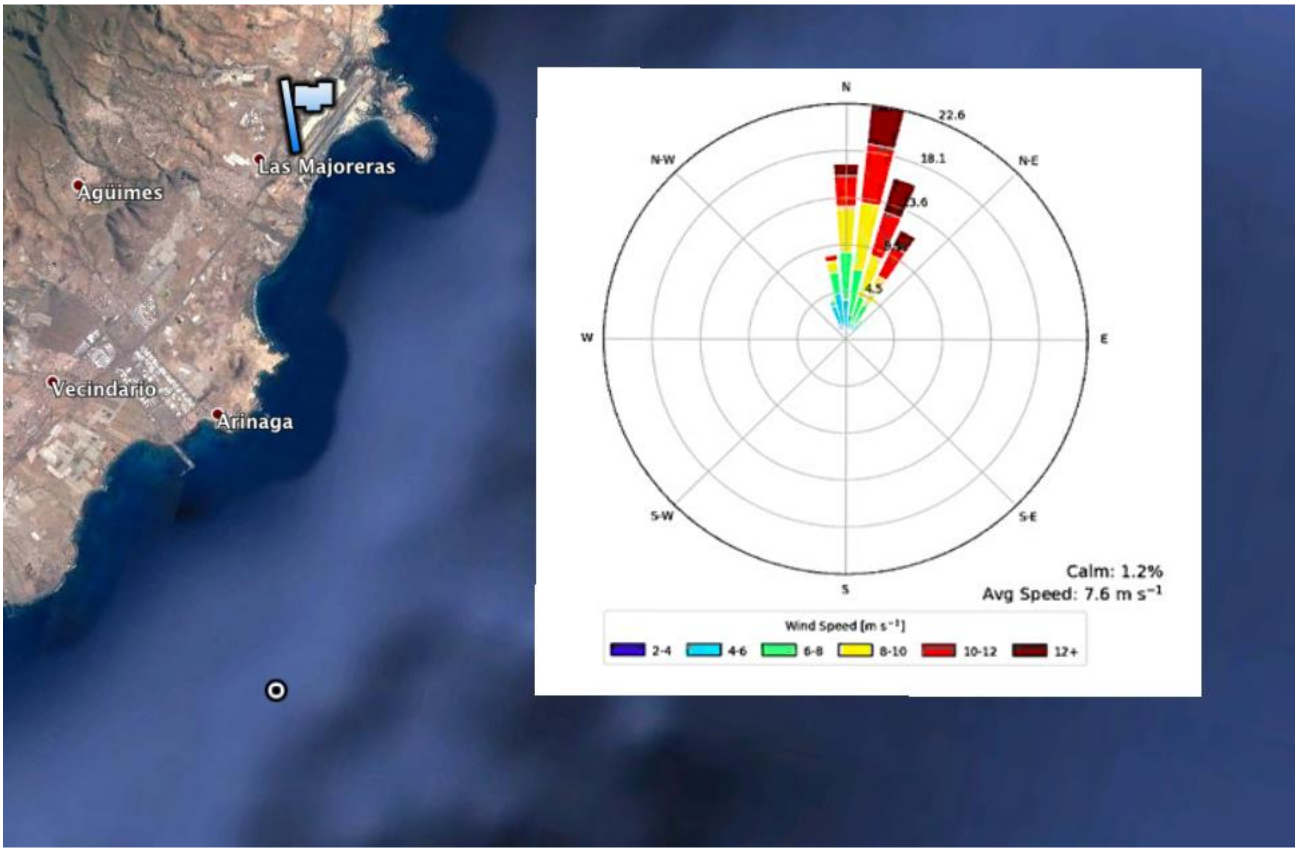

Figure 58: Windrose plot for Arinaga, period 22 Aug 2011- 14 Jul 2018 ;

Flag: Recorder position; Point: selected site. (Source : [https://mesonet.agron.iastate.edu)](https://mesonet.agron.iastate.edu)

Table 34: Las palmas GC, windrose data ; latitude : 27.92250 ; longitude : -15.38944; elevation (m) = 25.

```
# Windrose Data Table (Percent Frequency) for LAS PALMAS/GANDO (GCLP)
# Observations Used/Missing/Total: 117184/5287/122471
# Period: 22 Aug 2011 - 14 Jul 2018
# Hour Limiter: All included
# Month Limiter: All included
# Wind Speed Units: meters per second
# Generated 26 Jul 2018 09:11 UTC, contact: akrherz@iastate.edu
# First value in table is CALM
         ,  0.0- 1.9,  2.0- 3.9,  4.0- 5.9,  6.0- 7.9,  8.0- 9.9, 10.0-11.9, 12.0- inf,
355-005,      1.326,     0.751,     3.021,     4.580,     4.426,     2.955,     1.122,
005-015,      0.049,     0.473,     1.876,     4.417,     6.439,     5.661,     3.776,
015-025,      0.044,     0.376,     1.271,     2.633,     4.116,     4.323,     3.441,
025-035,      0.036,     0.368,     1.103,     2.201,     3.134,     3.168,     1.713,
035-045,      0.044,     0.323,     0.823,     0.759,     0.425,     0.088,     0.004,
045-055,      0.051,     0.283,     0.437,     0.146,     0.021,     0.001,     0.000,
055-065,      0.065,     0.405,     0.380,     0.036,     0.000,     0.000,     0.000,
065-075,      0.063,     0.316,     0.156,     0.008,     0.001,     0.000,     0.000,
075-085,      0.093,     0.275,     0.066,     0.009,     0.000,     0.000,     0.000,
085-095,      0.100,     0.345,     0.042,     0.019,     0.000,     0.000,     0.000,
095-105,      0.079,     0.321,     0.062,     0.010,     0.001,     0.000,     0.000,
105-115,      0.067,     0.242,     0.054,     0.042,     0.009,     0.000,     0.000,
115-125,      0.054,     0.198,     0.060,     0.020,     0.000,     0.000,     0.000,
125-135,      0.075,     0.273,     0.059,     0.011,     0.000,     0.000,     0.000,
135-145,      0.067,     0.287,     0.118,     0.003,     0.001,     0.000,     0.000,
145-155,      0.040,     0.287,     0.207,     0.018,     0.002,     0.000,     0.000,
155-165,      0.038,     0.227,     0.365,     0.113,     0.005,     0.000,     0.000,
165-175,      0.032,     0.117,     0.147,     0.086,     0.008,     0.000,     0.000,
175-185,      0.025,     0.092,     0.109,     0.094,     0.029,     0.000,     0.000,
185-195,      0.044,     0.126,     0.118,     0.128,     0.065,     0.015,     0.002,
195-205,      0.042,     0.133,     0.137,     0.125,     0.087,     0.043,     0.018,
205-215,      0.073,     0.215,     0.137,     0.098,     0.073,     0.036,     0.009,
215-225,      0.067,     0.207,     0.123,     0.061,     0.032,     0.016,     0.024,
225-235,      0.071,     0.137,     0.042,     0.032,     0.006,     0.007,     0.013,
235-245,      0.067,     0.099,     0.020,     0.007,     0.012,     0.000,     0.003,
245-255,      0.102,     0.118,     0.010,     0.009,     0.003,     0.002,     0.002,
255-265,      0.150,     0.222,     0.005,     0.003,     0.000,     0.001,     0.000,
265-275,      0.106,     0.095,     0.003,     0.004,     0.000,     0.000,     0.000,
275-285,      0.090,     0.067,     0.005,     0.000,     0.000,     0.000,     0.000,
285-295,      0.169,     0.154,     0.003,     0.002,     0.000,     0.000,     0.000,
295-305,      0.259,     0.394,     0.013,     0.003,     0.000,     0.000,     0.000,
305-315,      0.267,     0.622,     0.039,     0.011,     0.001,     0.002,     0.000,
315-325,      0.215,     0.695,     0.152,     0.021,     0.009,     0.002,     0.000,
325-335,      0.218,     0.964,     0.474,     0.132,     0.053,     0.017,     0.003,
335-345,      0.145,     1.341,     1.928,     0.556,     0.212,     0.055,     0.001,
345-355,      0.096,     1.158,     3.232,     2.071,     1.158,     0.528,     0.133,
```

REFERENCES

Ayrshire Shoreline Management Plan, Appendix C: Data Gap Analysis – Coastal Processes. (2018). IBE1107/D03. Draft D01.

Barasan F., Ozbilgin H., & Ozbilgin Y. D. (2007). Comparison of the swimming performance of farmed and wild gilthead seabream, Sparus aurata. *Aquaculture Research*. 38: 452-456.

Besio, G., Mentaschi, L., & Mazzino, A. (2016). Wave energy resource assessment in the Mediterranean Sea on the basis of a 35-year hindcast, *Energy,* 94: 50–63.

Boccotti, P. (2004). *Idraulica marittima*. Torino, Utet.

Booth, R.K., McKinley, R.S., Okland, F. & Sisak, M.M. (1997). In situ measurement of swimming performance of wild Atlantic salmon (*Salmo salar*) using radio transmitted electromyogram signals. *Aquatic Living Resources* 10: 213-219.

Bozzi. S, Besio. G, & Passoni. G. (2018). Wave power technologies for the Mediterranean offshore: Scaling and performance analysis. *Coastal Engineering* 136: 130-146.

Brett, J. R. (1964) The respiratory metabolism and swimming performance of young sockeye salmon. *J Fish Res Board Can* 21: 1183–1226.

Burnett, N.J., Hinch, S.G., Braun, D.C., Casselman, M.T., Middleton, C.T., Wilson, S.M., & Cooke, S.J., (2014). Burst swimming in areas of high flow: delayed consequences of anaerobiosis in wild adult sockeye salmon. *Physiological and Biochemical Zoology* 87: 587-598.

Carbonara P., Scolamacchia M., Spedicato M.T., Lembo G., Zupa W., & McKinley R.S. (2006). Swimming performances as a well being indicator of reared seabass *Dicentrarchus labrax* (Linnaeus, 1758). Preliminary results. *Biol. Mar. Mediterr*., 13 (1): 488-491.

Colmenar-santoa, A., Perera-Perez, J.,Borge-Diez, D., & de Palacio-Rodriguez, C. (2016). *Renewables and Sustainable Energy.* 64: 1-18.

Cooper. B, Jackson. C, Moore. J, Brown. C, Russell. R, Petrey. D, Elmes. M, & Lacey. P. (2008). Atlas of UK Marine Renewable Energy Resources: *Technical Report. R 1432*. ABP Mer Marine Environmental Research.

Dempster, T., Korsøen, O., Folkedal, O., Juell, J. E., & Oppedal, F. (2009) Submergence of Atlantic salmon (*Salmo salar* L.) in commercial scale sea-cages: A potential short-term solution to poor surface conditions. *Aquaculture* 288: 254–263.

Elliot. J. M, & Elliott. J. A. (2010). Temperature requirements of Atlantic salmon Salmo salar, brown trout Salmo trutta and Arctic charr Salvelinus alpinus: predicting the effects of climate change. *Journal of Fish Biology* : 77: 1793–1817.

Gansel, L. C., McClimans, T. A., & Myrhaug, D. (2012). Average Flow Inside and Around Fish Cages With and Without Fouling in a Uniform Flow. ASME. *J. Offshore Mech. Arct. Eng*.134(4): 041201-041201-7.

Gómez, M., Pérez Gómez, B., De Alfonso, M., Pérez, S. & Ruiz, M. I. 2015. Waves and tides in the Canary Current Large Marine Ecosystem. In: *Oceanographic and biological features in the Canary Current Large Marine Ecosystem*. Valdés, L. & Déniz-González, I. (eds). IOC Technical Series, 115: 115-131. Paris, IOC-UNESCO.

Gonçalves. M, Martinho. P, & Guedes Soares. C. (2014). Assessment of wave energy in the Canary Islands. *Renewable Energy* 68 : 774-784

Guedes Soares, C., Rute Bento, A., Gon¸calves, M., Silva, D., & Martinho, P. (2014). Numerical evaluation of the wave energy resource along the Atlantic European Coast. *Computers & Geosciences,* 71: 37-49.

Hasselmann, K., Barnett, T.P., Carlson, H., Cartwright, D.E., Enke, K., Ewing, J.A., Gienapp, H., Hasselmann, D.E., Krusemann, P., Meerburg, A., Muller, P., Olbers, D.J., Richter, K., Sell, W., & Walden, H., (1973). Measurements of Wind-Wave Growth and Swell Decay during the Joint North Sea Wave Project (JONSWAP). Deutches Hydrographishes Istitut – Hamburg. *Reihe* A(8), 12.

Herskin, J., & Steffensen, J.F., (1998). Energy savings in sea bass swimming in a school: measurements of tail beat frequency and oxygen consumption at different swimming speeds. *Journal of Fish Biology* 53: 366-376.

Hill. G. (2003). *Wind prospecting on the canary islands*. Department of Physical Geography, Goteborg University B348.

Hvas, M.; Folkedal, O.; Solstorm, D.; Vågseth, T.; Fosse, J. O.; Gansel, L. C.; & Oppedal, F., (2017) Assessing swimming capacity and schooling behaviour in farmed Atlantic salmon Salmo salar with experimental push-cages. *Aquaculture.* vol. 473.

Hwang, C.L.; Lai, Y.J.; & Liu, T.Y. (1993). "A new approach for multiple objective decision making". Co*mputers and Operational Research*. 20: 889–899.

Hwang, C.L.; & Yoon, K. (1981). *Multiple Attribute Decision Making: Methods and Applications*. New York: Springer-Verlag.

Inall. M. E & Sherwin. T. J. (2006). *SEA7 Technical Report – Hydrography.* SAMS Research Services Ltd. SEA7 Hydrography.

Jain K.E., Birtwell I.K., & Farrell A.P. (1998) - Repeat swimming performance of mature sockeye salmon following a brief recovery period: a proposed measure of fish health and water quality. *Can. J. Zool.,* 76: 1488-1496.

Johansson, D., Juel,l J.E., Oppedal, F., Stiansen, J. E., & Ruohonen, K. (2007) The influence of the pycnocline and cage resistance on current flow, oxygen flux and swimming behaviour of Atlantic salmon (*Salmo salar L.*) in production cages. *Aquaculture* 265: 271–287.

Johansson, D., Laursen, F., Fernö, A., Fosseidengen, J.E., Klebert, P., Stien, L.H., Vågseth, T.,& Oppedal, F., (2014). The interaction between water currents and salmon swimming behaviour in sea cages. PLoS One 9, e97635.

Klebert P., Gansel L., Lader P., & Oppedal F. (2013) Flow hydrodynamics through nets and floating cages: a review. *Ocean Engeneering* 58: 260–274.

Li L., Fu S., Xu Y., Wang J., & Yang, J. (2013). Dynamic responses of floating fish cage in waves and current. *Ocean Engeneering* 72: 297-303.

Luna-Acosta, A., Lefrancois, C., Millot, S., Chatain, B., & Bégout, M.L., (2011) Physiological response in different strains of sea bass (Dicentrarchus labrax): swimming and aerobic metabolic capacities. *Aquaculture* 317: 162–167

Martin Mederos, A.C., Medina Padron, J.F., & Feijoo Lorenzo, A.E., (2011). Renewable and *Sustainable Energy Reviews*. 15: 612-620.

Martinez, A., Perez, E., & Bruno, M. (1997) Variation of the tidal properties around Gran Canaria. *Oceanologica Acta,* 22 , 1: 19-30.

Neill. S. P, Vogler. A, Goward-Brown. A. G, Baston. S, Lewis. M. J, Gillibrand. P. H, Waldman. S, & Woolf. D. K. (2017). The wave and tidal resource of Scotland. R*enewable Energy* 114 :3-17.

Offshore Energy SEA. (2009). *Appendix 3 - Environmental baseline* : Page 374.

Onea. F, Deleanu. L, Rusu. L, & Georgescu, C. (2016). Evaluation of the wind energy potential along the Mediterranean Sea coasts. *Energy Exploration & Exploitation.* Vol. 34(5): 766–792

Oppedal F, Dempster T, & Stien L (2011). Environmental drivers of Atlantic salmon behaviour in sea-cages: a review. *Aquaculture* 311: 1–18.

Plaut, I., (2001). Critical swimming speed: its ecological relevance. Comparative Biochemistry and Physiology Part A: *Molecular & Integrative* Physiology 131: 41-50.

Remen M., Solstorm F., Bui S., Klebert P., Vågseth T., Solstorm, D., Hvas M., & Oppedal F. (2016) Critical swimming speed in groups of Atlantic salmon Salmo salar. *Aquacult. Environ. Int.* 8:659–664.

Schallenberg-Rodríguez. J, & Montesdeoca. N. G. (2017). Spatial planning to estimate the offshore wind energy potential in coastal regions and islands. Practical case: the Canary Islands, Energy. doi: 10.1016/j.energy.2017.10.084.

Schlütter. F, Petersen. O. S, & Nyborg. L. (2015). *Resource Mapping of Wave Energy Production in Europe* . Proceedings of the 11th European Wave and Tidal Energy Conference 6-11th September 2015, Nantes, France.

Soukissian, T.H., Axaopoulos, P. & F. Karathanasi (2015) Offshore wind power in the Mediterranean Sea using Blended Sea Winds, OCEANS'15 International Conference, MTS/IEEE, Genova, May 18-21, 2015, ISBN: 978-1-4673-7164-3.

Soukissian T. H, Denaxa. D, Karathanasi. F, Prospathopulos. A, Sarantakos. K, Iona. A, Georgantas. K, & Mavrakos. S. (2017). Marine renewable energy in the Mediterranean Sea: status and prospectives. Review. *Energies.* 10: 1512

Stien, L. H., Dempster, T., Bui, S., Glaropoulos, A., Fosseidengen, J. K., Wright, D. W., Oppedal, F. (2016). 'Snorkel' sea lice barrier technology reduces sea lice loads on harvest-sized Atlantic salmon with minimal welfare impacts. *Aquaculture* 458: 29–37.

Twidell, J., & Weir, A., (2006). *Renewable Energy Resources*. 2nd ed. New York, Taylor & Francis,.

Vannucchi. V., , Cappietti. L., & Falcão. A.F.O. (2012). *Estimation of the offshore wave energy potential of the Mediterranean Sea and propagation towards a nearshore area*. 4th International Conference on Ocean Energy, 17 October, Dublin

Veigas. M & Iglesias. G. (2013). Wave and offshore wind potential for the island of Tenerife. Energy Conversion and Management 76 : 738–745.

Veigas. M & G. Iglesias. G. (2015). A hybrid wave-wind offshore farm for an island. *International Journal of Green Energy*, 12:6, 570-576.

Wood, C.M., (1991). Acid-base and ion balance, metabolism, and their interactions, after exhaustive exercise in fish. *J. Exp. Biol.* 160: 285-3.

Zanuttigh B., Angelelli E., Kortenhaus A., Koca K., Krontira Y. and P. Koundouri. (2016). Methodology for multi-criteria design of multi-use off-shore platforms for marine renewable energy harvesting. *Renewable Energy,* 85: 1271-1289

http://www.fao.org/fishery/culturedspecies/

http://www.marine.copernicus.eu